

RCA REVIEW

a technical journal

**RADIO AND ELECTRONICS
RESEARCH • ENGINEERING**

VOLUME XII

SEPTEMBER 1951

NO. 3

Part I

RCA REVIEW

GEORGE M. K. BAKER
Manager

CHAS. C. FOSTER, JR.
Editorial Manager

THOMAS R. ROGERS
Business Manager

SUBSCRIPTIONS:

United States, Canada, and Postal Union: One Year \$2.00, Two Years \$3.50, Three Years \$4.50
Other Countries: One Year \$2.40, Two Years \$4.30, Three Years \$5.70

SINGLE COPIES:

United States: \$.75 each. Other Countries: \$.85 each

Copyright, 1951, by RCA Laboratories Division, Radio Corporation of America

Published quarterly in March, June, September, and December by RCA Laboratories
Division, Radio Corporation of America, Princeton, New Jersey

Entered as second class matter July 3, 1950, at the
Post Office at Princeton, New Jersey, under the act of March 3, 1879

RADIO CORPORATION OF AMERICA

DAVID SARNOFF, *Chairman of the Board*

FRANK M. FOLSOM, *President*

LEWIS MACCONNACH, *Secretary*

ERNEST B. GORIN, *Treasurer*

RCA LABORATORIES DIVISION

C. B. JOLLIFFE, *Executive Vice President*

PRINTED IN U.S.A.

RCA REVIEW

a technical journal

RADIO AND ELECTRONICS
RESEARCH • ENGINEERING

Published quarterly by

RADIO CORPORATION OF AMERICA
RCA LABORATORIES DIVISION

in cooperation with

RCA VICTOR DIVISION

RADIOMARINE CORPORATION OF AMERICA

RCA INTERNATIONAL DIVISION

RCA COMMUNICATIONS, INC.

NATIONAL BROADCASTING COMPANY, INC.

RCA INSTITUTES, INC.

VOLUME XII

SEPTEMBER, 1951

NUMBER 3

PART I OF TWO PARTS

CONTENTS

	PAGE
FOREWORD <i>The Manager</i> , RCA Review	291
Utilization of Printed Components in a Television Tuner D. MACKEY AND E. SASS	293
Photoconductivity in Insulators ALBERT ROSE	303
The Vidicon—Photoconductive Camera Tube P. K. WEIMER, S. V. FORGUE AND R. R. GOODRICH	306
Photoconductivity in Amorphous Selenium P. K. WEIMER AND A. D. COPE	314
Properties of Some Photoconductors, Principally Antimony Trisulfide S. V. FORGUE, R. R. GOODRICH AND A. D. COPE	335
Some Aspects of the Photoconductivity of Cadmium Sulfide R. W. SMITH	350
An Outline of Some Photoconductive Processes ALBERT ROSE	362
Studies of Externally Heated Hot Cathode Arcs, Part I—Modes of the Discharge L. MALTER, E. O. JOHNSON AND W. M. WEBSTER	415
RCA TECHNICAL PAPERS	436
AUTHORS	438

RCA Review is regularly abstracted and indexed by *Industrial Arts Index Science Abstracts* (I.E.E.-Brit.), *Engineering Index*, *Electronic Engineering Master Index*, *Abstracts and References* (Wireless Engineer-Brit. and Proc. I.R.E.) and *Digest-Index Bulletin*.

UTILIZATION OF PRINTED COMPONENTS IN A TELEVISION TUNER*

BY

DONALD MACKEY and EARL SASS

Tube Department, RCA Victor Division,
Camden, N. J.

Summary—Printed coils are found to be practical in a turret-type television tuner which has individual coil strips. The coils on these strips are produced by means of a relatively unconventional photoetching process. Possible economic and electrical advantages of using the printed coils are indicated, and a circuit employing the coils is described.

INTRODUCTION

AS a step in the investigation of the practicability of using printed construction in television circuits, research has been carried out utilizing a photoetching process to produce coils for a television tuner. A circuit which employs a large number of coils was chosen so that an application which would be suitable for mass production of printed coils could be tested. It was found that the range, precision, and stability of inductance values obtained with the photoetching process are satisfactory for the tuner.

PRINTING TECHNIQUES

Before an attempt was made to construct a tuner using printed coils, various processes for the manufacture of printed components were studied. One process involves the application of metallic paints through stencils. This method, it was found, cannot readily produce lines of precision width or of uniform conductivity. The same disadvantages result from the use of the somewhat similar process of spraying conducting films through a stencil. The latter process may, in addition, produce poor particle adhesion and consequent low conductivity.

A third method employed to produce printed units is that of chemical deposition. After a thin metallic film of relatively low conductance is formed, the film is built up by electroplating. With this process, when the pattern is complicated, difficulty is experienced in obtaining uniform line thickness. The same problem arises in vacuum

* Decimal Classification: R583.5.

processes utilizing cathode sputtering and evaporation to produce thin metallic films which must then be plated.

A fifth method, that of hot-die stamping, is often used. But here too the fineness of the lines is limited by the process. In addition, because tool changes are necessary for each modification, the tooling required for development work is not only costly but slow. Moreover, die stamping permits little flexibility for rapid production changes.

PHOTOETCHING TECHNIQUE

Disadvantages having been found in the various conventional processes, further studies were made of methods of printing circuit components. The result of this investigation was the adoption of a photoetching process similar to the photoengraving technique used in the printing industry. A copper-clad sheet of phenolic plastic or glass-base melamine is coated with a light-sensitive material. A contact print is made photographically on this sheet from a negative of a pattern of the required circuit. To facilitate mass production, a multiple pattern is used. The contact print is developed and placed in an etching solution. The part of the copper not covered by the pattern is eaten away, with the result that the required copper circuit appears on the phenolic sheet. The sheet is then placed in a die where it is cut into the desired shape and holes are pierced for the provision of terminals.

The photoetching process has several advantages over previously mentioned systems. It facilitates circuit development in that only a new negative is necessary for a circuit change. It follows that production-tool cost is very low. This economy is especially important if inductance changes are necessary during a production run. The highest cost is that involved in providing a blanking and piercing die, the design of which is fixed by mechanical considerations. Because a pure conductor is used, resistance variations are negligible. Reproducibility is excellent, the ultimate limits of detail and precision approaching those of conventional photographs. A pattern using a line-width of as little as 10 mils is completely practical.

TUNER MODELS

After the photoetching process was developed, it was used in producing a television tuner. The first design model employed the drum-type assembly shown in Figure 1. The disc assembly could be rotated by means of the thumb wheel. A single disc (Figure 2) was used with printed coils on both sides. The advantages of this system are: (1)

only a minimum number of components is used; (2) the tuning system is mechanically simple; (3) the layout is good from the standpoint of controlling wiring inductance. These advantages, however, are outweighed by the following disadvantages: (1) the yield would probably be low because of the large number of coils on each disc; (2) the unconventional shape of the tuner and thumb wheel presents a styling problem for the cabinet designers; (3) shielding between the antenna, radio-frequency primary, and radio-frequency secondary circuit is difficult.

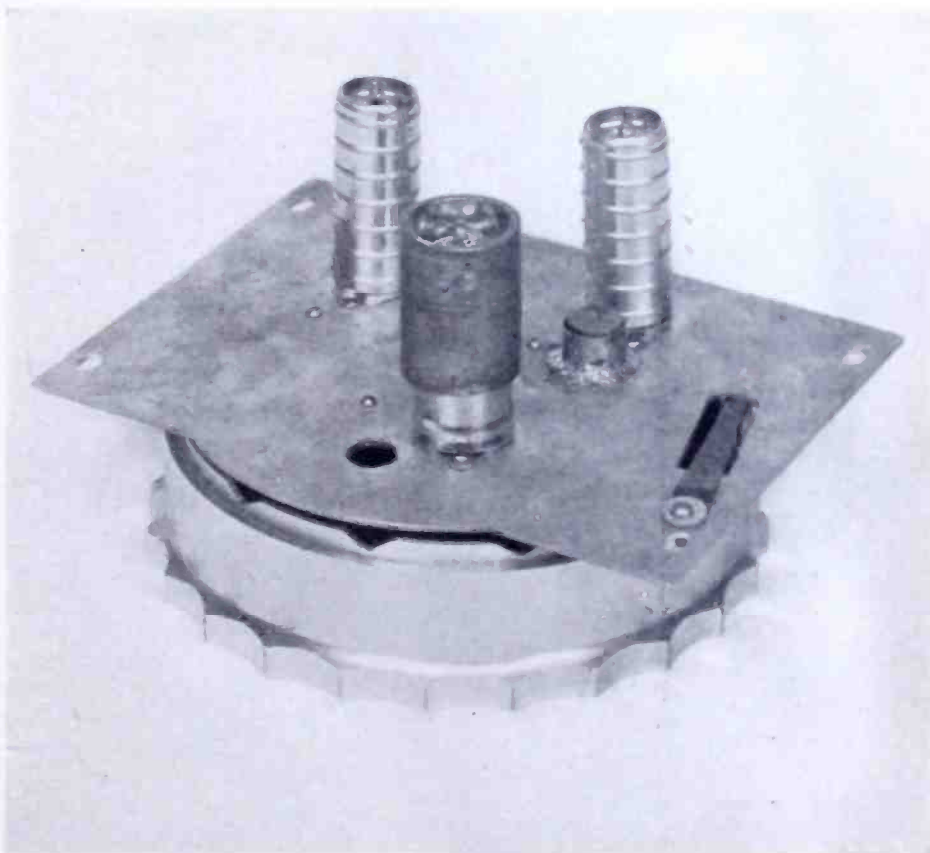


Fig. 1—View of original "thumb wheel" tuner components.

Primarily because of the disadvantages of the drum-type assembly, the cylindrical turret-type tuner shown in Figure 3 was selected for development. Here each set of coils for a particular channel is located on an individual mounting strip. Because a defect in one coil does not cause rejection of all the others, the probable yield is much greater than when all coils are on one disc. In addition, the use of a turret assembly greatly simplifies circuit shielding and reduces the styling problem. Moreover, the use of individual strips for each channel provides flexibility in case of frequency allocation changes, permits adjust-

ment of each channel to optimum condition, and contributes to easier control during development and in production.

TUNER CIRCUIT

The basic circuit of the tuner is given in Figure 4, the printed elements shown being those for channel 7. A tabulation of operating characteristics is given in Table 1. The input circuit consists of a

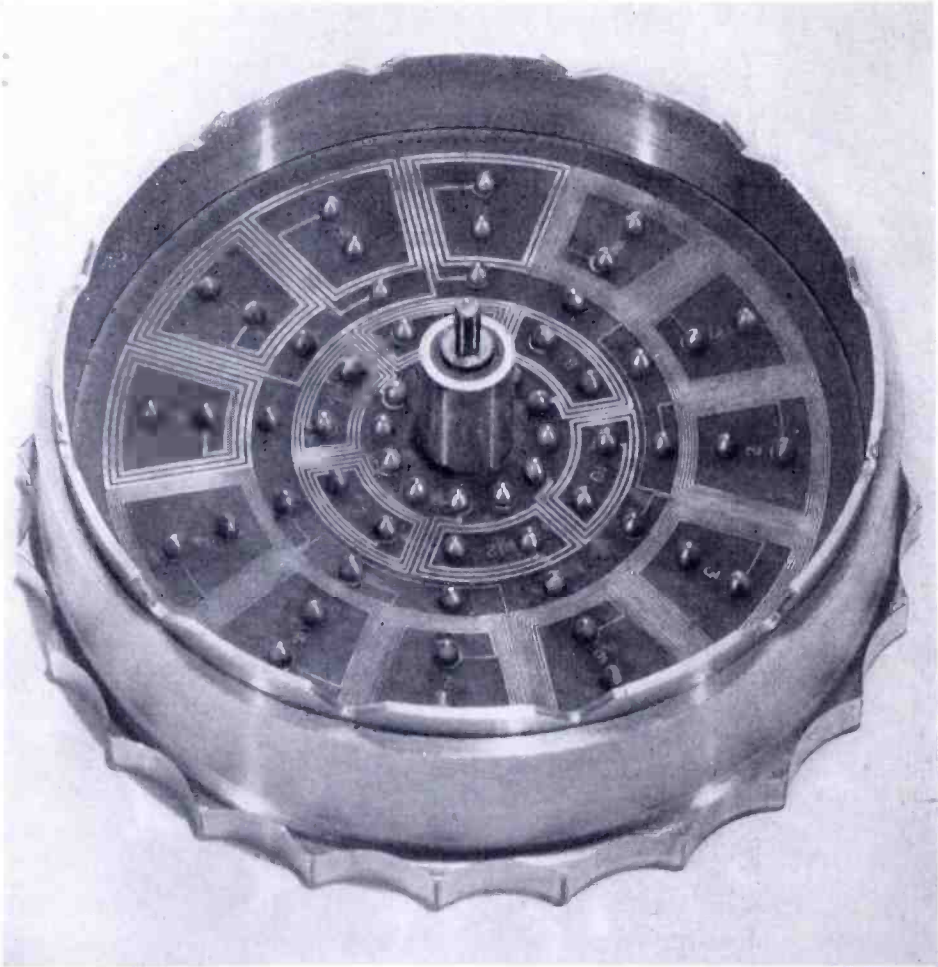


Fig. 2—Original tuner knob with all the coils printed on the one disc.

pair of elevator transformers for matching the tuner to a balanced 300-ohm line, followed by a high-pass filter section with cutoff at approximately 47 megacycles and maximum attenuation at 23 megacycles for intermediate-frequency rejection, and a tuned input section. The tuned input section is composed of a printed coil (L_{107} in this case), L_8 and L_9 , the capacitors C_4 , C_5 , and C_{10} together with the input capacitance and resistance of the radio-frequency amplifier tube. These

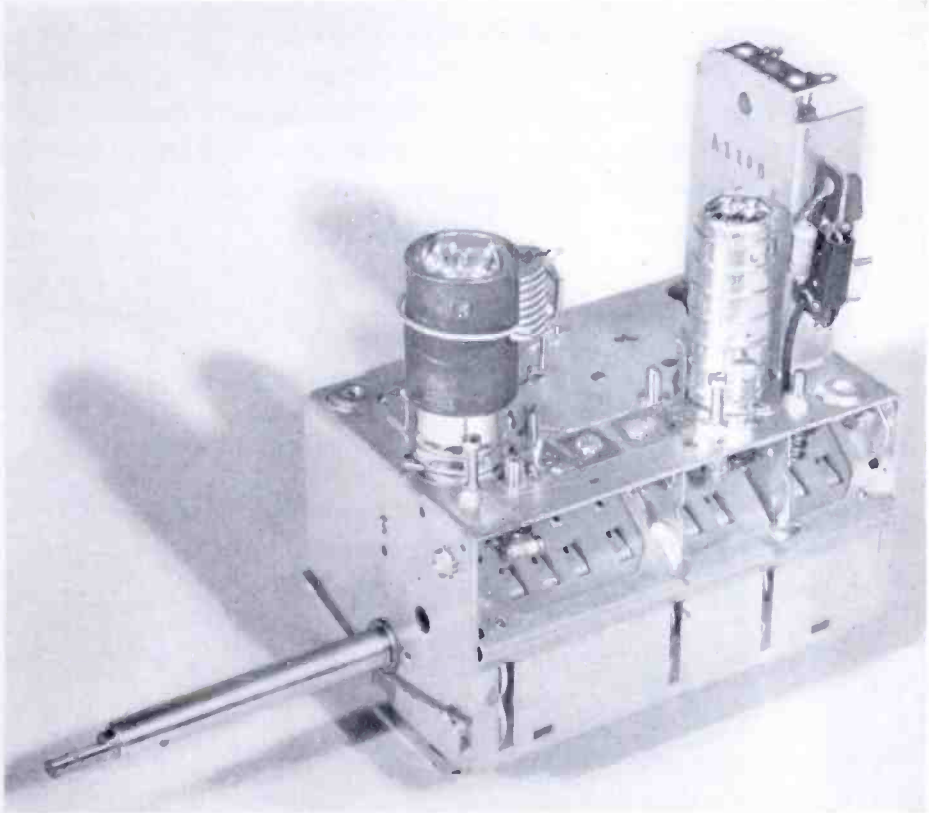


Fig. 3—Turret-type tuner.

components constitute a low-pass pi network with cutoff tuned for each channel, so that signal selectivity is provided and oscillator-frequency radiation from the antenna is reduced.

The constants, variables, and configuration of the pi network are arranged to provide a varying impedance transfer to the grid with change in frequency. On channel 13 the voltage across the arm composed of L_{107} and L_9 , approximately equals the voltage across L_8 ahead of C_5 . As larger values of switched inductance are inserted on lower-

Table I — TYPICAL TUNER OPERATING CHARACTERISTICS

Channel No.	2	3	4	5	6	7	8	9	10	11	12	13
Gain (db)*	28.9	28.5	27.6	25.9	25.3	24.5	25.7	26.2	24.9	24.0	22.9	22.7
Noise Factor	6.5	7.7	8.1	9.4	10.2	13.7	13.8	13.8	13.4	13.7	13.1	13.2
Image Rejection (db)	86.0	86.0	86.4	76.5	76.5	83.0	77.0	77.0	74.5	75.0	74.5	86.4
IF Rejection (db)	82	82	**	81	78.5	80	80	79.5	79.5	80.5	83.0	78.5
Signal-Image Rejection (db)	Greater than 100 db						73	77.5	—	—	—	—
Harmonic Interference (db)	Greater than 100 db											
Sound-IF Rejection (db)	17.5	17.5	17.5	17.5	17.5	17.5	17.5	17.5	17.5	17.5	17.5	17.5
Oscillator Radiation (μ v)	Less than 3000 μ v						4500	7000	10000	9000	8000	7000
Reflection Coefficient	0.33	0.43	0.43	0.33	0.13	0.14	0.18	0.29	0.25	0.18	0.21	0.29

* Based on ratio of voltage at first intermediate-frequency grid to that on antenna and includes 6db termination loss.

** Not measured because 3rd harmonic of intermediate-frequency signal generator falls in this channel.

frequency channels, the voltage across the terminating arm becomes greater than that across the input arm. Consequently, C_5 has greater effect on the input impedance as lower channels are tuned in. The fact that the effective input capacitance increases with decreasing frequency tends to offset the accompanying decrease of tube conductance and thus tends to maintain a good impedance match,

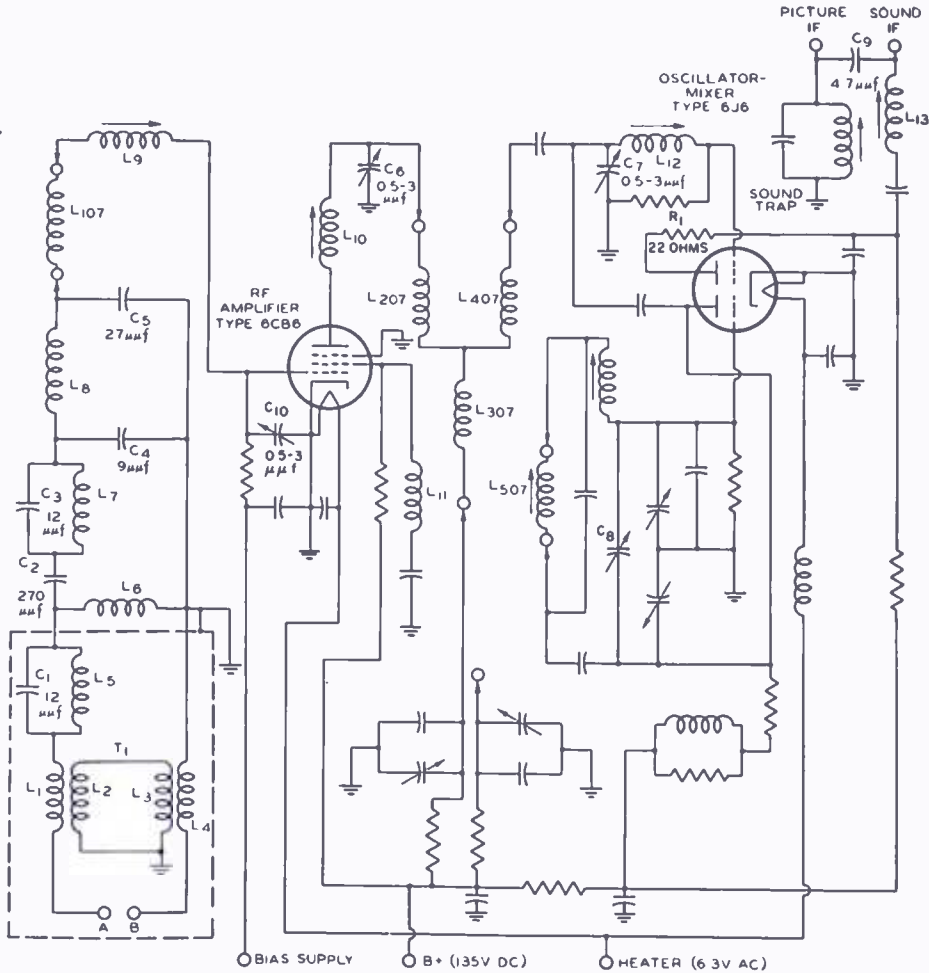


Fig. 4—Tuner circuit.

However, the major criterion in the selection of the circuit parameters was the attainment of optimum average signal-to-noise ratio rather than optimum average impedance match over the complete band of frequencies. The minimizing of noise favors operation with indoor and built-in antennas and is not incompatible with good impedance match.

Type 6CB6 is used in the radio-frequency amplifier stage because this tube, an improved version of the 6AG5, features high transconductance, low interelectrode capacitances, and moderate cost. Coil L_{11}

in the screen circuit causes a regenerative effect which minimizes the rate at which the input conductance of the 6CB6 increases with frequency. In addition, L_{11} partially neutralizes the effects of cathode inductance, thereby somewhat reducing the rate at which the noise factor increases with frequency.

The output of the radio-frequency amplifier contains a double-tuned M-derived band-pass filter with maximum attenuation at approximately the image frequency of each channel. The M-derived circuit provides unusually high image attenuation and reduces oscillator feed-through to the radio-frequency amplifier. Shunt trimmers C_6 and C_7 and variable inductors L_{10} and L_{12} are adjusted to compensate for

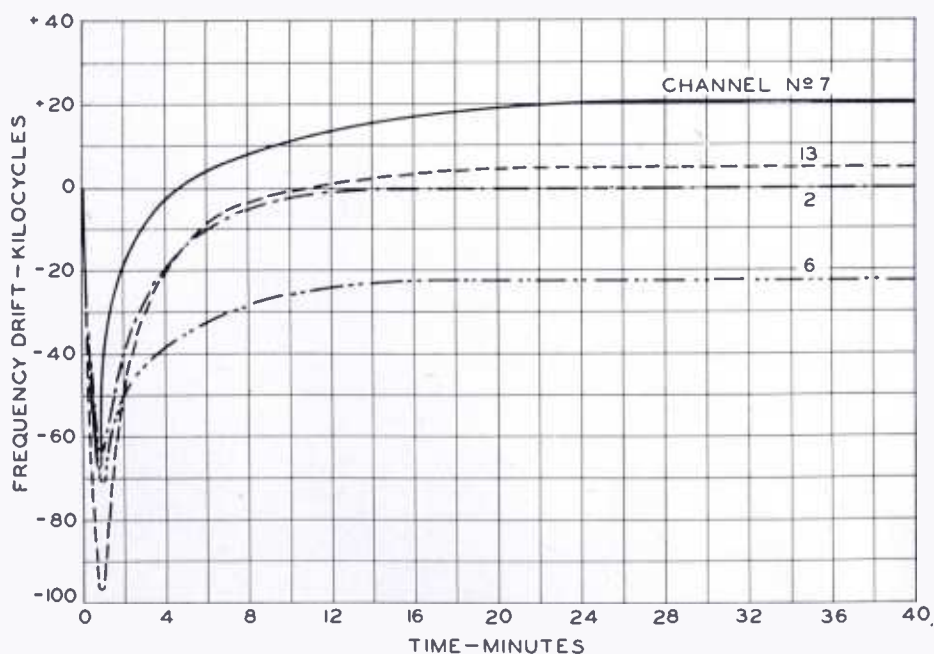


Fig. 5—Warm-up drift of oscillator frequency.

variations in chassis capacitance and wiring inductance. Because L_{10} and L_{12} are large compared with the printed inductances for the high channels, the trimmers are effectively tapped down on the higher frequencies, a fact which increases the L/C ratio on these channels.

OSCILLATOR SECTION

The oscillator section employs one unit of a 6J6 tube in a temperature-compensated circuit. Figure 5 shows that maximum frequency change occurs during the first minute of operation. This maximum change varies from 95 kilocycles on channel 13 to 65 kilocycles on

channel 2. After the warm-up drift the oscillator frequency becomes stable.

The base material for the low-frequency coils is made of glass-base melamine rather than of phenolic plastic because the latter has a relatively high temperature coefficient of dielectric constant. If phenolic bases are used for printed low-channel oscillator coils, variations in temperature cause appreciable changes in distributed capacitance and hence in oscillator frequency. This effect is not as pronounced on the high channels, for there the printed portion of the oscillator contributes only a small portion of the tank inductance and any change in the effective printed inductance causes only a small percentage change in the total inductance. Therefore, the less costly phenolic base is used for the strips for channels 7 to 13.

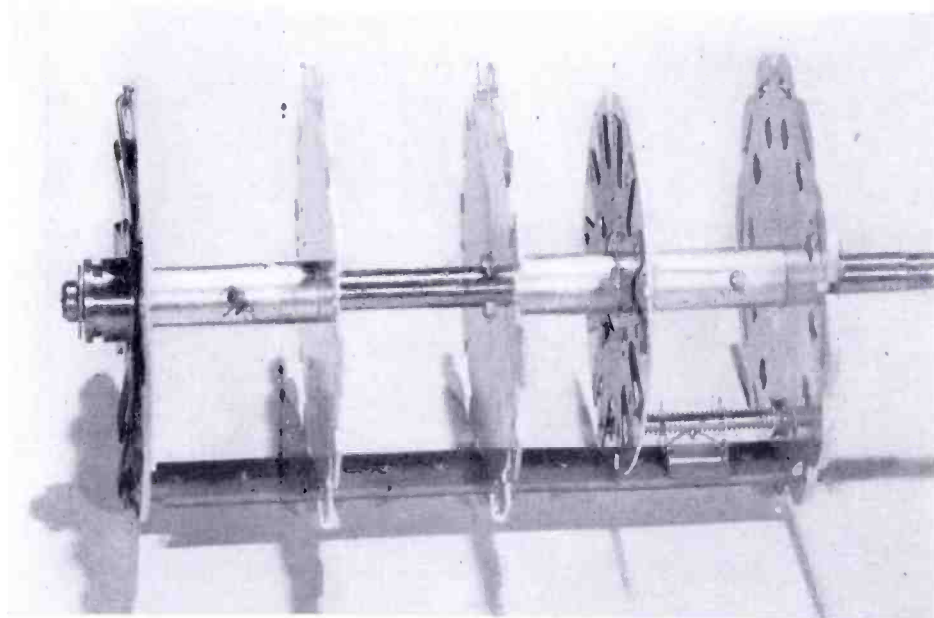


Fig. 6—Turret assembly with one coil strip in place.

The oscillator frequencies are adjusted by varying the position of sliding plates under the printed coils. Figure 6 shows a turret with one coil strip in place. The sliding plate, lower right, is adjusted by means of a screw. Fine tuning is provided by variable-dielectric capacitor C_8 connected directly across the tank circuit.

MIXER SECTION

The mixer-tube unit is the other half of the 6J6. The mixer plate circuit contains series elements which are resonant at approximately 140 megacycles. These elements are C_9 and the wiring inductance

associated with R_1 . The resonance effect provides negative resistance in the mixer grid circuit on channels 7 to 13 and positive resistance on channels 2 to 6, thereby giving the circuit a Q which is nearly proportional to frequency. Consequently, for the same degree of coupling, the circuit bandwidth is approximately constant on all channels. The resistive component of R_1 serves to damp out unwanted resonances.

The intermediate-frequency output section shown in Figure 4 is intended for use with stagger-tuned intermediate-frequency systems. However, the output circuit can be revised to suit any other intermediate-frequency system now in use. The mixer plate circuit contains a tuned low-pass section which passes intermediate frequencies and a high- Q trap which absorbs the sound output, thus shunting it away from the picture intermediate-frequency terminals and providing output for the sound intermediate-frequency terminals. The low-pass filter, in addition, minimizes oscillator feed-through to the intermediate-frequency stages. The filter is composed of L_{13} , C_D , the output capacitance of the mixer tube, and the input capacitance of the picture intermediate-frequency tube. Coil L_{13} has sufficient range of adjustment to cause resonance over a wide enough range of frequencies in the vicinity of 22 megacycles to be suitable for various stagger-tuned intermediate-frequency combinations.

PRINTED COMPONENT CONSIDERATIONS

Some of the physical features of the tuner should be noted. The copper sheet cemented on each channel strip at the start of the process is 1.35 mils thick. The coil strips have T-slots into which are inserted metal plates that serve to lock the strips in the turret and also to function as shields between coils. Figure 7 depicts the coil strip for channel 13.

The inductance values of the printed coils range from approximately 1.00 microhenry on channel 2, to 0.002 microhenry on channel 13. The Q of these coils is approximately 70, the dielectric losses in the strip being the primary controlling factor. The geometry of the coil has only a secondary effect on Q . As to uniformity, the great majority of strips could be interchanged at random in a tuner with no effect on the response curve. The maximum variation of effective inductance resulted in between $\frac{1}{4}$ and $\frac{1}{2}$ per cent change of the resonant frequency with this variation being nearly equally divided between variation in inductance and distributed capacitance. Figure 8 shows a coil strip for channel 2. Here the printed lines are 10 mils wide with 10 mils between lines.

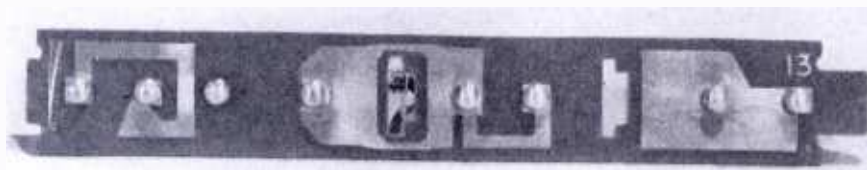


Fig. 7—Coil strip for channel 13.

CONTACT FEATURES

The head and shank dimensions of the rotor contact rivets are such that the rivets may be hopper fed. The radius of curvature of the head is large, therefore the head has a small angle of contact with the stator contact springs. The stator contact springs, which are made of spring silver, are in the form of a loop. This shape is used both to minimize inductance and to reduce inductance changes due to any variation in position of the rivet head on the spring. The loop provides two paths in parallel, the combined length of the paths being a constant; therefore, variation in the contact point does not appreciably change the effective inductance of the parallel paths. In addition, the stator terminal is formed in such a manner as to provide both a highly favorable ratio of detent to contact pressure, which results in very positive detent action with low switching torque, and a long switching wipe with the rotor contacts to insure positive contact. Exhaustive life tests in which turrets were revolved more than 40,000 times have shown substantially no wear on the contact rivets and springs. It is of interest to note that the most destructive life test consists of rotating the rotor at a very slow rate, permitting the stator terminals to complete their full train of mechanical oscillations as contact is broken, and thus obtaining the maximum number of stress reversals.

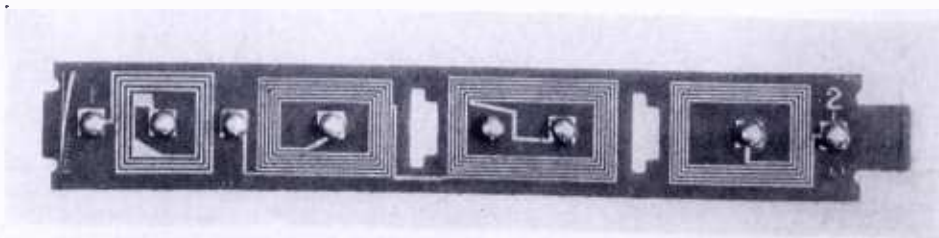


Fig. 8—Coil strip for channel 2.

PHOTOCONDUCTIVITY IN INSULATORS*

BY

ALBERT ROSE

Research Department, RCA Laboratories Division,
Princeton, N. J.

THE series of papers which this note introduces originated in a project aimed at adapting photoconductive materials to television pickup tubes. It is at once interesting and significant that photoconductivity entered into some of the earliest proposals for pickup tubes; that it continued intermittently to attract the attention of all of the major groups working on these tubes; and that only recently have useful photoconductive tubes been developed. The high sensitivity advantage of a volume effect, like photoconductivity, compared with a surface effect, like photoemission, was a steady goal of these efforts. But the many attempts to incorporate this advantage into useful tubes encountered one or all of three problems: objectionable time lag, objectionable non-uniformities over the target area and, least expected, low sensitivity. Of these, time lag is perhaps the most fundamental. A television system normally requires that each picture be exposed, scanned and erased in one thirtieth of a second. But photoconductivity, once initiated in an insulator, is not easily terminated, particularly at the low light levels consistent with a sensitive pickup tube. As few as one electron out of every 10^{15} atoms need be excited in order to generate a good television signal. A simple computation of the length of time such an electron will wander around before it returns to its ground state, a computation based on the most optimistic values one can assume for an ideal (trap free) insulator, leads to times of a tenth second or longer. Unless some other ways of terminating the life of a free electron or departures from an ideal insulator (such as the introduction of traps) could improve this time constant, the hopes of realizing highly sensitive, fast photoconductive pickup tubes would indeed be sharply limited.

The fact that one free electron per 10^{15} atoms is able to generate useful currents is a measure of the "purity" of the photoconductive effect in insulators. Departures from an ideal crystal need only exceed this ratio to have a significant effect on the currents. But a common departure is the formation of localized states (trapping states) at

* Decimal Classification: 535.3.

crystal imperfections. And the density of such states is found normally to exceed one part in 10^8 . The overwhelming ratio of trapping states to free electrons becomes, then, not a correction factor to be applied after computing the currents in an ideal crystal, but rather *the* starting point for the computation itself.

The variety of photoconductive behavior as reported in the literature generously outstrips the few simple properties that may be deduced from an ideal insulator model. This same variety both expands the choice of properties available for designing sensitive pickup tubes and complicates the models needed to understand the photoconductive processes. Much of the work reported in the succeeding papers was aimed at improving this understanding. To this end, the scanning arrangement of the pickup tube has proved to be a valuable supplementary tool for making basic measurements. Some of the observations on the properties of holes in amorphous selenium were facilitated by the scanning technique.

The first paper, which originally appeared in *Electronics*, is reprinted in order to review the scanning method of observation and to point up the compactness of television equipment which these pickup tubes allow. The second paper discusses some unexpected and almost unique properties of the highly insulating and photoconductive amorphous form of selenium. To the writer's knowledge this is the only well attested case of carriers injected at one end of an insulator being *steadily* drawn through the insulator. The third paper discusses chiefly one member, antimony trisulfide, of a large class of materials whose photoconductive properties are similar and are the more frequently encountered. This class of materials is characterized by its spectral response — it is sensitive only to those wave lengths that can substantially penetrate the interelectrode distance, in contrast to amorphous selenium in which the light need only excite carriers at one electrode. The fourth paper reports some experimental results of measurements on single crystals of cadmium sulfide. The aim was to measure some basic parameters of a photoconductor. It is still not entirely clear how much of the behavior of a photoconductor can be characterized by a few significant constants — nor what constants should be selected. In fact, the last two papers are exploratory in this field. The last of the series outlines formally some of the variety of photoconductive processes that may be expected in semiconductors and treats in detail a particular method for computing the effect of traps.

The emphasis on insulators does not mean that pickup tubes cannot be made with semiconducting materials. A number of moderately sensitive experimental tubes were made using materials whose re-

sistivity was insufficient to provide charge storage. What was stored was a state of increased conductivity. The sensitivity was provided by the inherent time constant of the photoconductive effect. An insulator, however, permits even greater sensitivity to be obtained by combining charge storage with storage of the photoconductive effect and at the same time permits a greater freedom from spurious signal currents in the dark areas of a picture.

This work has been carried on with the close cooperation of H. W. Leverenz and other members of the Chemico-Physics group, particularly S. M. Thomsen, who have prepared, purified and synthesized many of the materials used. The single crystals of CdS and CdSe were grown by S. M. Thomsen and K. F. Stripp by deposition from the vapor phase in modifications of an arrangement described by R. Frerichs.* Many of the results reported have been confirmed and extended by the parallel work of R. B. Janes**, R. W. Engstrom**, B. H. Vine**, and F. S. Veith**. The application of vidicons to various industrial, educational and scientific problems has been steadily urged by V. K. Zworykin and has been effectively demonstrated in equipment designed by R. C. Webb, L. E. Flory and J. M. Morgan. The results of these applications have aided the evaluation and understanding of the photoconductive materials.

* R. Frerichs, "The Photoconductivity of Incomplete Phosphors", *Phys. Rev.*, Vol. 72, p. 594, 1947.

** RCA Victor Division, Lancaster, Pa.

THE VIDICON — PHOTOCONDUCTIVE CAMERA TUBE*†

BY

PAUL K. WEIMER, STANLEY V. FORGUE AND ROBERT R. GOODRICH

Research Department, RCA Laboratories Division,
Princeton, N. J.

Editors' Note: The first commercially successful application of photoconductivity in a television pickup tube is described in this paper, which originally appeared in the May 1950 issue of *Electronics*. It is reprinted here for the convenience of the reader. *RCA Review* is indebted to the publishers of *Electronics* for granting permission to reproduce the paper.

Summary—Simplification of design, high sensitivity and good resolution are available in a new tube having a photoconductive target. Its application results in economy of equipment designed for unattended industrial applications as well as broadcast use.

THE phenomenon of photoemission of electrons has been widely used for the light-sensitive surface of television pickup tubes. This is true for the image orthicon¹ as well as for its predecessors, the orthicon and the iconoscope.

The related phenomenon of photoconductivity has not been employed in any commercially useful pickup tube. However, this application of photoconductivity has by no means been ignored either in the experimental laboratories or in the patent literature. In fact, one of the earliest proposals for a television system envisioned the use of a selenium photoconductive cell in combination with a mechanical scanning disc. Actually, the sluggish frequency response of the selenium cells made them inadequate for this application. Photoemissive cells which became available in the early part of this century were found to be much more suitable.

During the middle 1930's, work on photoconductive targets for television pickup tubes was carried on in this country,² as well as in England³ and Germany.⁴ In these experiments an electron beam similar to that used in the iconoscope scanned the photoconductive target. This mode of operation allowed the possibility of obtaining increased

* Decimal Classification: 621.388.

† Reprinted from *Electronics*, May, 1950.

¹ Rose, Weimer and Law, "The Image Orthicon—A Sensitive Television Pickup Tube", *Proc. I.R.E.*, Vol. 34, No. 7, p. 424, July, 1946.

² Iams and Rose, "Television Pickup Tubes with Cathode Ray Beam Scanning", *Proc. I.R.E.*, Vol. 25, No. 8, p. 1048, August, 1937.

³ Miller and Strange, "The Electrical Reproduction of Images by the Photoconductive Effect", *Proc. Phys. Soc.*, Vol. 50, p. 374, 1938.

⁴ Knoll and Schroeter, "Transmission of Pictures and Signals by Insulating and Semi-conducting Surface", *Phys. Zeitschrift*, Vol. 38, p. 330, 1937.

sensitivity by means of storage. Furthermore, the photoconductor needed to respond to changes in light intensity no faster than thirty cycles per second as compared to the several million per second that is required for nonstorage operation.

None of these experiments resulted in a useful tube able to compete with the iconoscope available at that time. The principal defects were insensitivity, retention of images and spurious spots on the target. Once again photoconductivity for pickup tubes was set aside at least temporarily in favor of photoemission whose processing art was somewhat more advanced.

Work done during the war on photoconductive materials for infrared detectors has served to focus attention on the basic advantages which photoconductivity has to offer to television pickup tubes. It is well known that the light sensitivity obtainable with photoconductive cells greatly exceeds that reported for any photoemissive cells. Whereas a sensitivity of 50 microamperes per lumen (about 0.10 electron per quanta) is considered good for photoemission, tens of thousands of microamperes per lumen (many electrons per quanta) are not uncommon with some photoconductive materials. (An image orthicon employing a photocathode giving 50 microamperes per lumen has an operating sensitivity comparable to that of the human eye.)

If high-sensitivity materials suitable for pickup tube targets could be found, the benefits could be used in two ways. Perhaps least important at present would be the possibility of developing tubes capable of operating at much lower light levels. An improvement of about 10 times over that of the present day image orthicon⁵ is theoretically possible, assuming that on the average, the best photoemitting surfaces are only 10 per cent efficient. Second and more important, any sizeable increase in target sensitivity would permit such simplification in pickup tube design as to open up entirely new fields of application. The electron image section and the electron multiplier, which have been required in the image orthicon for good sensitivity, may be entirely eliminated. The tube is reduced to the basic elements of gun and target. This makes for economy, compactness and simplicity of operation.

In addition, all the tube dimensions may be scaled down, if desired, because the extra target sensitivity is available to compensate for the reduction in target area. It was easily conceivable that a simple, compact and dependable television pickup tube would find many applications in industry, business and in scientific investigations far wider than that of entertainment broadcasting.

⁵ Janes, Johnson and Moore, "Development and Performance of Television Camera Tubes", *RCA Review*, Vol. 10, No. 2, p. 191, June, 1949.

Work on photoconductive pickup tubes has been carried on intensively at RCA Laboratories during the past several years. High-sensitivity materials suitable for targets have been found and many experimental photoconductive tubes of various sizes have been tested. The name "vidicon" has been coined to distinguish these tubes from the photoemissive tubes.

The particular form of vidicon to be described is in an advanced stage of experimental development. It is one inch in diameter and six inches long, and is particularly suited to industrial applications. It appears likely that both larger and smaller forms of vidicons will eventually become available for other applications.

The comparative sizes of the vidicon and the image orthicon are shown in an accompanying photograph. A miniature television camera⁶ employing the vidicon is also illustrated.



Experimental one-inch-diameter vidicon, with the standard commercial image orthicon in the background.

ONE-INCH VIDICON

The cross-sectional diagram of an experimental tube given in Figure 1 shows the relative positions of the gun and the target.

As shown in Figure 2, the photoconductive material is deposited on the transparent conducting signal plate and scanned directly by the electron beam. A uniform magnetic field is used to focus the beam. The velocity of impact of the beam may be either below first crossover as in the orthicon, or above first crossover as in the iconoscope. The video signal is taken from the target by connecting the amplifier to the transparent signal plate. The wall screen shown in Figure 1 provides a uniform field in front of the target, but does not appear in the transmitted picture.

⁶ Webb and Morgan, "Industrial Television System", paper presented at IRE National Convention, New York, March, 1950.



Miniature television camera employing the vidicon pickup tube⁶, monitor in background.

CHARGE-DISCHARGE CYCLE

For purposes of explanation, assume that a low-velocity orthicon-type scanning beam is used. A fixed potential of about 20 volts positive, relative to the thermionic cathode, is applied to the transparent signal plate. The beam deposits electrons on the scanned surface of the photoconductor charging it down to thermionic cathode potential. Although considerable field is thereby developed across the opposite faces of the photoconductor, its conductivity is sufficiently low that very little current flows in the dark.

If a light image is focused on the target, its conductivity is increased in the illuminated portions, thus permitting charge to flow. In these areas the scanned surface gradually becomes charged a volt or

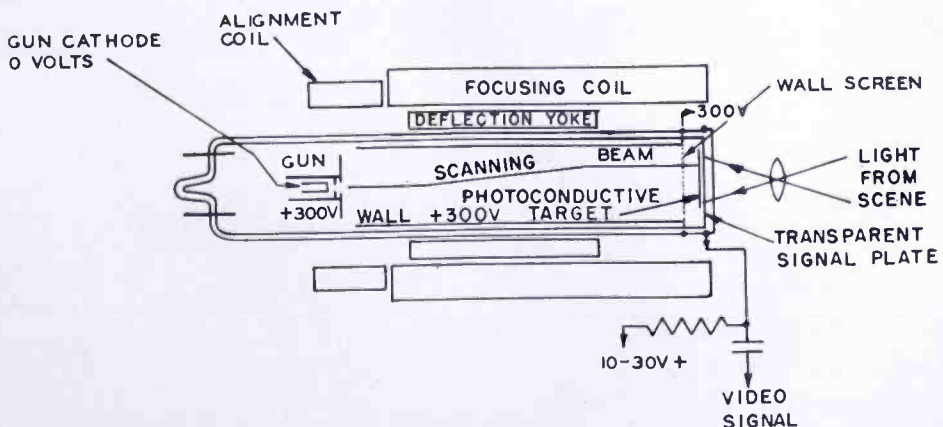


Fig. 1—Cross-sectional diagram of an experimental vidicon photoconductive television pickup tube.

two positive with respect to the cathode during the 1/30-second interval between successive scans.

The beam deposits sufficient electrons to neutralize the accumulated charge, and in doing so generates the video signal in the signal plate lead. It will be noted that the target is sensitive to light throughout the entire frame time permitting full storage of charge.

The charge-discharge cycle is identical to that of the orthicon with the exception that the positive charging effect is achieved by photoconduction through the target itself, rather than by photoemission from the scanned surface. This mode of operation requires that the resistivity of the photoconductive target be sufficiently high that its

time constant exceeds the 1/30-second television frame time. A dark resistivity of 10^{12} ohm-centimeter or greater is satisfactory.

Many materials such as selenium, sulfur, as well as the sulfides, selenides and oxides are known to be photoconducting. Several of these materials when properly processed have been found suitable for pickup tube targets. The spectral response is a function of the material and the processing. Targets which are sensitive to the entire visible range of the spectrum have been made.

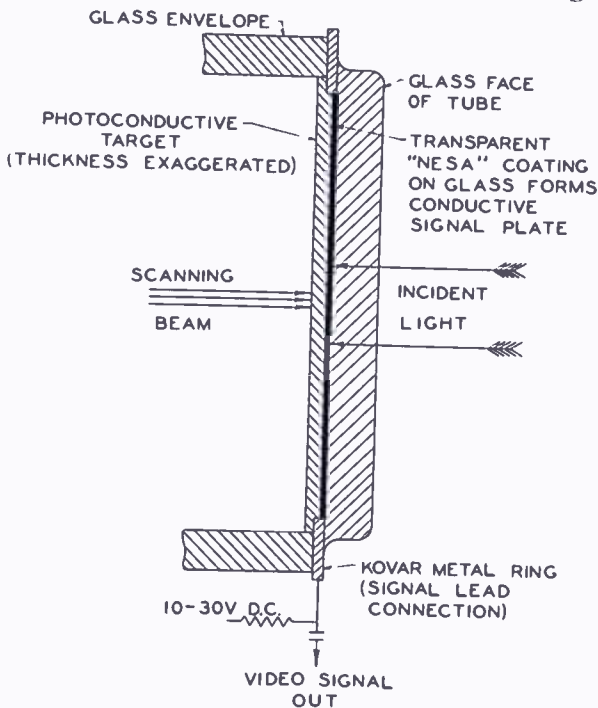


Fig. 2—Detail of the target construction in the experimental photoconductive camera tube.

OPERATING CHARACTERISTICS

Photoconductive targets free from the spurious spots and lag which troubled the earlier workers, have been made. Sensitivities in excess of 1,000 microamperes per lumen are obtainable. Resolution is limited only by the electron optics of the beam while in the image orthicon a fine mesh screen at the target limits resolution.

The one-inch diameter vidicon is capable of resolving more than 600 lines. Under similar conditions the larger image orthicon will give about fifteen hundred lines. The capacity of the target may be made

sufficiently large in any size target that the high light signal-to-noise ratio of the output signal can be as high as needed.

The signal-versus-light curve is linear at low lights as in an orthicon, but with some flattening off at high light levels. In general, the photoconductive targets made to date will not accommodate as wide a range of light levels for a given lens aperture as an image orthicon. For extremely bright illumination on the target, the picture loses contrast without any tendency for unstable charge up as in the early orthicon. An image orthicon under similar conditions would maintain good contrast by virtue of the redistribution of secondary electrons on the picture side of the glass target.



Photograph of picture transmitted by a one-inch vidicon.

In general, pickup tubes with photoconductive targets are simpler in operating adjustments than an image orthicon. The electron image focusing control is completely eliminated, and the target voltage adjustment is somewhat less critical.

The high signal level obtainable at the target removes the need for an electron multiplier whose contribution to spurious spots and shading in the image orthicon has been a steady source of concern. The beam-current adjustment is accordingly less critical. In short, the simplicity of operation of the photoconductive targets combined with

their adaptability for small tubes has made them particularly suitable for equipment designed for unattended industrial applications.

Sufficient satisfactory tubes have been constructed in the laboratory to demonstrate the advantages listed above. However, questions of tube life, allowable temperature limits and reproducibility of results will require additional intensive development before equipment reliable enough for industrial use can be made available.* For example, conditions necessary to ensure targets free of objectionable time lag are still in an experimental stage.

SENSITIVITY OF THE TUBE

A one-inch vidicon possessing a target sensitivity of 300 microamperes per lumen will transmit a noise-free picture with a scene brightness of several foot-lamberts using an $f/2$ lens. Since this light level is less than ordinarily present in most laboratories or factories, special lighting is not required.

It is impossible to compare the relative sensitivities of the vidicon and the image orthicon without specifying at what light level the comparison is being made. At intermediate light levels, with a few foot-lamberts scene brightness, the two tubes will transmit a picture having about the same signal-to-noise ratio. At higher light levels, the vidicon will deliver a higher signal-to-noise ratio than the image orthicon since its target capacity is higher. At lower light levels its signal-to-noise ratio will be inferior to that of an image orthicon with a multiplier.

This follows from the fact that the noise background for the vidicon is the amplifier noise that remains fixed at all light levels, while for the image orthicon it is shot noise in the scanning beam, which may be reduced somewhat for low signal levels. With the development of still more sensitive targets, the vidicon without a multiplier may be expected to exceed the present image orthicon at all light levels.

It will be noted that the elimination of the electron multiplier will require a stronger beam current at the target of the vidicon than in the image orthicon. Assuming the input noise of the video amplifier to be 2×10^{-3} microampere, a target current of 0.2 microampere is required for a signal-to-noise ratio of 100. This current is about ten times that required in the image orthicon.

Some explanation as to why a smaller pickup tube may require a

* Since this paper was written, developmental camera equipment and tubes have been field tested in a variety of industrial applications with encouraging results.

more sensitive target for equal scene brightnesses is in order. If the entire tube and optical system are scaled down in size, keeping the same *f* number lens, the quantity of light in lumens intercepted by the lens is reduced. The output signal of the tube in microamperes is also reduced unless the target sensitivity in microamperes per lumen is increased.

On the other hand, if the lens diameter for the small tube were kept the same as for the large tube, no increase in target sensitivity is necessary. However, for the same angle of view this means a faster or slower *f* number lens. Such lenses, if available at all, are likely to be less highly corrected and more expensive. Thus, in general, the smaller tube will be operated with smaller diameter lenses requiring higher scene brightnesses or more sensitive targets. The gain in depth of focus accompanying the use of the smaller diameter lens may, however, be very useful. Sixteen-millimeter motion picture lenses have been found to be satisfactory.

ACKNOWLEDGMENT

The writers wish to thank V. K. Zworykin and Albert Rose for their continued interest and advice during the course of this work. The construction and testing of tubes has been greatly aided by the cooperation and assistance of A. D. Cope and P. G. Herkart. We are indebted to S. M. Thomsen for preparation of photoconductive materials. The development of miniature camera equipment by R. C. Webb and J. M. Morgan has facilitated the evaluation of tube performance.

PHOTOCONDUCTIVITY IN AMORPHOUS SELENIUM*

BY

PAUL K. WEIMER AND A. DANFORTH COPE

Research Department, RCA Laboratories Division,
Princeton, N. J.

Summary—Photoconductivity in amorphous selenium has recently been utilized in certain types of vidicon television camera tubes. Further studies of photoconductivity in this material by television scanning techniques and by conventional methods have shown it to possess interesting and unusual properties. Sustained photocurrents, generated at one electrode and approaching unity quantum yield, are obtained through evaporated selenium films which are highly insulating in the dark. Hole conduction is predominant over electron conduction, the range of the holes in the selenium exceeding 10^{-3} centimeter. The spectral response is a maximum at 4000-4500 Å and extends into the far ultraviolet. The maximum response does not coincide with the optical absorption edge, as is usually the case; the absorption edge occurs at much longer wave lengths (6000 Å). The time constant for the rise and decay of photocurrent is less than 50 microseconds. Space-charge-limited currents are observed with excess light for low fields across the material. Evidence for primary and secondary photocurrents is discussed. The application of the television scanning method to photoconductive measurements is presented and its advantages and limitations are discussed.

INTRODUCTION

THE element selenium has long been noted for its photoconductive properties. Selenium exists in four polymorphic forms which exhibit different optical and electrical characteristics. The common hexagonal form¹ has a gray, metallic appearance and consists of parallel chains of selenium atoms. Its dark resistivity falls in the semiconductor range (approximately 10^6 ohm-centimeter) and the photoconductivity gives maximum response to red light. Early photoconductive cells employed this form of selenium. Two monoclinic forms, α and β , are red insulating crystals and consist² of Se_8 rings and Se_8 chains. Monoclinic crystals of selenium were used by Gudden

* Decimal Classification: 535.3.

¹ A. J. Bradley, "The Crystal Structures of the Rhombohedral Forms of Selenium and Tellurium", *Phil. Mag.* Vol. 6, No. 48, p. 477, 1924.

² R. D. Burbank, Technical Report XXXVII, ONR Contract N50R1-07801, Laboratory for Insulation Research, MIT, May, 1950.

and Pohl³ for their early studies of primary and secondary photo-current. Amorphous selenium is obtained as a red, glassy film when heated and condensed upon a cold surface. The amorphous form is highly insulating and presumably consists of a random orientation of chain molecules.

Photoconductivity in amorphous selenium had apparently not been studied until comparatively recently.⁴⁻⁶ Earlier references⁷ had stated explicitly that amorphous selenium was not a photoconductor; in fact, the early selenium photocells were very carefully heat treated to convert the selenium from the amorphous to the gray metallic form. It is interesting that photoconductivity in amorphous selenium was discovered, apparently independently, by several separate groups whose primary objective was the development of a picture reproducing device. The application in one case was the electrostatic photography process^{6,8} called "Xerography" while in the other it was the development of a photoconductive television pickup tube.⁹ In each case the photoconductive current flowing between opposite faces of a thin film of selenium could be detected without actually building a selenium photocell, as might have been done with a more conventional approach.

The present paper is principally concerned with the results of photoconductive measurements on amorphous selenium using television scanning techniques. These measurements have shown that amorphous selenium exhibits photoconductive properties which appear to be highly unique among other insulating materials.

MEASURING TECHNIQUE FOR PHOTOCONDUCTIVITY IN INSULATORS

Photoconductivity measurements in highly insulating materials illuminated at one electrode are ordinarily handicapped by space charge accumulating in the material and preventing the steady flow of cur-

³ B. Gudden and R. Pohl, "Über Lichtelektrische Leitung im Selen", *Zeits f. Physik*, Vol. 35, p. 243, 1926.

⁴ P. K. Weimer, "Photoconductivity in Amorphous Selenium", *Phys. Rev.*, Vol. 79, p. 171, 1950.

⁵ M. A. Gilleo, "Optical Absorption and Photoconductivity in Amorphous and Hexagonal Selenium", *Bul. Amer. Phys. Soc.*, Vol. 26, p. 43, February 1, 1951.

⁶ P. H. Keck, "The Electrical Properties of Selenium Coatings", *Jour. Opt. Soc. Amer.*, Vol. 41, p. 53, 1951.

⁷ A. L. Hughes and L. A. DuBridge, *PHOTOELECTRIC PHENOMENA*, McGraw-Hill Book Company, Inc., New York, N. Y., 1932.

⁸ R. M. Schaffert and C. D. Oughton, "Xerography: A New Principle of Photography and Graphic Reproduction", *Jour. Opt. Soc. Amer.*, Vol. 38, p. 991, 1948.

⁹ P. K. Weimer, S. V. Fergie and R. R. Goodrich: "The Vidicon—Photoconductive Camera Tube", *Electronics*, Vol. 23, May, 1950.

rent. This limitation can be reduced by using an alternating applied voltage, but the photocurrents are likely to be small and not convenient for certain types of measurements. The effect of space charge in an insulator can be greatly reduced by using closely spaced electrodes with applied voltages which give a high field across the material. A so-called "sandwich" type photocell is illustrated in Figure 1. One, or preferably both, of the electrodes must be sufficiently transparent to admit the light.

Part of the measurements on amorphous selenium reported in this paper were made using sandwich type cells. Sustained direct photocurrents of the order of 1 microampere per square centimeter were obtained through selenium layers 5 or 10 microns thick with approximately 30 volts applied across the electrodes. The cells were formed

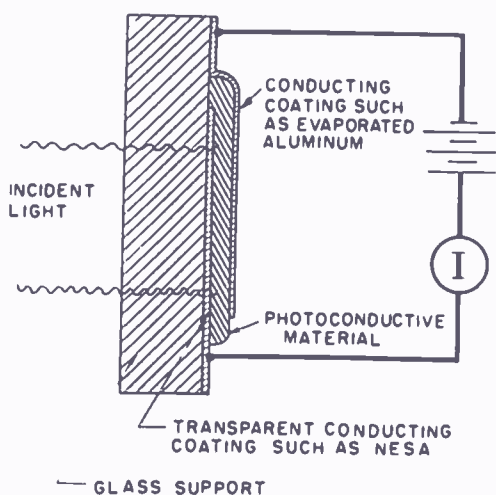


Fig. 1—"Sandwich" type photocell for photoconductivity measurements.

by evaporating selenium onto a glass plate which had been previously coated with a transparent conducting film such as "Nesa"*. The second electrode could be deposited on top of the selenium in various ways, such as, by evaporating a thin layer of aluminum.

An alternative method of measuring photoconductivity of insulators, very similar to the "sandwich" type photocell, is to scan the selenium surface directly with an electron beam. The cell or "target" is formed in the same manner on a Nesa-coated glass plate except that the electron beam itself serves as the second electrode. Figure 2 shows a cross-sectional drawing of a demountable scanning tube with external circuits for measuring photoconductivity. Such a tube is identical to a vidicon television pickup tube except that provision is made

* "Nesa" is a registered trademark of the Pittsburg Plate Glass Co.

for opening the scanning tube to insert the targets which were formed in another evaporating chamber.

Owing to the interest in the development of photoconductive pickup tubes, a large part of the data reported in this paper was taken using the scanning method. This method of measurement has certain advantages and limitations which will be discussed here. Its principal asset is that a detailed point-by-point examination of the entire area of the photoconductor is possible. As the beam is swept over the target area a television signal corresponding to a picture of the target is caused to flow in the wire lead connected to the signal plate. This television picture can be viewed on the kinescope screen where the areas which appear brightest correspond to areas of highest conductivity in

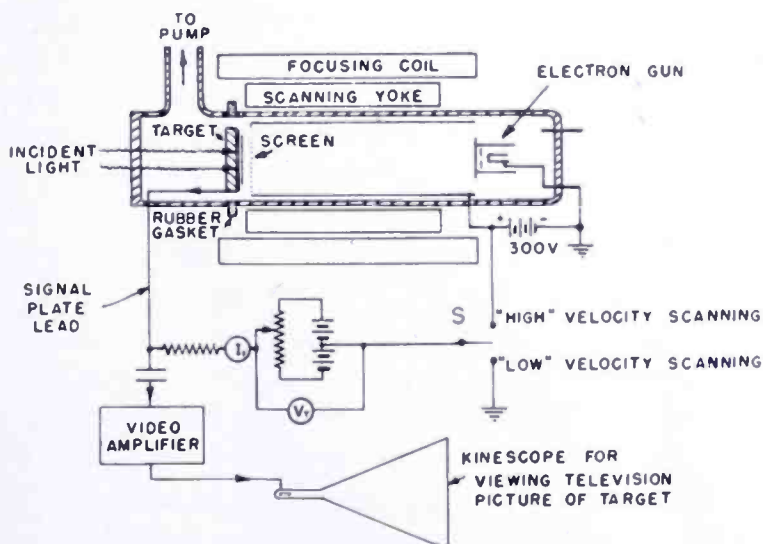


Fig. 2—Demountable television scanning tube with associated circuits for photoconductivity measurements.

the target. When uniform light is projected on the target, the screen is uniformly white and the magnitude of the photocurrent can be read on the direct-current microammeter in the target circuit.

The effect of the beam on the target was to drive the scanned surface to some constant potential whose value depended on the velocity of impact of the beam. For "low-velocity" operation (switch S in Figure 2 at "low" position) the scanned surface was driven to the potential of the gun cathode. For "high-velocity" operation, where the secondary emission ratio of the beam was greater than unity, the scanned surface assumed a potential approximately equal to that of the collector of the secondary electrons (a fine mesh screen operated at 300 volts in Figure 2). The actual potential difference, V_T , appear-

ing across the photoconductor was determined by adjusting the voltage applied to the signal plate. For low-velocity operation the signal plate had to be positive with respect to the scanned surface, but for high-velocity operation it could be either positive or negative.

While the television scanning method of measurement is not necessarily limited to the highly insulating photoconductors, target materials having a dark resistivity in excess of 10^{12} ohm-centimeter were of primary interest. A photoconductive layer of such a material forms a condenser having a time constant in excess of the 1/60-second television scanning period.* That is, in the dark, the potential difference V_T , established across the layer by the beam, will remain substantially unchanged from one scan to the next. If light is allowed to fall on the target, photoconductivity through the film will cause the potential of the scanned surface to drift slowly toward that of the signal plate. When the beam reaches each element of the target, once every 1/60 second, it deposits sufficient charge to return the scanned surface to its dark potential. In practice, the light intensity is so adjusted that the scanned surface cannot change in potential by more than a few volts between scans. This procedure ensures that the beam will be able to deposit sufficient electrons to neutralize the charge which accumulated on the scanned side in the interval between scans.

The principal disadvantage of the scanning method, aside from the considerable amount of equipment required, arises from the inherent current limitation of the electron beam. This limitation was particularly evident in making time constant measurements (See Figure 10).

The possibility that the beam impinging directly on the photoconductor may affect its conductivity can be argued either as an advantage or disadvantage of the scanning method. For example, it was found that a beam of several hundred volts energy causes bombardment-induced conductivity in selenium films of several microns thickness, far too thick to be penetrated by an electron beam of this low an energy. In most insulating materials, bombardment-induced conductivity is not appreciable unless the films are thin enough to be completely penetrated by the beam.¹⁰ Even at low velocity it is conceivable that the beam might inject electrons directly into the conduction band. If this did occur in selenium, the dark currents so induced were negligible. In general, low-velocity scanning measurements have been

* The true television scanning period is 1/30 second. However, for these tests the beam size covered two scanning lines so that the interlaced scanning pattern caused each element to be reached each 1/60 of a second.

¹⁰ L. Pensak, "Conductivity Induced by Electron Bombardment in Thin Insulating Films", *Phys. Rev.*, Vol. 75, p. 472, 1949.

considered more dependable than high-velocity measurements partly because of freedom from bombardment induced conductivity effects and from spurious effects due to secondary emission. Greater care must be taken with the electron optics of a low velocity beam, however, in order to ensure normal incidence of the beam on the target. Without normal incidence the entire scanned surface may not be held at gun cathode potential.

It may be noted that in cases where many materials are to be tested, the scanning method more readily provides considerable qualitative information than the construction and testing of a "sandwich" photo-cell. In the latter, a single pinhole in the thin photoconductor may

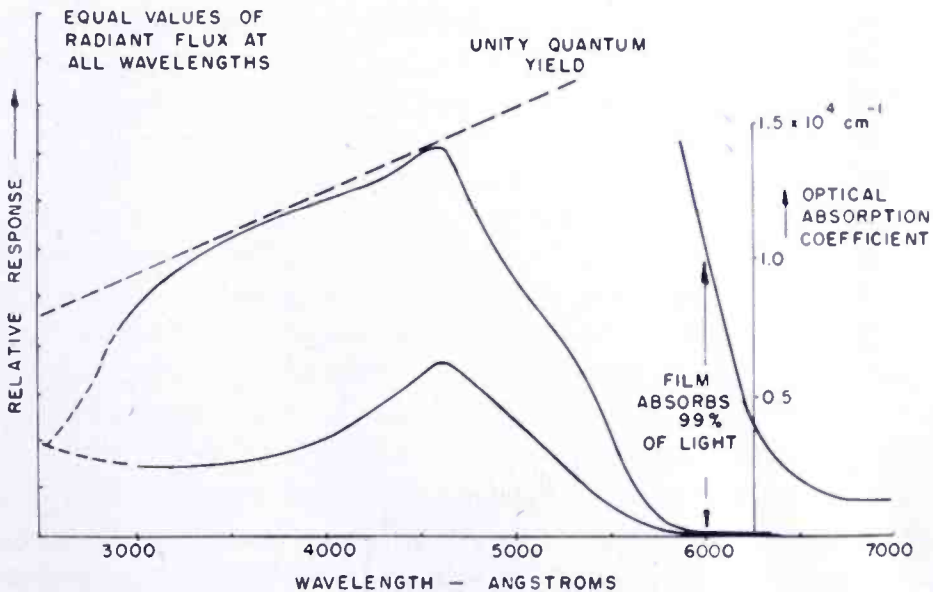


Fig. 3—Spectral response curves for amorphous selenium targets measured by the scanning method. The optical absorption edge is seen to be displaced toward considerably longer wave lengths than the photoconductive response.

make the cell inoperative, while it would appear merely as a tiny white spot on the television screen when scanned by an electron beam.

GENERAL CHARACTERISTICS OF PHOTOCONDUCTIVITY IN AMORPHOUS SELENIUM

The following observations on amorphous selenium are based largely on experiences with many targets tested in the demountable scanning system of Figure 2, or in numerous sealed-off vidicon pickup tubes. Mallinckrodt ultrapure selenium was evaporated or condensed on to Nesa-coated glass targets which were held at room tempera-

ture. The thickness of the selenium films ranged from less than a tenth of a micron (light orange color) to more than 10 microns (a deep red).

Figure 3 shows some response curves for amorphous selenium plotted against wave length of the incident light. Response was measured in terms of the change in current, ΔI , observed when the light was turned off and on. (Ordinarily the dark current was sufficiently small that the photocurrent represented the total current.) The absorption coefficient curve was taken from the literature¹¹ and was in agreement with independent measurements made by R. E. Shrader of these laboratories.

An interesting feature of the curves shown in Figure 3 is that the peak in photoconductivity is displaced so far on the short wavelength side of the absorption edge. In most photoconductive materials¹² the maximum response coincides with the absorption edge. Furthermore, in selenium, sustained photocurrents can be measured for film thicknesses exceeding the range of penetration of the light by a factor of 10 or more. This appears to be a unique feature among insulating photoconductors. In other evaporated sulfides and selenides tested in a similar manner,¹³ the light needs to penetrate substantially the entire thickness of the film in order to give appreciable photoconductivity. The sign of the carrier in selenium is readily determined from the polarity of the applied field. As indicated in the following section the range for holes greatly exceeds that of electrons.

A third point of interest in Figure 3 is that some targets exhibit a quantum yield* approaching unity over a considerable spectral range. In no case has a selenium target, free of impurities, given a quantum yield exceeding unity. This fact is consistent with, but, of course does not prove, that the photoconductivity in selenium is a primary process — i.e., electrons and holes freed by the light move directly to the proper electrodes without influencing other charges in any way which may give rise to additional secondary photocurrents. Further evidence for and against the primary photoeffect is discussed in a later section.

¹¹ A. Becker and I. Shaper, "Über die Lichtdurchlässigkeit des Amorphsen Selens", *Zeits f. Physik*, Vol. 122, p. 49, 1944.

¹² B. Gudden, *LICHTELEKTRISCHE ERSHEINUNGEN*, p. 151, Julius Springer, Berlin, 1928.

¹³ S. V. Fergue, R. R. Goodrich and A. D. Cope, "Properties of Some Photoconductors, Principally Antimony Sulfide", *RCA Review*, Vol. XII, No. 3, p. 335, September, 1951.

* Unity quantum yield means that one light quantum will produce a photocurrent equivalent to one carrier traversing the entire thickness of the target.

EVIDENCE FOR THE PREDOMINANCE OF HOLE CONDUCTION
OVER ELECTRON CONDUCTION

Light of 4000 Å wavelength is reduced to a few per cent of its original intensity in passing through a layer of amorphous selenium 0.1 micron thick. Sustained photocurrents approaching unity quantum efficiency were obtained through layers up to 5 or 10 microns thickness provided that the illuminated side of the film was of positive polarity. The conclusion must be that the photocurrent under these conditions is due to hole conduction and that the range of the holes in the selenium is approximately 10 microns. The potential difference across the target was of the order of 25 to 50 volts giving an internal field of about 5×10^4 volts per centimeter.

Selenium targets operated with low velocity scanning and with the signal plate 25 to 50 volts positive depend on hole conduction for a signal when the light enters the target through the transparent signal plate. If light entered the selenium from the scanned side instead of through the signal plate any photocurrent obtained under the same field condition would have to be electron conduction. When such an experiment is performed with a target 5 microns thick the response to blue light drops by a factor of a thousand from its previous value. This was interpreted as meaning that the electron range was insufficient to penetrate a selenium layer of this thickness. However, if the thickness of the layer is reduced to one micron, comparable sensitivity is obtained for blue light incident on either side. Thus an electron range of approximately one micron may be compared with the hole range of 10 microns.

The predominance of hole conduction over electron conduction has been found also with the sandwich photocells of Figure 1. Here again with thicker layers of selenium the maximum response is obtained when the positive electrode is illuminated.

Electron bombardment-induced conductivity in amorphous selenium shows the same preference for hole conduction as does the photoconductivity. Pensak¹⁴ found that when the positive side of the selenium film was bombarded, conductivity is produced for bombarding voltages too low to penetrate the film. The present work indicates that a 300-volt beam (switch *S* of Figure 2 at "high velocity" position) generates sufficient holes and electrons that a spurious high dark current reading is obtained if the signal plate is biased negative with respect to the scanned surface. This result is not obtained with other

¹⁴ L. Pensak, "Electron Bombardment Induced Conductivity in Selenium", *Phys. Rev.*, Vol. 79, p. 171, 1950.

insulating sulfides and selenides in which the range of the holes is considerably less than in selenium. A thin film of antimony sulfide on top of the scanned surface of the selenium will greatly decrease its dark current for high velocity scanning with the signal plate negative.

EVIDENCE FOR INJECTION OF HOLES INTO SELENIUM

Considerable evidence that the holes may also be injected into the selenium from the supporting electrode or from semiconducting films in contact with the selenium arises from the following observations:

(1) The dark resistance of the selenium film is a sensitive function of the electrode material. This can be demonstrated by coating different areas of the Nesa signal plate with various metals or semiconductors prior to evaporation of selenium over the entire target. The relative difference in dark signal between the adjacent areas provides a sensitive test of minute variations in dark current.

In one test with Sb_2S_3 covering half the Nesa signal plate and selenium evaporated over the whole target, low dark currents were observed on both sides of the boundary, while an exceptionally high dark current was observed at the boundary where the Sb_2S_3 tapered off to zero thickness. This test has a remarkably close parallel in the emission of electrons into a vacuum. A monolayer of thorium on tungsten produces thermionic currents several orders of magnitude higher than either clean tungsten or a thick layer of thorium on tungsten. The present case is one of thermionic emission of holes into a dielectric greatly enhanced by a thin layer of Sb_2S_3 .

Another indication of injection of holes into the selenium from the back plate occurs when the field across the film is increased almost to the breakdown point. An interesting twinkling effect is observed on the television screen indicating intermittent flow of excessive charge at random points in the film. Again the magnitude of the effect for a given film depends on the signal plate material.

(2) A layer of photoconductive material in contact with the selenium, when illuminated, will allow holes to be injected into the selenium. This can be readily demonstrated by making two double layer targets as shown in Figure 4. In (A) a red-sensitive photoconductive sulfide, such as antimony-sulfide, forms an intermediate layer between the selenium and the signal plate. In (B) the same material is deposited on top of the selenium. A red-sensitive material is useful because its response can be identified in the presence of the selenium whose response is almost entirely in the blue-green portion of the spectrum.

When the signal plate is positive with respect to the scanned surface the double layer A responds only to red light, indicating that holes freed by the red light in the sulfide enter the selenium and are carried across the film. The blue light is absorbed in the sulfide without appreciable response. Under the same field conditions the double layer B exhibits only blue response even though the red light penetrates the selenium and frees approximately the same number of holes and electrons in the sulfide as it did in A. This is consistent with the fact that holes are much more readily transmitted in selenium than are electrons. However, if the field is reversed, the same condition now obtains in B as was previously true in A. The holes released by the red light in the sulfide now return to the signal plate through

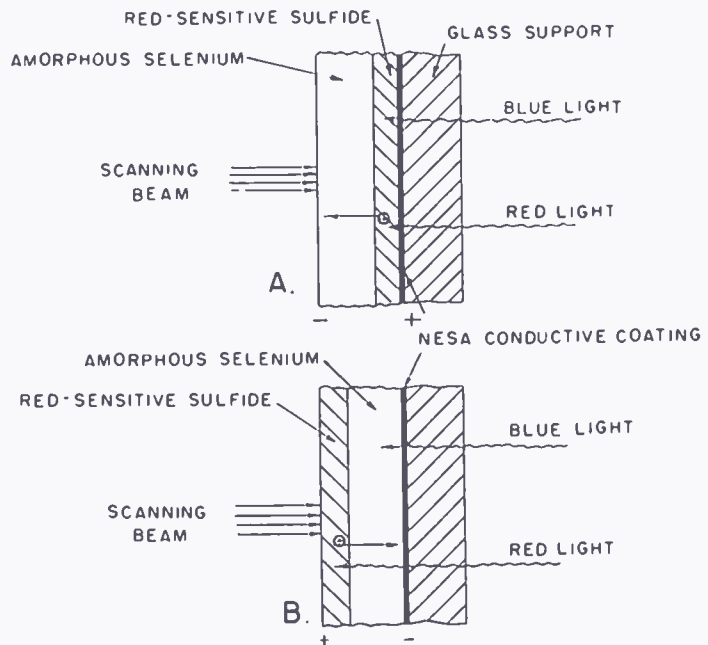


Fig. 4— Two types of double layer targets utilizing the long range of hole conduction in amorphous selenium.

the selenium but the electrons released by the blue light in the selenium are unable to cross the selenium.

Double layer targets of the type shown in Figure 4 offer an interesting possibility in the design of targets for picture reproducing devices. In the target of Figure 4A the requirements of photosensitivity and high resistance for storage of charge are divided between two separate materials. Thus by depositing a layer of insulating material such as amorphous selenium, possessing the property of long range carriers, on top of a photoconductive material having the proper spectral response, a useful target can be made.

MEASUREMENTS

The following measurements were taken mostly by scanning the targets, either in the demountable tube of Figure 2 or in sealed-off selenium-type vidicon pickup tubes. Low-velocity scanning with the signal plate positive was used throughout. Additional tests were made with sandwich type cells. Results quoted here are believed to be typical for pure selenium. Targets formed from impure or contaminated selenium, which behaved quite differently, are discussed in a later section.

a. *Dark Current versus Voltage*

Figure 5 shows a plot of dark current versus voltage across a selenium film approximately 10 microns thick. The target thickness and light levels employed were typical values encountered in operation of the selenium-type vidicons.

The dark current curves in amorphous selenium were characterized

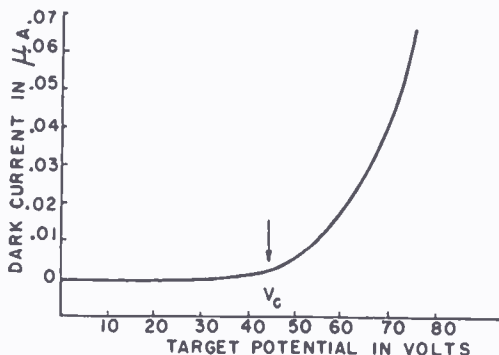


Fig. 5—Dark current plotted against the voltage applied across the amorphous selenium layer.

by a very slow rise in current with voltage until a critical voltage V_c was reached beyond which the rise was much more rapid. In television operation of this type of vidicon the target voltage was set just below V_c .* At potentials higher than V_c , the dark current was sufficiently high that the scanning beam generated a video picture of the target itself. Figure 6 is a photograph of the kinescope for target potentials below and above V_c . The white spots correspond to areas of very much higher dark current than the surrounding area. Spots which were not visible at target fields below V_c , become quite prominent at more and more positive potentials above V_c .

The high dark-current spots are oriented sometimes at random and sometimes in circular patterns which may be correlated with marks made in cleaning the glass target prior to deposition of the selenium.

* The spectral response curves of Figure 3 were taken under these field conditions.

It is likely that in these areas a partial crystallization of the selenium to the monoclinic or hexagonal form has occurred. The fact that most of the spots do not show at target voltages below V_c indicates that the crystal size must represent a small fraction of the total thickness of the amorphous layer. The high current in these areas must be carried in the amorphous selenium by holes which are probably injected by the high field into the amorphous layer from the higher-conducting crystals.*

The dark current plotted in Figure 5 is averaged over the entire scanned area of the target including both the spots and the surround. It is difficult to determine what fraction of the rapid rise for voltage

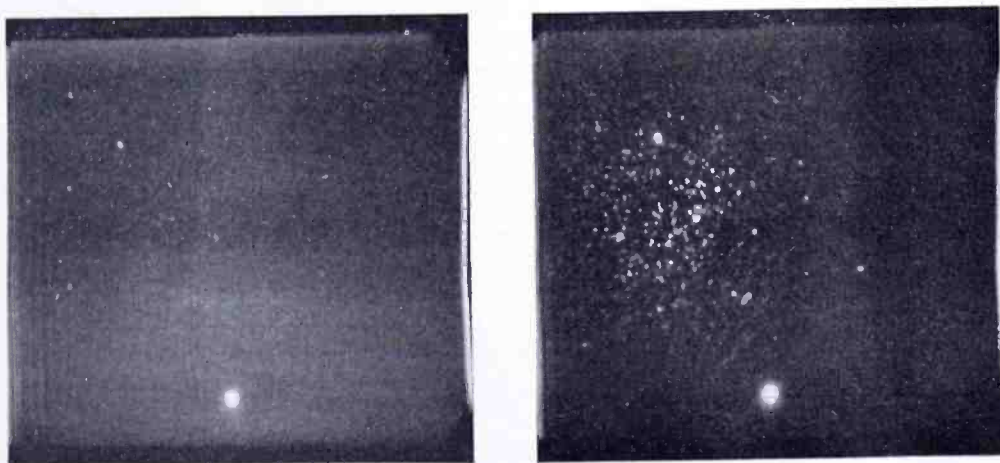


Fig. 6—Photograph of a kinescope picture of an amorphous selenium target in the dark for target potentials below and above the critical potential V_c (see Figure 5). The higher field (right) shows many more conducting spots than the slightly lower field (left).

greater than V_c is due to the spots as compared with the surround. The television picture certainly indicates that at these high fields the selenium cannot be considered as a homogeneous layer.

b. Photocurrent versus Voltage

The total target current for several values of incident light are plotted in Figure 7 as a function of voltage across the selenium layer. At low light levels the current increases nearly linearly with voltage. At excessively high light levels the current increases approximately

* An observation supporting this statement is that a double layer target consisting of amorphous selenium in contact with a metallic selenium layer has a much higher dark current than the same film in contact with the Nesa.

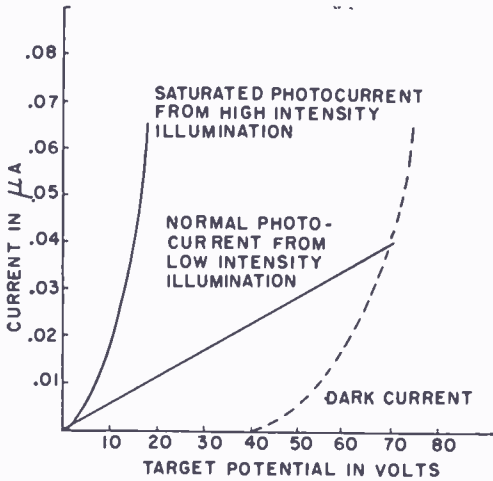


Fig. 7—Photocurrent plotted against target voltage for two levels of illumination.

as the square of the voltage. This variation of current with voltage is consistent with space charge limited currents.¹⁵

Considerable attention has been given to determine whether or not for moderate light levels the current-versus-voltage curves show any saturation at the high voltage end. Such a leveling off of current with voltage has been found in only a few targets. At high target voltages the rapidly increasing dark signal makes current measurements difficult. For measurements using an electron beam for one electrode, care must be taken to ensure that inadequate beam current does not cause a false leveling off of signal.

c. Photocurrent versus Light

Signal current versus incident light is plotted in Figure 8. At low lights and high target voltages the curve is of the form $I \propto L^n$ where n has a value in the neighborhood of 0.9. The selenium-type vidicons are ordinarily operated under these conditions. For lower target voltages and excessive high-light levels the signal current saturates

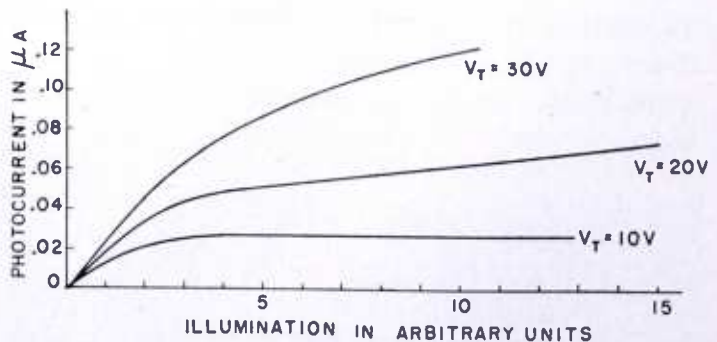


Fig. 8—Photocurrent in amorphous selenium plotted against incident light intensity for three different target voltages.

¹⁵ N. F. Mott and R. W. Gurney, *ELECTRONIC PROCESSES IN IONIC CRYSTALS*, Oxford Press, Second Edition, 1948.

with light. The photocurrent under these conditions is believed to be space-charge limited, as evidenced by the square law current-versus-voltage curve plotted in Figure 7.

The nearly linear signal-versus-light curve, for selenium with weak illumination, is to be contrasted with similar curves for antimony sulfide where the exponent n is nearer 0.5 volt than unity.

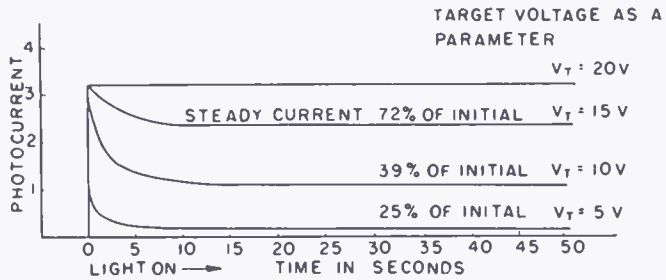
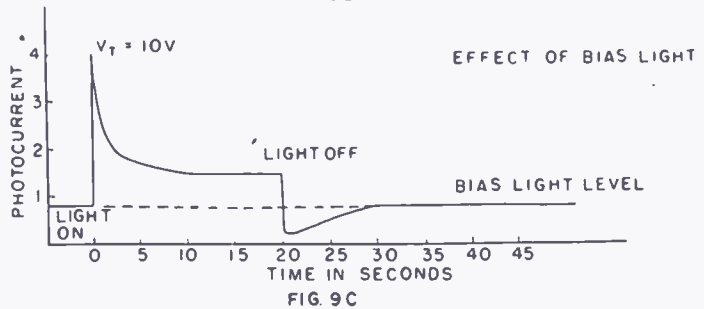
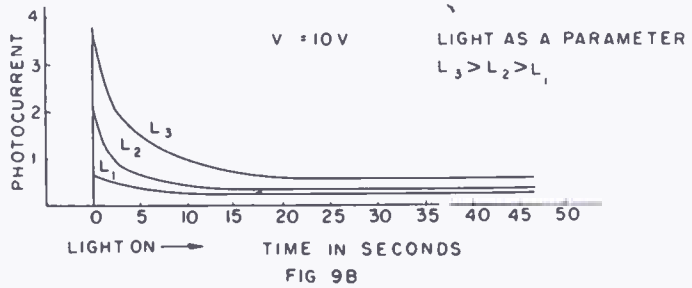


Fig. 9—Fatigue in photocurrent in amorphous selenium for various target voltages and light levels. The percentage “slumping off” of current from its initial value is largest for low target voltages and most intense illumination.



d. Photocurrent versus Time

In Figure 9a, a fatigue* effect in the photocurrent, obtained initially when the light is flashed on, is shown in a plot of photocurrent versus time. At low target fields the current drops by more than 50 per cent from its initial value. As the field is increased, the fatigue effect diminishes and becomes very slight for target voltages approaching V_c , the so-called critical field. For a given target voltage the effect

* The term “fatigue” is used in this paper to describe a slumping off of current. The effect is reversible and is believed to be electronic in nature, rather than indicating any permanent structural or chemical change in the photoconductor.

is more prominent for higher light levels (Figure 9b). A constant bias light was left on for the curve in Figure 9c. The time taken to recover to the initial steady value after the intermittent light was flashed off was comparable with the time taken to reach a steady value when it was flashed on.

In television pickup tube operation the fatigue effect plotted in Figure 9 gives rise to a negative image of previous scenes being superimposed on the transmitted picture. By operating with the target voltage near V_c this "negative after-image" can be made sufficiently small in many tubes as to be completely unnoticed. In other tubes the effect cannot be eliminated even at high target voltages. In the latter case the fatigue may be ionic in nature rather than electronic. Its

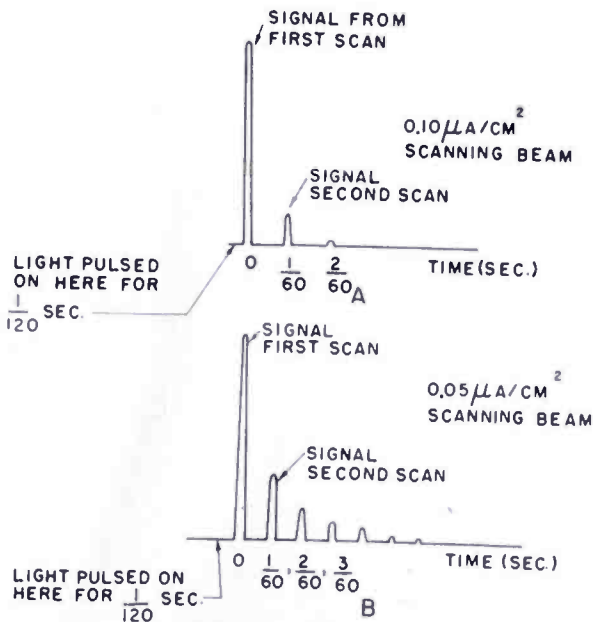


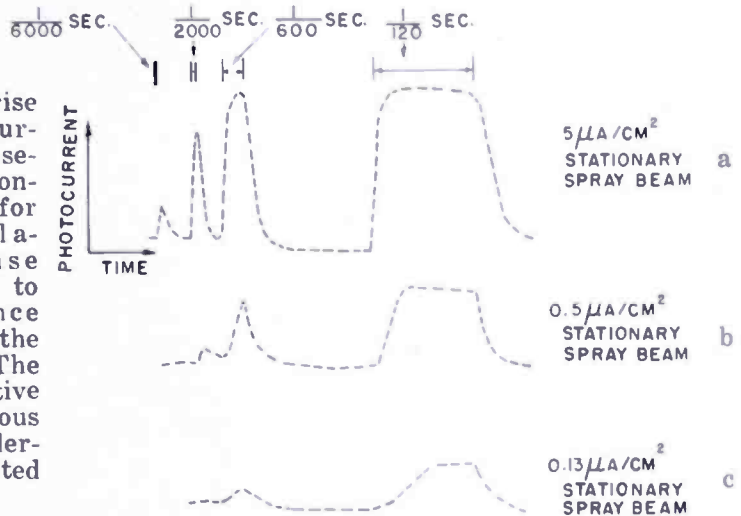
Fig. 10—Signal taken off the target of a selenium-type vidicon in successive scans after the light has been cut off. Lack of complete discharge in one scan gives rise to "smearing" of moving images. Such smearing could be caused by inadequate beam current or by photoconductive lag. As indicated in Figures 11 and 12, the photoconductive time constant in selenium is much less than a television scanning period. The incomplete discharge shown here arises from the resistance of the beam. The velocity distribution of the electrons make the discharge of the target less effective for small signals.

magnitude appears to be a function of tube processing and can be exaggerated by addition of certain impurities to the selenium.

The rate of rise and decay of photocurrent was studied using a slotted wheel to produce light pulses having a duration of $\frac{1}{120}$, $\frac{1}{600}$, $\frac{1}{2000}$, and $\frac{1}{6000}$ second. First tests were made with a selenium-type vidicon operated with a defocused stationary low-velocity electron beam instead of the customary well-focused scanning beam. The scanning process would have limited the time constant measurement to units of $\frac{1}{60}$ second, the interval between successive scans.* The

* Figure 10 shows the signal taken off a conventional vidicon operating in normal manner during successive scans after a uniform light was flashed off. In the absence of photoconductive lag, an ideal beam should completely remove the charge in one scan.

Fig. 11—Apparent rise and decay of photocurrent in amorphous selenium using a stationary defocused beam for discharge. The relatively slow response shown here is due to the beam resistance which increases as the signal is reduced. The true photoconductive response of amorphous selenium is considerably faster as indicated in Figure 12.



beam was defocused in order to cover sufficient area of the target to give measurable photocurrent without requiring excessive light intensities. The rise and decay curves obtained from an oscillograph trace are plotted in Figures 11a, b and c. These curves do not represent the true photoconductive response of amorphous selenium but are too slow owing to resistance limitations of the low-velocity beam. It is well known that the inherent spread in the electron velocities would make the beam less and less effective as the scanned surface approaches its equilibrium potential. Calculations based on an assumed exponential beam current versus target voltage curve show that the observed time constant should be inversely proportional to the target current quite independently of any photoconductive lag. The apparent increase of time constant with reduced signal current is shown in Figure 11.

In order to eliminate the effect of the beam in the time constant measurements, a sandwich type photocell was operated with a similar toothed wheel containing one additional slot corresponding to a 1/20,000-second light pulse. The response curves plotted in Figure 12 are very much steeper, indicating at least a 60 per cent response for the 1/20,000-second pulse. The true photoconductive response of

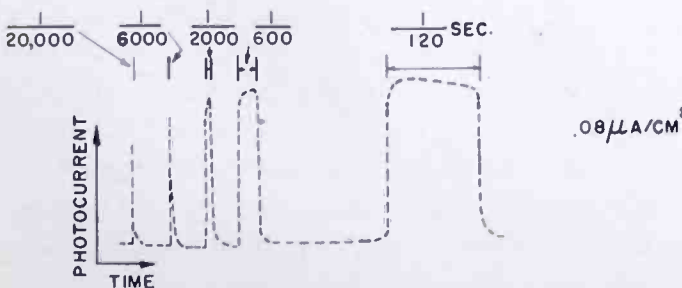


Fig. 12 — Rise and decay of photocurrent in an amorphous selenium sandwich photocell for light pulses of various lengths. The time constant of 50 microseconds indicated here can only be taken as an upper limit.

amorphous selenium may be still faster than this owing to limitations of the experimental setup. No change in response was noted for variations in light level by a factor of 50 or of target voltage by a factor of 5.

EFFECT OF TEMPERATURE

A shift of the absorption edge^{5,11} and photoconductive response⁵ in amorphous selenium toward shorter wave lengths with decreasing temperature has been reported in the literature. In the present work photoconductivity in amorphous selenium has been measured over a temperature range from zero degrees centigrade up to about fifty degrees. For temperatures higher than this, irreversible changes occur in the targets owing to the greatly accelerated crystallization. After a fifteen minute bake at 80°C, for example, measurements at room temperature indicate a greatly increased dark current, time constants of several seconds or more, enhanced red sensitivity and a profusion of conducting spots. These changes in electrical characteristics occur before sufficient crystallization has occurred to change the visual appearance of the amorphous layer. Prolonged heating will, of course, entirely convert the red selenium to the gray metallic form.

Qualitatively, a lowering of the temperature from room temperature to around 0°C causes the direct-current response to fall to very low values. Although the initial response when the light is flashed on is comparable to that obtained at room temperatures, the fatigue effect at low target fields is greatly exaggerated. In Figure 13 photocurrent is plotted against temperature for very high light levels and low target fields as in the lower curve of Figure 8. The exact shape of these curves cannot be relied on, since they varied from tube to tube and depended strongly on past history, etc.

LIFE MEASUREMENTS

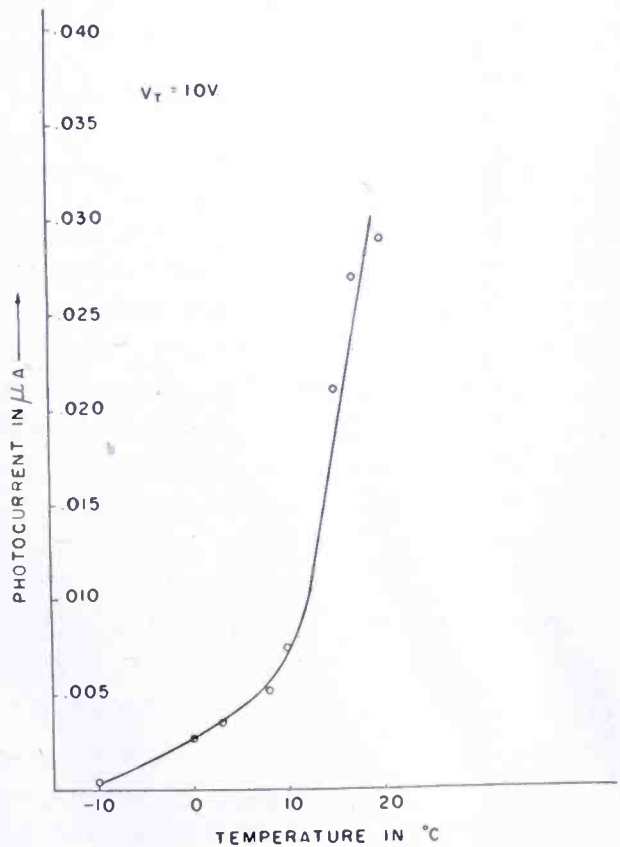
The tendency for amorphous selenium to convert to the hexagonal metallic form would be expected to set a limit on the useful life of devices employing this form of selenium. The rate of conversion is quite slow at room temperature: selenium-type vidicons tested two years after their manufacture have shown only a few more converted spots than when new. However, on life test after several hundred hours of continuous operation at 30-35°C, experimental targets have shown an increased number of spots, higher dark current and in some cases, objectionable time lag. This rate of deterioration can be speeded up or slowed down by raising or lowering the temperature. It also

depends upon other processing factors which might affect crystallization rates.

EFFECT OF IMPURITIES

The deliberate or accidental addition of impurities to amorphous selenium changes its characteristics considerably from those described above. Antimony, cadmium, and cadmium sulfide have been evaporated simultaneously with selenium giving targets whose composition was largely selenium but with an estimated few per cent of impurity.

Fig. 13—Photocurrent measured with low target voltage, intense light plotted against temperatures for an amorphous selenium target.



An attempt was made to ensure a homogeneous distribution of the impurity by "flash" evaporation of the finely powdered constituents or by use of shutters with separate evaporator boats.

The results were not reproducible quantitatively, but the following trend was clearly evident:

(1) Sensitivities greatly increased over the pure form, reaching in some cases many thousands of microamperes per lumen. Quantum yields exceeding unity are encountered here.

(2) Dark current increased by a factor of 10 to 100.

(3) The time constant is increased to many seconds. Fatigue effects also were observed. An area, previously illuminated with light, shows temporary reduction of dark current when the light is cut off, similar to that illustrated in Figure 9c for normal selenium with a bias light.

(4) Spectral response may remain blue-sensitive or in some cases have greatly enhanced red response.

The high quantum yields indicate that the additional photoresponse must be of secondary nature. The undiminished blue sensitivity for thick targets shows that the impurities did not prevent the holes from passing across the film. In another target, where the impurity was germanium, no increase in sensitivity over normal selenium was observed, but instead the fatigue effect was enhanced.

DISCUSSION

The evidence for long range carriers in amorphous selenium, originating at or near the transparent signal plate and passing across the relatively thick film, is quite definite. It is equally clear that the polarity of the charges exhibiting the longest range is positive, indicating hole conduction. The observed range of holes is longer than would be expected, either from what is known about the molecular structure of amorphous selenium, or from experience with other evaporated insulating photoconductors.

These results, of course, do not necessarily imply that amorphous selenium is so free of traps that all of the holes are able to traverse the entire distance without interruption. The reduction of photocurrent with temperature indicates that a large fraction, if not all, of the holes are trapped at various times in transit and depend upon the temperature for release to give sustained photocurrents.

The fatigue effect illustrated in Figure 8 is undoubtedly caused by the partial filling of these traps. The space charge of the trapped holes reduces the interior field, lowering the current from its initial value. The higher the applied field, the less the effect of the trapped charges and the less the fatigue in current. Similarly, for a given temperature and applied field, a higher light level will mean more trapping and more fatigue.

The reduced range of electrons as compared with holes presumably indicates a greater density or depth of electron traps as compared with hole traps. Very little attention has been given to the photoconductive properties of selenium measured under field conditions which require electrons for conduction.

The exact process by which the incident light excites holes in a thin layer along one face of the selenium is not clear from the data. For a primary process, the absorption of each quantum of light would presumably raise an electron from the filled band to the conduction band, the resulting vacancy or hole would be carried across the selenium, and the excited electron would enter the nearby transparent signal plate. On the other hand, it may be that the excited electron can remain near the interface sufficiently long that it can attract many holes from the signal plate into the selenium. These additional holes would be carried by the field across the selenium and would produce a so-called "secondary" photocurrent. The primary process would not permit a quantum yield greater than unity, while a secondary process would permit a photocurrent equivalent to many charges per light quanta.

For impure selenium there can be no doubt of the existence of secondary photocurrents resulting perhaps from the above-described process or some other. For pure selenium, on the other hand, the primary process is a possibility although the evidence for it is not clean-cut. Good evidence for primary photocurrent would be for the photocurrent-versus-voltage curve to saturate at unity quantum yield. The measured quantum yields for uncontaminated selenium have ranged from a few tenths up to unity for normal target voltages. However, the photocurrent-versus-voltage curves have not consistently shown saturation at high target voltages. For voltages much greater than V_0 (see Figure 5) the dark current becomes very high and measurements are difficult. At these higher voltages, where large hole currents are being drawn out of the signal plate into the selenium, it seems quite likely that additional holes would be drawn out by the field of the electrons excited by light. Thus, a bona fide primary photoeffect for low target voltages might very well be enhanced by a secondary photoeffect at high voltages. If such is the case, it prevents the observation of saturation at high voltages as a test for primary photoeffect.

The linear photocurrent-versus-voltage curve at low light levels could occur with either primary or secondary photocurrents, but is suggestive of the former. In this case the light produces electrons and holes throughout a thin layer near the signal plate. The number of holes drawn out of this layer would be proportional to the applied field in the voltage range below saturation. The remaining electrons and holes can be disposed of by recombination. Since a simple bimolecular recombination would lead to a half-power signal-versus-

light curve instead of the nearly linear curve observed, some additional mechanism such as trapping¹⁶ needs to be introduced.

The comparatively rapid rise and decay of photocurrent in selenium could be obtained with either primary or secondary photoeffect. There was no indication that the observed time constant depended on target voltage or transit time of the holes across the selenium. This may indicate that the frequency response is set by the time for recombination of the holes and electrons in the thin layer near the signal plate.

CONCLUSIONS

The photoconductive properties of amorphous selenium studied in this paper may be summarized as follows:

(1) Evaporated selenium films, highly insulating in the dark, will permit sustained currents to flow, approaching unity quantum yield, when illuminated by light strongly absorbed at one electrode.

(2) The spectral sensitivity extends from 5500 Å to the far ultraviolet. The peak response, occurring near 4000 Å does not coincide with the absorption edge at 6000 Å.

(3) Hole conduction is predominant over electron conduction. The range of the holes with an applied field of 5×10^4 volts per centimeter is of the order of 10^{-3} centimeter, as compared with 10^{-4} centimeter for electrons.

(4) Evidence for injection of holes into the selenium from the supporting electrode or from another photoconductor is presented.

(5) The rise and decay of the photocurrent has a time constant of less than 50 microseconds.

(6) Fatigue effects in the photocurrent are observed and shown to be consistent with space-charge limitations.

(7) Signal-versus-light curves are nearly linear for low incident light levels, but saturate with intense light and weak applied fields.

(8) Signal-versus-target voltage curves increase more or less linearly for low light levels, but increase as the square of the voltage for intense light, consistent with space-charge-limited current.

(9) Photocurrent decreases with decreasing temperature indicating the presence of traps.

(10) Primary photocurrent is believed to account for at least part of the photoconductivity in the purest selenium targets. Strong secondary photoeffects are encountered when impurities are added.

¹⁶ A. Rose, "An Outline of Some Photoconductive Processes", *RCA Review*, Vol. XII, No. 3, p. 362, September 1951.

PROPERTIES OF SOME PHOTOCONDUCTORS, PRINCIPALLY ANTIMONY TRISULFIDE*

BY

S. V. FORGUE, R. R. GOODRICH AND A. D. COPE

Research Department, RCA Laboratories Division,
Princeton, N. J.

Summary—The electrical properties of a photoconductor necessary to fit it for use as a television pickup tube target material are outlined. Red antimony trisulfide has been studied extensively and found to satisfy many of the requirements. Plots of the variation of dark current with voltage and of photocurrent with light for this material are given. Its spectral response, sensitivity and quantum efficiency are discussed. These and other physical properties of antimony trisulfide pertinent to its use as a photoconductor may be affected by impurity addition, heat treatment and method of preparation. It has been found possible to form a single photoconductive layer from combinations of two different sulfides or selenides having useful electrical properties intermediate between those of the constituents.

INTRODUCTION

TWO observations have consistently stood out in the application of sulfide and selenide compounds as photoconductive target materials in television pickup tubes. One is the infrequency of making a target which will not produce a transmitted picture of some kind, and second, the difficulty of making a target which will give a picture which simultaneously fulfills all of the several rigid requirements dictated by modern television applications.

The most important of these requirements are sensitivity, freedom from time lag, uniformity, and a reasonable operating life. In addition particular applications for a pickup tube require certain spectral response characteristics and stable operation over a range of temperatures.

It is not difficult to make photoconductive targets, usually of relatively low or intermediate sensitivity, employing materials having insufficient resistivity to permit charge storage type of operation. These targets operate by storing a change in resistivity. Storage operation permits most effective use to be made of the photoproperties of a material, and thus leads to tubes of the highest possible sensitivity. In this operation the charging effect of the photoaction at any point on the target takes place continuously throughout the frame time.

* Decimal Classification: 535.3.

For a frame time of $1/30$ second, this specifies a material resistivity of at least 10^{11} ohm-centimeter. However, an even higher resistivity is preferable to permit greater freedom from spurious signals in the dark areas of the picture. For these reasons the photoconductivity investigation has been carried out on materials which fall substantially within the classification of insulators.

To avoid visible trailing or lag, it is necessary that each picture be erased in a frame time. Both capacity and photoconductive lag effects are encountered. To eliminate the former, it is necessary that the product of beam resistance and target capacitance be less than a frame time.¹ The photoconductive lag has been a much more elusive problem. In its less objectionable forms, it has appeared as a faint residual lag following a rapid initial decay. Photoconductive lag has been found to vary with impurity content, processing, and operating conditions.

Evaporation has proved to be one of the most effective methods of preparation of a target layer from the standpoint of uniformity. Very uniform, nongrainy targets have been made by this method. While in some cases it has been possible to obtain reasonably uniform targets by other methods such as sublimation, settling, precipitation, or spraying, the precautions necessary to insure uniformity have been considerably more involved than in the case of evaporation. For this reason all of the measurements to be described below will be associated with evaporated layers unless otherwise specified.

As is the case with most photocell applications, the use of photoconductors in pickup tubes calls for a reasonably long operating life. A long life is intimately associated with reversible electronic processes as opposed to nonreversible ionic processes. The materials to be described below are believed to show predominantly electron conduction. While most of the measurements which follow were taken with the television pickup tube application in mind, they have, at the same time, general interest in illustrating the photoconductive properties of the materials.

Figure 1 shows the electron beam scanning arrangement in which the photoconductive materials were tested. The beam can scan the target at either low or high velocity, that is either below or above unity secondary emission ratio, depending upon the relative voltage applied to the transparent conducting signal plate. In the absence of light the beam will bring the scanned photoconductive surface to about

¹ For a discussion of the mechanism of beam discharge of the target capacity see S. V. Forgue, "The Storage Orthicon and Its Application to Teleran", *RCA Review*, Vol. VIII, No. 4, pp. 633-650, December, 1947.

cathode (ground) potential in the low-velocity case or to approximately collector screen potential in the high-velocity case. Light will bring the scanned surface toward the signal plate potential. A video signal is generated when the beam returns the surface to either the cathode or screen potential.

At high velocity the signal plate may be biased either positive or negative with respect to the collector screen. In both cases the low-velocity secondary electrons act as a resistance to restore the target surface to collector potential. At low velocity, the signal plate may, of course, only be biased positively to the scanned surface maintained at cathode potential by the beam. While the photoconductive properties have usually been the same under these several conditions of operation, some interesting and significant exceptions have been observed.

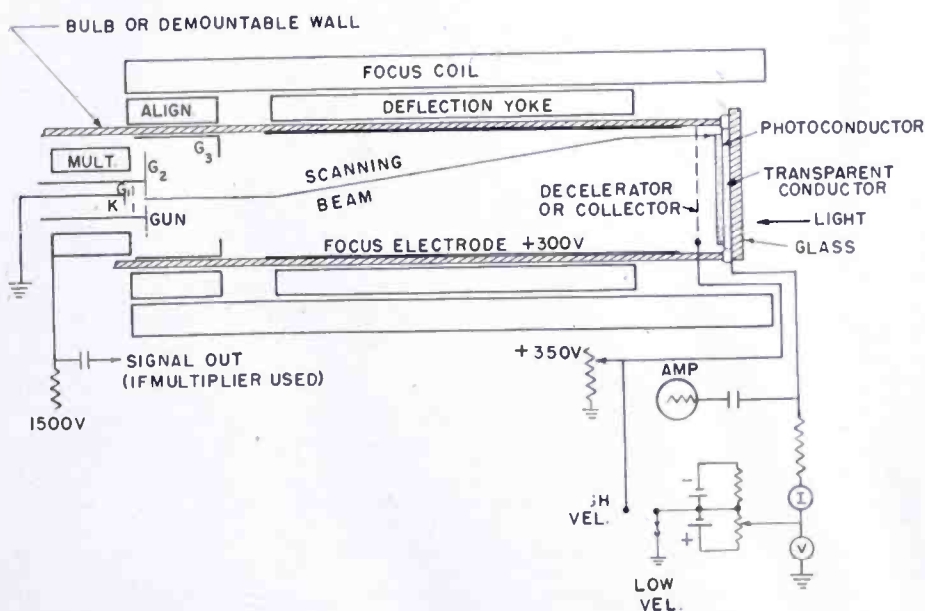


Fig. 1—Scanning arrangement for test of photoconductors.

PHOTOCONDUCTIVE PROPERTIES OF EVAPORATED ANTIMONY TRISULFIDE LAYERS

Resistivity—Dark Current versus Voltage

One of the photoconductive materials which has given much promise toward filling the several requirements mentioned above is red antimony trisulfide (Sb_2S_3). Electron diffraction analysis* has shown evidence of microcrystallinity in evaporated layers of this material. Differences in crystal structure between the evaporated layers and

* The electron diffraction analyses were made by S. G. Ellis of these laboratories.

the raw material before evaporation have also been shown. The normal x-ray diffraction analysis** has indicated no evidence of crystallinity. This may be interpreted as evidence of a large amorphous content or very small crystal size. The photoconductive properties may be widely varied with processing and impurity introduction. Suitably prepared layers have produced targets with very useful characteristics for several pickup tube applications. In its normally evaporated form antimony trisulfide has a dark resistivity of about 10^{11} to 10^{13} ohm-centimeter. Added impurities can shift the resistivity in either direction. It will be noted that this value is sufficient to allow charge storage type of pickup tube operation mentioned earlier, with the resulting possibility of high operating sensitivity.

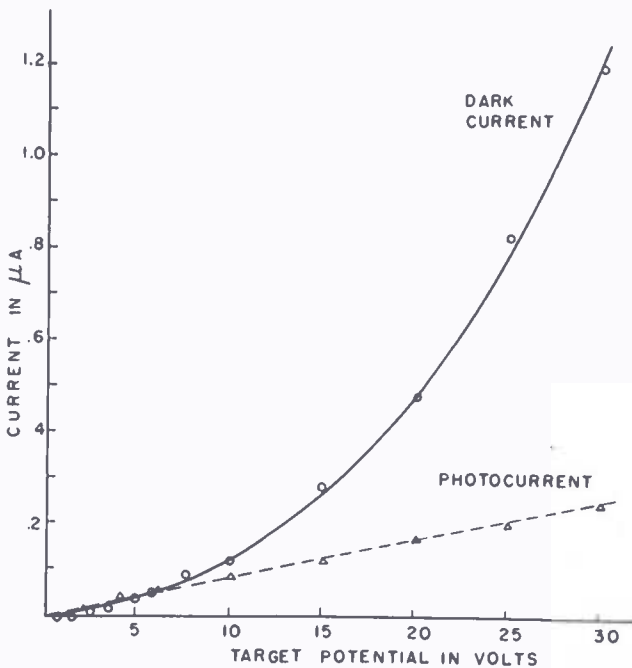


Fig. 2 — Dark current and photocurrent versus potential for antimony trisulfide target.

The dark resistivity has been found to decrease with voltage as shown by the following typical plot of dark current through a layer of antimony trisulfide versus voltage across the layer (see Figure 2). As a typical layer thickness is of the order of 0.1 mil (2.5 microns), a voltage of 100 volts represents a very high gradient, namely 400,000 volts per centimeter. Since the dark current-voltage curve has frequently been of the form $I \sim V^2$, it is possible to interpret this current as a space-charge-limited current generated by a thermal reservoir of carriers either at the signal plate or scanned surface. This form of curve is particularly significant because the photocurrent versus voltage as shown in the same figure is ohmic.

** The x-ray diffraction analyses were made by I. J. Hegyi of these laboratories.

Photocurrent versus Light Intensity

It is an advantage for a television pickup tube to have a current output versus light input relationship that is substantially less than linear. This allows a large range of light intensity to be accommodated by the tube. For example, a current-versus-light curve having an exponent of 0.5 will allow a 100-to-1 range of light intensities with a 10-to-1 range of photocurrent.

The exponent representing the current-light characteristic for antimony trisulfide has fallen within a range near 0.5 (i.e., square root response). The curves of Figures 3 and 4 are current-light plots for a typical antimony trisulfide target at different voltages across



Fig. 3—Photocurrent as a function of illumination for an antimony trisulfide layer with target potential V_T as a parameter.

the film. It is to be noted that the exponent of the curves does not vary with target voltage.

Optical Transmission and Spectral Response

It has been found that the range of carriers in antimony trisulfide is generally short compared with the layer thickness when this thickness is great enough (above two microns) to avoid capacity time lag effects. This means that light of a given wave length must substantially penetrate the layer for photoconductivity to take place. As expected, antimony trisulfide exhibits photoconductivity peaked in the red, which penetrates the target, and is very low in the blue which is

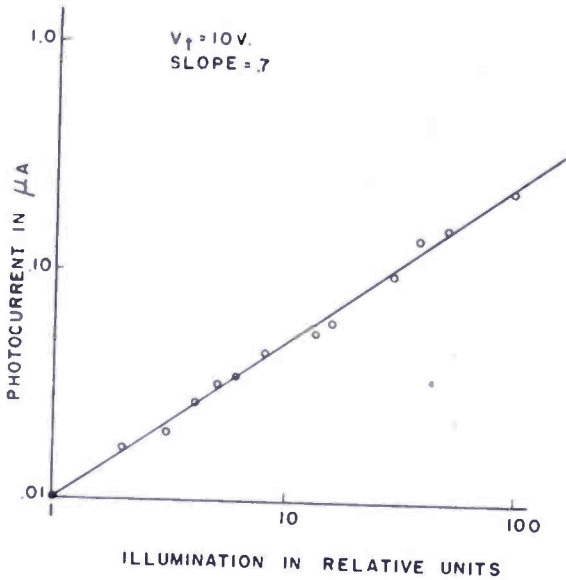


Fig. 4—Photocurrent as a function of illumination for an antimony trisulfide target. Slope of the log-log plot indicates current varies with 0.7 power of light intensity.

highly absorbed in a thin layer at the illuminated face of the material. As layer thickness is decreased, however, the light transmission shifts from red to yellow and the photoconductivity peaks in the green with only a slightly lower response in both the blue and red. A very thin layer will give a peak response in the blue. Here the red efficiency is very low because of the low absorption of this wave length by the thin layer. Figure 5 shows the response versus wave length, along with the corresponding light absorption versus wave length curve.

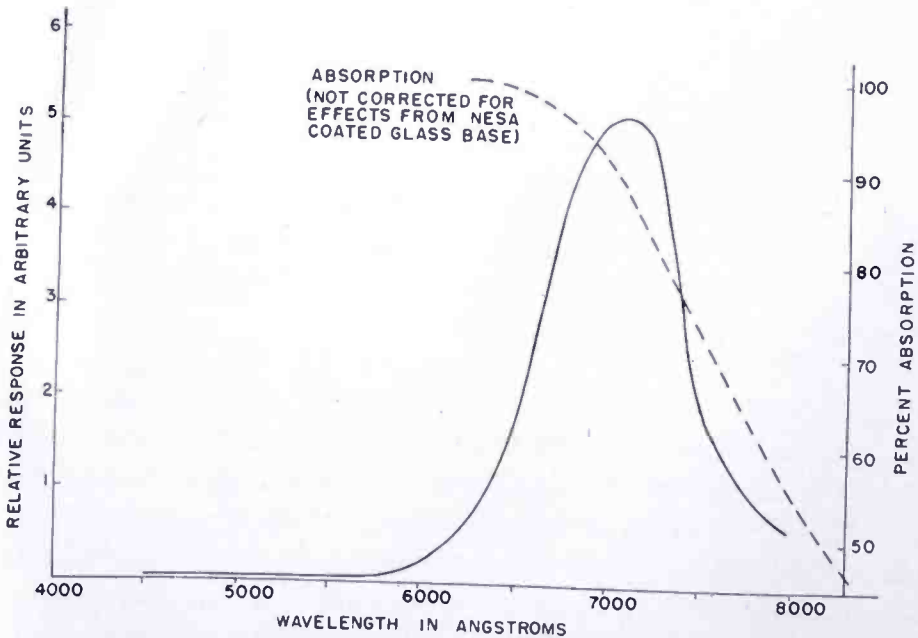


Fig. 5—Spectral response and absorption curves for an antimony trisulfide target.

The response ordinate is given in terms of the inverse power needed to excite equal signals at each wave length.

A second source of low sensitivity for strongly absorbed radiation is implied by the fact that the exponent of the current-versus-light curve is less than unity. This means that the material is less sensitive at higher concentrations of excitation. The same total lumens of blue light by virtue of its higher absorption coefficient produces a higher concentration of excitation than does red light.

The spectral response curves were obtained by using as a monochromator a Beckman spectrophotometer. By varying the slit width of this instrument the intensity of each illuminating wave length was adjusted to excite the same signal output from the photoconductor. From the known spectral distribution of the light source and the dispersion versus slit width relationship for the monochromator, it was possible to compute the relative energy at each wave length falling on the photoconductive layer to excite equal signal. This "constant signal" method of measuring the spectral response avoided the problem of making correction for the nonlinear current-versus-light curve of the antimony trisulfide layers. While this gives a spectral distribution curve for only one gradient across the film, antimony trisulfide has not generally shown a significant change of spectral response with field strength.

A very few antimony trisulfide layers, visibly red by transmission, have shown appreciable blue sensitivity. While this normally indicates a range of charge carrier greater than the blue light penetration, this conclusion is not unambiguous. Another likely possibility is that the photoconductive layer is not homogeneous, but composed of two or more thinner layers such that the major potential drop is in a thin layer adjacent the signal plate. A third possibility is that the absorbed blue light excites a red or infrared luminescence which can penetrate the target thickness and thus give rise to a measurable photocurrent. However, independent tests showed no evidence for this luminescence.

While pictures have been produced by antimony trisulfide layers excited by x-rays, the sensitivity has been low owing to the small absorption of the x-rays by the relatively thin film. Increased sensitivity has been obtained by allowing the x-rays to be absorbed by and excite luminescence in an intermediate screen.

Sensitivity and Quantum Efficiency

Like the other electrical properties, the photosensitivity has varied considerably from sample to sample. Of the many sulfides, selenides and tellurides tested, however, antimony trisulfide has consistently

shown the highest sensitivity when operated as a pickup tube target. Frequently layers have had operating sensitivities of several hundred microamperes per lumen; a few experimental ones have substantially exceeded a thousand microamperes per lumen. It is interesting to note that the frequently cited association of good photoconductivity with high index of refraction fits antimony trisulfide quite well.

The plots of response versus wave length in Figures 5 and 6 are response curves based on equal photocurrent through the layers at each wave length. The actual value of the incident power correspond-

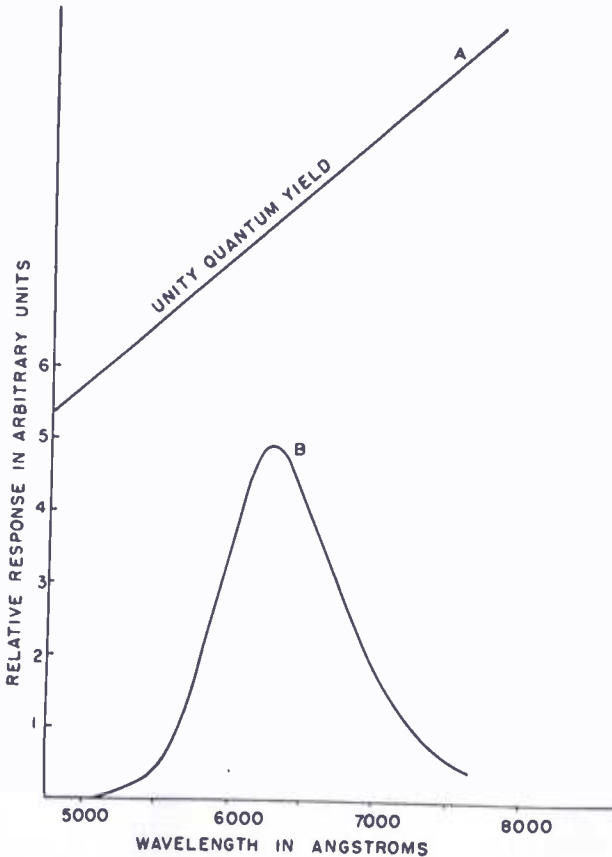


Fig. 6—Spectral response of an antimony trisulfide target shown relative to curve for unity quantum yield.

ing to any point on these curves was found by substituting a photocell of known sensitivity for the layer being measured. Curve A of Figure 6 was drawn showing the incident radiant power required at each wave length for the constant photocurrent to represent unity quantum yield. That is, curve A is plotted in the same units of reciprocal power as curve B. A comparison of curve A with the current response curve B of the photoconductive layer shows the quantum efficiency of the layer at each wave length.

Speed of Response

The decay of photocurrent through an antimony trisulfide layer

after exposure to light has been characterized by an initial relatively rapid decay down to about ten per cent of the light signal in a few frame times. Thereafter a faint residual signal (positive after image) can be observed in some cases for as much as a few seconds. This has limited the low-light range of the material to applications where observation of rapid motion is not important. The observable time lag can be improved by operating at a higher light level. Like most photoconductors, the speed of response of antimony trisulfide increases with excitation density. The sensitivity of this material is normally high enough that the excess light required is readily available for improving its time constant. Figure 7 shows a set of photocurrent

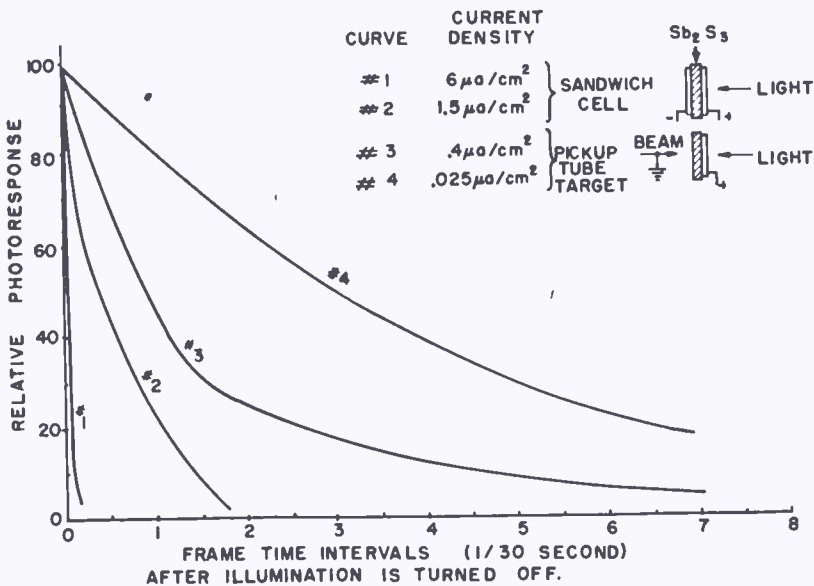


Fig. 7—Photocurrent decay after various initial illuminations.

decay curves for various initial light intensities. The curves are normalized to have the same current value at the instant the light is turned off. The improvement of speed of response with light intensity is evident. Although the decay shown by curves (1) and (2) is believed to be due entirely to the time lag of the photoconductive process, curves (3) and (4) may reflect some limitation of the beam resistance as well, since they depended upon an electron beam for one contact.

While the sensitivity of antimony trisulfide layers has exceeded a thousand microamperes per lumen, an analysis of time lag versus sensitivity² indicates that for the observed lag a much higher quantum

² A. Rose, "An Outline of Some Photoconductive Processes", *RCA Review*, Vol. XII, No. 3, p. 362, September, 1951.

efficiency should be observed. Effort is being made to either close this discrepancy in sensitivity or to understand the reason for its existence.

Temperature Characteristics

While it is unlikely that a photoconductive material in pickup tube use would be subjected to much over 70°C, antimony trisulfide has shown reversible behavior in its properties at temperatures in excess of this value. Upon subsequent cooling to room temperature, there is found to be no significant change in either dark or light current from the initial room temperature values. However, when heated above about 200° in a vacuum, very pronounced permanent increases occur in both light and dark currents. Between 200° and 250°C a permanent visible color change from red to black takes place. Pictures transmitted by the black form have been inferior to those of the red form for uniformity, dark current and sensitivity.

Figure 8 shows a plot of temperature versus light and dark currents measured between two electrodes on a surface of antimony trisulfide. This sample was carried to a temperature in a vacuum where slight permanent darkening of the sample could just be noticed. In the range from room temperature to about 180°C, the variation of current with temperature may be assumed to be reversible since no change occurred while holding the target for ten minutes at each temperature reading. However, the target did undergo a permanent change on standing slightly above 200°C, as shown in Figure 8. Although the light sensitivity shows a permanent increase after cooling from the more than 200°C bake, this does not necessarily represent a higher sensitivity in pickup tube operation. If the increase in conductivity of the material, as indicated by the increase in dark current is great enough to prevent the charge storage type of operation, this could cause a net loss in operating sensitivity. Less than 50 per cent reversible drop in sensitivity has been noted on cooling antimony trisulfide layers to 0°C.

Life Properties

Two antimony trisulfide layers have been life tested under scanning operation with stationary light patterns projected upon them. One surface showed no significant change in photoconductive properties after more than 500 hours operation. The other showed no significant change after 1500 hours operation, and only a slight drop of sensitivity after over 2000 hours of operation, which could be accounted for by other causes. During part of this test the surface was heated to over 70°C. Both tests were terminated by causes not related to the

life properties of the layers. Two antimony trisulfide layers exposed to strong alpha particle bombardment for a prolonged period showed no permanent change in electrical properties. The stability of these layers during extended periods of operation is felt to be evidence of the electronic character of the photoprocess. As opposed to this, migration of material with resulting permanent changes of electrical properties, has been associated with ionic processes.

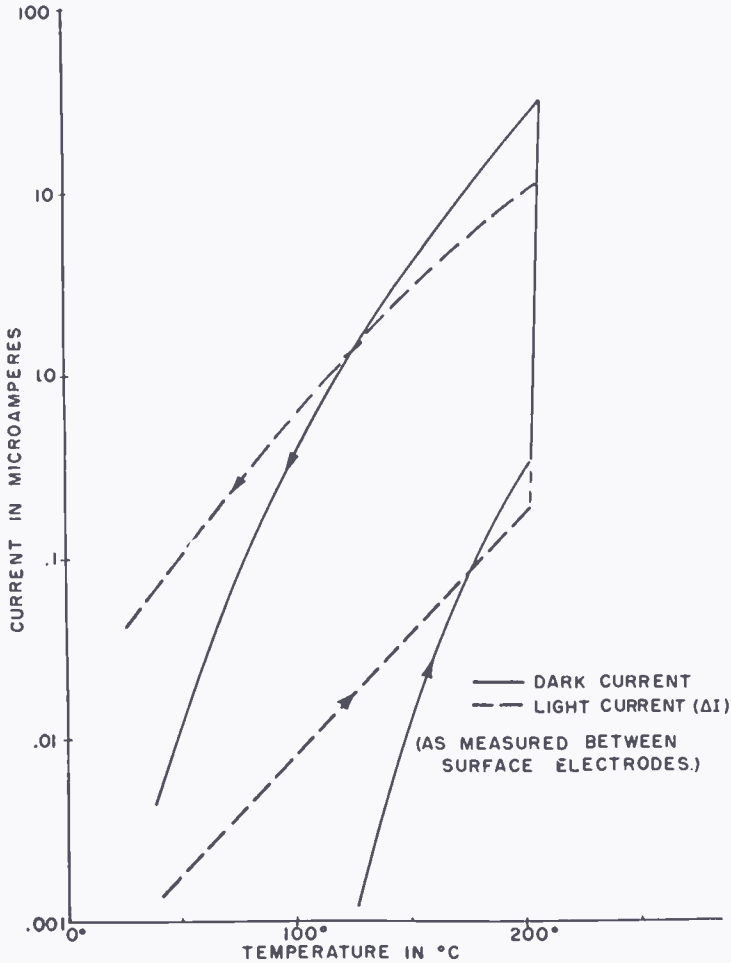


Fig. 8—Dark current and light current (ΔI) vs. temperature during vacuum baking of antimony trisulfide target. Sample held 10 minutes at each temperature point.

PROCESSING VARIATIONS OF ANTIMONY TRISULFIDE LAYERS

Effects of Air Baking

Air baking of an antimony trisulfide layer can both lower its dark current and increase its sensitivity. It has been found, however, that subsequent operation of such a layer in a vacuum will produce a generally slow reversion to the original characteristics. The rate of

reversion to the initial electrical properties may be changed as a function of variation in baking procedure. However, it has in all cases been short compared with the lifetime to be expected from a layer that has not been baked.

Effects of the Substrate

Layers of antimony trisulfide have been evaporated over a substrate consisting of distinct islands of several different semitransparent conductive materials. While antimony trisulfide, unlike selenium,³ has not generally shown any first order effects of this substrate on its electrical properties, small differences have been noted. The dark current seems to be the property most affected by the substrate and may be higher or lower on the part of the photoconductor over the metallic substrate than over the Nesa*, generally used as the transparent conducting signal plate.

Impurity Addition

Many foreign substances have been added in varying amounts to antimony trisulfide for the purpose of making desirable changes in the photoconductive properties. These additions have produced rather large changes in both dark current and sensitivity, but have been for the most part singularly characterized by the small effect they have had on speed of response. For example, a few per cent antimony oxide added to the sulfide can increase the dark resistivity by more than an order of magnitude. Although the sulfide alone has a resistivity high enough for storage operation, the higher resistivity introduced by the oxide is an advantage for use in pickup tube operation. The increased resistivity permits higher operating voltage which produces a flatter background signal over the whole target area for the same total dark current. This advantage has outweighed the disadvantage of a small decrease in average sensitivity from that of the normal antimony trisulfide layer.

Other Methods of Preparing Antimony Trisulfide Layers

Although evaporated photoconductive layers have been most satisfactory from the standpoint of uniformity, other means of forming layers of antimony trisulfide have been investigated.

Settled targets have had medium to low sensitivity, good resistivity and fairly good speed of response characteristics. While layers made

³ P. K. Weimer and A. D. Cope, "Photoconductivity in Amorphous Selenium", *RCA Review*, Vol. XII, No. 3, p. 314, September, 1951.

* Trade name for transparent conducting coating developed by Pittsburgh Plate Glass Co.

by this method have been grainy, it is likely that smaller initial particle size would improve the uniformity; however, this solution would raise the question of influence of particle size on other photoconductive properties such as sensitivity.

A number of layers of red antimony trisulfide were prepared by spraying solutions onto heated Nesa coated glass plates. The resulting films showed more dark current, less sensitivity and lower speed of response than the normal antimony trisulfide.

SOME OTHER MATERIALS AS PHOTOCONDUCTIVE LAYERS

In addition to antimony trisulfide, many other photoconductive materials have been examined. One set of compounds whose constituents were examined both individually and in certain combinations with each other will be discussed as a group. The individual compounds making up this group are cadmium sulfide and selenide and zinc sulfide and selenide. Cadmium sulfide in sublimed or evaporated layers has generally been characterized by a very high intrinsic photoconductive sensitivity and a resistivity too low for charge storage in scanning operation. This low resistivity prevents effective use being made of the high sensitivity. If these layers are baked in air or in some other gases the resistivity can be increased by several orders of magnitude. Some of these heat treated layers have had a resulting resistivity high enough for storage operation, with a usable, but not outstandingly high operating sensitivity as a pickup tube target. The photoconductive peak for cadmium sulfide, as has been reported in the literature,⁴ occurs in the green region (5200 Å) of the spectrum.

Cadmium selenide has also exhibited a high intrinsic photoconductive sensitivity. Here again the dark resistivity has generally been insufficient, but can be improved by an air bake. Its peak sensitivity lies in the red end of the spectrum.

Unlike the preceding two compounds, zinc sulfide has exhibited a very high dark resistivity, but a relatively low photoconductive sensitivity. Layers of this material, as used in pickup tubes, have had only a low sensitivity peaked in the blue end of the spectrum.

Similarly zinc selenide has had more than adequate resistivity for storage and, with few exceptions, a relatively low sensitivity. Its peak photoconductive response lies in the blue-green region of the spectrum.

In an attempt to combine the desirable properties of these materials, layers were formed by combining one of the high intrinsic

⁴ R. Frerichs. "The Photoconductivity of 'Incomplete Phosphors'", *Phys. Rev.*, Vol. 72, pp. 594-601, 1947.

sensitivity materials (CdS or CdSe) with one of the highly resistive materials (ZnS or ZnSe). Each of the several combinations was tested over a range of percentage mixtures of the two constituents. The CdSe-ZnSe series was most extensively investigated.

As desired, photoconductive layers formed by evaporation of various percentage mixtures of these two compounds displayed properties intermediate between those of the separate constituents. Thus, for example, spectral sensitivity shifted from the blue to the red as the percentage of CdSe was increased. Figure 9 shows the variation of both resistivity and "gap" sensitivity. The latter is measured as the photocurrent between two electrodes on the surface of the material. The sensitivity so obtained is a measure of the intrinsic sensitivity

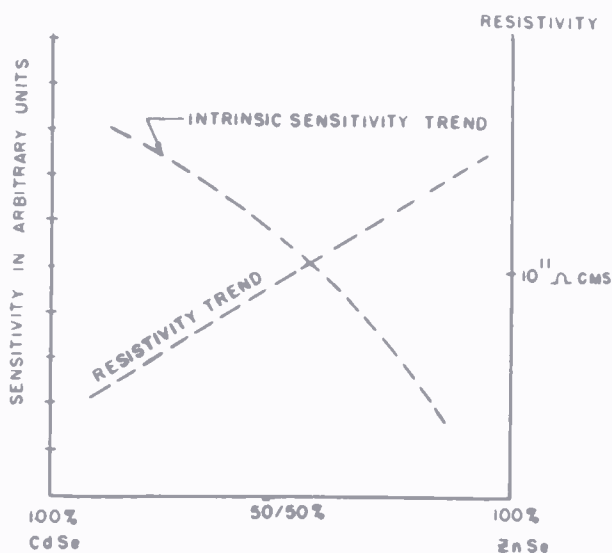


Fig. 9—Variation of resistivity and intrinsic sensitivity of CdSe-ZnSe mixtures with percentage of each component.

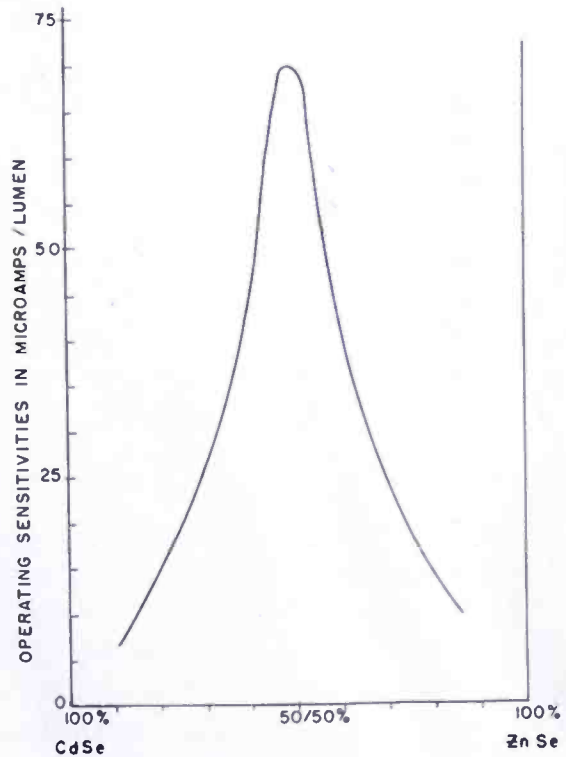
of the material separate from the question of resistivity. The operating sensitivity trend (which involves both intrinsic sensitivity and resistivity) is shown in Figure 10 as a function of composition. The curves of these two figures represent general trends as evidenced by averaging results from a large number of targets; well over a hundred were tested. No significance should be attached to the actual shape of the curves of Figure 9.

Sensitivities of individual layers have ranged up to many hundreds of microamperes per lumen. Very uniform pictures have been transmitted by these layers. However, the speed of response has not been sufficiently fast to be useful for normal television operation. For certain industrial applications the high sensitivity might recommend its use where speed of response is not critical.

CONCLUSIONS

From the variation of sensitivity, dark current and speed of response encountered in repeated evaporations of relatively pure antimony sulfide, it is clear that no precise meaning can be given to the results reported here as being characteristic material constants. They define rather probable ranges in which values for these properties fall. Nevertheless, the results with antimony sulfide have shown considerably better reproducibility than those obtained with many of the other sulfides and selenides tested. There is good evidence that dissociation of many of these materials during evaporation, as well as the sub-

Fig. 10—Average operating sensitivity for targets of various percentage mixtures of CdSe and ZnSe.



microscopic structure of the evaporated films, plays a large part in the variability of properties. These factors would be expected to be far more critical for insulators, for which small currents are being observed, than for semiconductors.

Sufficient reproducibility has been obtained in mixtures of certain sulfides and selenides to indicate that their properties may be varied continuously between the end-point properties of the individual components.

SOME ASPECTS OF THE PHOTOCONDUCTIVITY OF CADMIUM SULFIDE*

BY

ROLAND W. SMITH

Research Department, RCA Laboratories Division,
Princeton, N. J.

Summary—Measurements of the photoconductive behavior of cadmium sulfide crystals are described and include: photocurrent-versus-irradiation curves, time constant observations, Hall effect measurements, and probe examinations of the potential distribution. These are mainly aimed at determining how well the expression for quantum yield

$$\theta = \frac{\text{life time of a free carrier}}{\text{transit time of a free carrier}}$$

can be satisfied. If the observed time constant is used as a measure of the life time of a free carrier, the discrepancy is over four orders of magnitude at low lights and may be reduced to one order of magnitude or less at high lights. Trapping effects are believed to be responsible for the lack of complete agreement. A capture cross section of primary centers for free electrons is computed from the data to be 10^{-21} square centimeter.

INTRODUCTION

CRYSTALS of cadmium sulfide, grown from the vapor phase, are useful for a basic study of photoconductivity for a number of reasons. Prominent among these are their large size, convenient form, large variety and magnitude of photoeffects, low dark current, and predominantly electronic character of the current. Of the many effects that have been observed, this paper is concerned mainly with a simple relation that should hold generally for the photoconductive process regardless of the model used.

The relation is

$$\theta = \frac{(I/e)}{F} = \frac{\tau}{T}, \quad (1)$$

where θ is the quantum yield, τ the life time of a free carrier, I the photocurrent resulting from F excitations per second, T the transit time of a free carrier across the crystal, and e the electronic charge.

The basis for this expression, and the conditions under which it is

* Decimal Classification: 535.3.

expected to hold, are dealt with in another paper.¹ One of the main points is that the life time of a free carrier, τ , is not, in general, the time constant, τ_{obs} , observed from the decay of the photocurrent when the light is interrupted. Traps may drastically reduce the life time of a free carrier (and the photosensitivity) while leaving the observed time constant substantially unchanged. Unless the exact disposition of traps is known, the test should be performed under conditions that are expected to minimize trapping effects. This should obtain when the density of carriers in the conduction band is greater than the density of electrons in traps. Under these conditions the life time of a free carrier and the observed time constant are one and the same quantity.

The pertinent parameters for a test of Expression (1) were determined by the measurements described below. These measurements include an estimate of the mobility from observations of the Hall effect. In addition some of the general characteristics of photoconducting cadmium sulfide are recorded.

If Expression (1) is applied to a photoconducting insulator without distinguishing the two time constants, discrepancies as great as eight orders of magnitude are frequently encountered. From data on thin evaporated films of antimony trisulfide,² an expected quantum yield of 10^8 is computed using the observed time constant of 0.1 second as a measure of the life time of a free carrier. This is to be compared with quantum yields of unity actually observed. Similarly data on cadmium sulfide crystals taken at low irradiations fail to satisfy Expression (1) by as much as five orders of magnitude when the observed time constant is used for τ . The present paper may be regarded in the above light, as an attempt to satisfy Expression (1) by making measurements on cadmium sulfide crystals at very high irradiation such that trapping effects are minimized and the observed time constant approaches the life time of a free carrier.

MEASUREMENTS

The cadmium sulfide and selenide crystals used in this study were grown in these laboratories by the chemico-physics group. Generally, the larger crystals were mounted on pyrex plates by means of air-drying silver paste electrodes. Correlated measurements were made on

¹ A. Rose, "An Outline of Some Photoconductive Processes", *RCA Review*, Vol. XII, No. 3, p. 362, September, 1951.

² S. V. Forgue, R. R. Goodrich, and A. D. Cope, "Properties of Some Photoconductors, Principally Antimony Trisulfide", *RCA Review*, Vol. XII, No. 3, p. 335, September, 1951.

two cadmium sulfide crystals, A and B, measuring $7 \times 3 \times 0.5$ and $10 \times 3 \times 0.5$ millimeters respectively. The measurements were taken at room temperature and represent static characteristics.

Figure 1 shows schematically the experimental arrangement. The crystals were housed in a light-tight box, and were irradiated with radiation from high pressure A-H6 mercury arcs. The radiation passed through suitable band selecting filters and a neutral wedge attenuator, to a beam splitter; part of the radiation passing to the crystal, the other part to a photomultiplier.

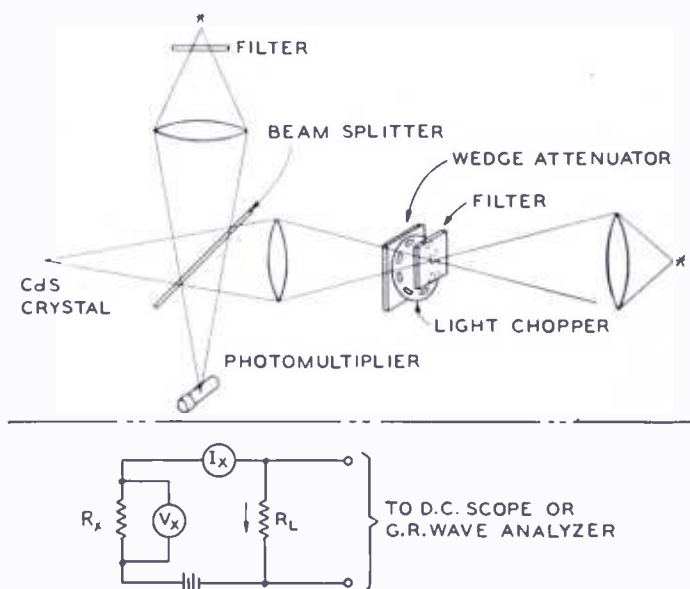


Fig. 1—Experimental arrangement.

For time constant observations two methods were used: (a) the time taken for the photocurrent to decay to one half its initial value was measured from the decay curve trace on a direct-current oscilloscope, the irradiation being cut off by means of a high speed photographic shutter; (b) the response to pulsed radiation obtained by a rotating sectored disc.

Potential Distribution

A knowledge of the potential distribution along the crystal is essential for a computation of the transit time of the free carriers. In order to determine the actual potential distribution, probe measurements were made on a large number of crystals. The probes were fine wires making pressure contact to the crystal surface, and could be moved to any position by a mechanical manipulator. Potential differences between probes were measured by very-high resistance ($\sim 10^{12}$ ohms) electrostatic voltmeters.

The results of these measurements can be summarized as follows:³

1. A uniform, linear potential distribution along the length of a crystal is the exception, rather than the rule, for the large number of crystals examined.
2. Generally the largest fraction (over 90 per cent) of the total potential drop is concentrated at either one or both ends of the crystal.
3. The potential drop at the ends is usually independent of the applied polarity.
4. The potential drop between any two points on the crystal is usually a very complicated function of the irradiation.
5. A few cadmium sulfide crystals have been found with an essentially linear potential distribution along their length.
6. Relatively large (10^1 - 10^3 microamperes) photocurrents have been drawn through crystals with linear potential distributions.

From the above it is concluded that though potential barriers are usually observed, crystals exist in which a major portion of the potential drop occurs along the body of the crystal and that large photocurrents can be drawn through them. This obviates the need for barriers which were earlier thought necessary to account for the high sensitivities observed in these crystals.^{1,4}

The origin of the barriers at the electrodes is not well understood, and efforts to alter them artificially, or produce crystal-electrode systems without barriers, generally have met with little success. Before making calculations involving the electric field, it is advisable to actually determine the potential distribution rather than to assume it to be uniform. In many discussions of photoconductivity of cadmium sulfide in the literature to date, there has been an implicit assumption of a uniform potential distribution. For the main test, to which this paper is addressed, it was determined that the potential distribution was essentially linear along the crystals.

Photocurrent-Voltage Characteristic

With irradiation as a parameter, the direct-current photocurrent was measured as a function of the applied voltage. Figure 2 is a typical characteristic. It is noted that there are usually three parts: (a) in the low-voltage region the photocurrent varies faster than the

³ These results are consistent with data obtained by R. H. Bube, "A Comparative Study of Photoconductivity and Luminescence", *Phys. Rev.*, Vol. 83, p. 393, 1951.

⁴ A. Rose, P. K. Weimer and S. V. Forgue, "Some Observations on the Photoeffect in Cadmium Sulfide", *Phys. Rev.*, Vol. 76, p. 179, 1949.

first power of the voltage; (b) a linear portion and, (c) a saturation region where the photocurrent is roughly independent of the voltage. The characteristics can be asymmetrical, though the current seldom changes by a factor of more than two for a reversal of polarity.

Photocurrent-Irradiation Characteristic

The photocurrent as a function of irradiation, at room temperature, has been determined for many cadmium sulfide and selenide samples. Figure 3 shows typical characteristics. In most cases the lowest photocurrents were over ten times the dark currents.

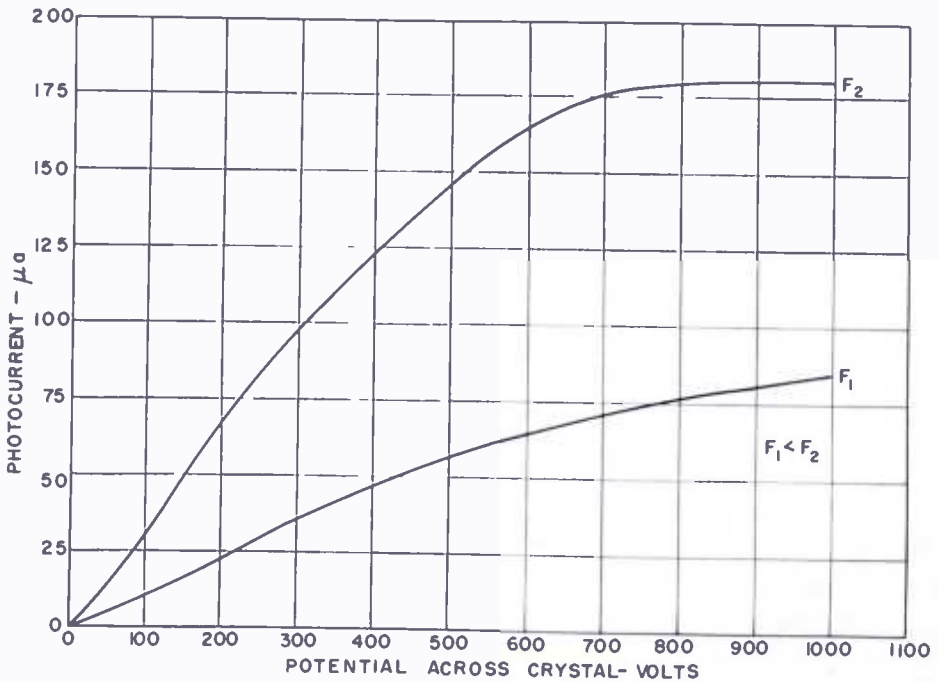


Fig. 2—Photocurrent—voltage characteristic.

In summary the following can be said about the photocurrent-irradiation characteristics:

1. A plot of log photocurrent versus log irradiation generally yields two straight line sections (over several orders of magnitude), with a relatively small transition region between, here referred to as the break-point.
2. In the region of low irradiation the exponent $n = 1 \pm 0.2$; in the high intensity region $n = 0.5 \pm 0.2$. Exponents of exactly 1 or .5 are seldom observed.
3. The form of the photocurrent-irradiation characteristic appears to be independent of the applied voltage.

4. Exponents greater than 1 in the low-intensity region have been observed for several crystals. The outstanding example being a cadmium selenide crystal with $n = 2.3$ in the low-intensity region and $n = 0.73$ in the high-intensity region.
5. No appreciable difference in the form of the photocurrent-irradiation characteristic is noted with irradiation on either side of the absorption edge.

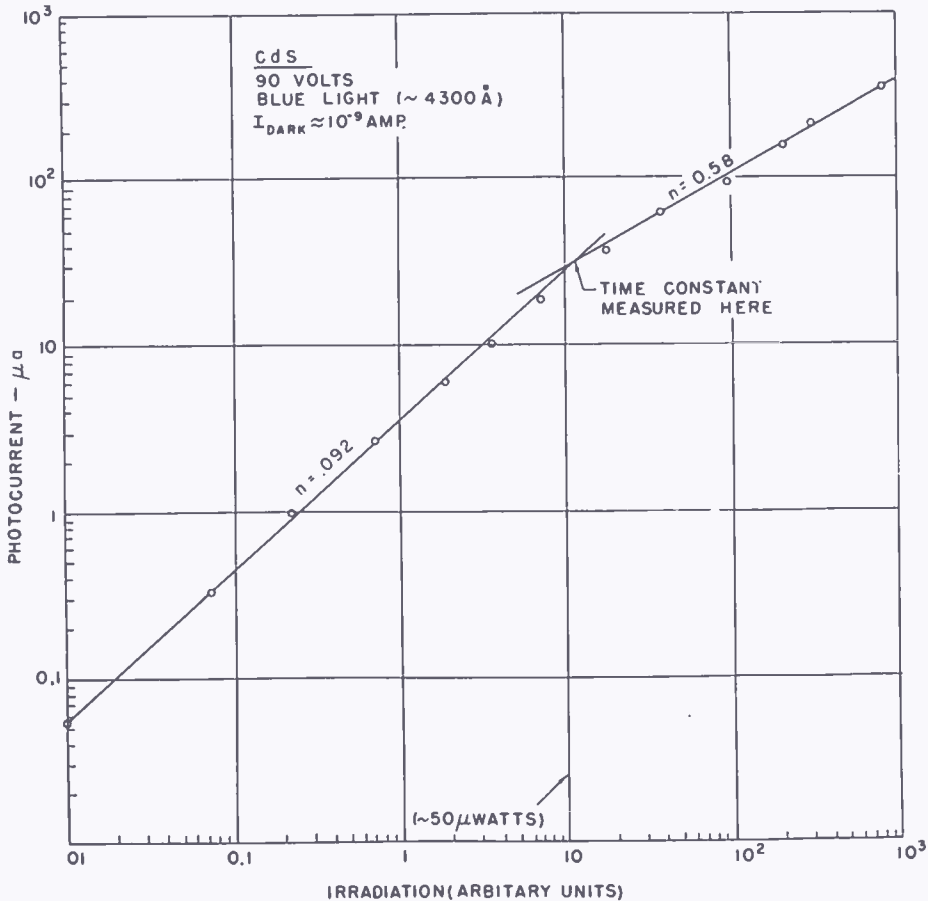


Fig. 3—Photocurrent-irradiation characteristic, crystal A.

Quantum Yield

In addition to uniformity of potential distribution, uniformity of photoresponse is important in quantitative measurements. This is pointed up by the fact that many crystals have been sensitive in small areas; that many crystals were not responsive to shadows or spots of irradiation on the body of the crystal; and that, by use of the television technique of flying spot scanning, the sensitive areas of a crystal were observed to shift position with amount, distribution, and wave length of bias light.

For the particular crystals under test, it was found that a portion along the length of the crystal was essentially uniform in photoresponse. Using a narrow band of frequencies, centered around 4300 Å, where the irradiation was completely absorbed by the crystal, it was determined by comparison with a 929 photocell, that irradiation, F , of 5×10^{13} quanta per second excites a photocurrent of 30 microamperes at 90 volts on one crystal (A) and an F of 3×10^{13} quanta per second produces a 50-microampere photocurrent at 90 volts on the other crystal (B). The corresponding quantum yields, θ , calculated from $I = e\theta F$, are 3.6 and 9.9 respectively. (A closer spacing of electrodes would have given the exceedingly high quantum yields usually reported

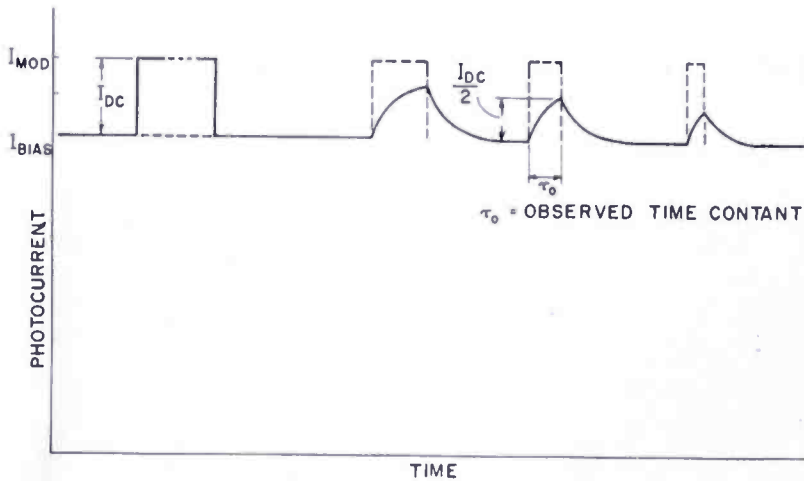


Fig. 4—Time constant measurement.

for cadmium sulfide.) The excitation values include a correction for 50 per cent reflection loss at the crystal face.

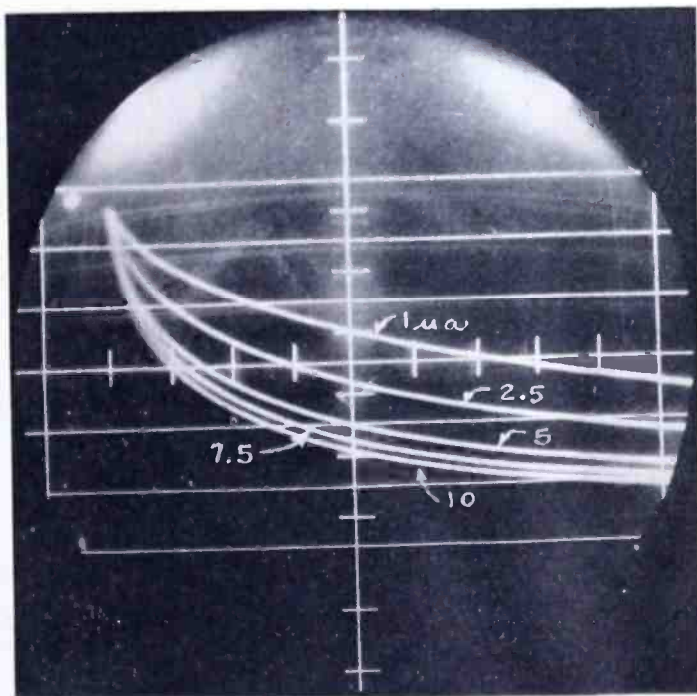
Speed of Photoresponse

One of the most obvious characteristics of photoconductors, as contrasted with photoemitters, is the time of response of the photocurrent to changes in irradiation. Figure 4 illustrates the method used to get the speed of response or observed time constant, for cadmium sulfide crystals. The photocurrent was raised to the level I_{BIAS} , the photocurrent at which it was desired to get the speed of response, by means of auxiliary irradiation. A rotating disc was then used to superpose square pulses of irradiation of known duration. The pulse time, τ_{obs} , for half the direct-current response, $I_{d.c.}$, was then taken as a measure of the speed of response. At the break-point of 30 microamperes photocurrent, a time constant of 0.008 second was recorded for crystal A. For crystal B, $\tau_{obs} = 0.0012$ second. For crystal B an additional

check was obtained using a high speed photographic shutter. Figure 5 is an oscillogram showing the decay curves for several different initial photocurrents.

It was further observed that the speed of response, τ_{obs} , was inversely proportional to the (bias) irradiation, in the region of linear response, Figure 6. This is a frequently observed but not general characteristic of cadmium sulfide crystals. Several samples have been observed for which the time constant did not change for several orders of magnitude change of irradiation.

Fig. 5—Oscillogram showing variation of observed time constant for various initial photocurrents. Constant sweep rate. Crystal B.



Hall Effect

The transit time, T , of a free carrier is given by $\frac{L^2}{\mu V_A}$, where L is the length of the crystal, V_A the applied potential, and μ the mobility.⁵ In order to get an estimate of the mobility, Hall measurements were performed on several cadmium sulfide crystals.

$$\mu_H = \sigma R = 10^8 \frac{V_H L}{H V_A W} \text{ cm}^2/\text{volt-sec.}, \tag{2}$$

⁵ Neither the precision nor the tentative character of the present measurements of the Hall effect on cadmium sulfide warrants a distinction between the microscopic and Hall mobility. See W. Shockley, *ELECTRONS AND HOLES IN SEMICONDUCTORS*, p. 209, D. Van Nostrand, New York, N. Y., 1950.

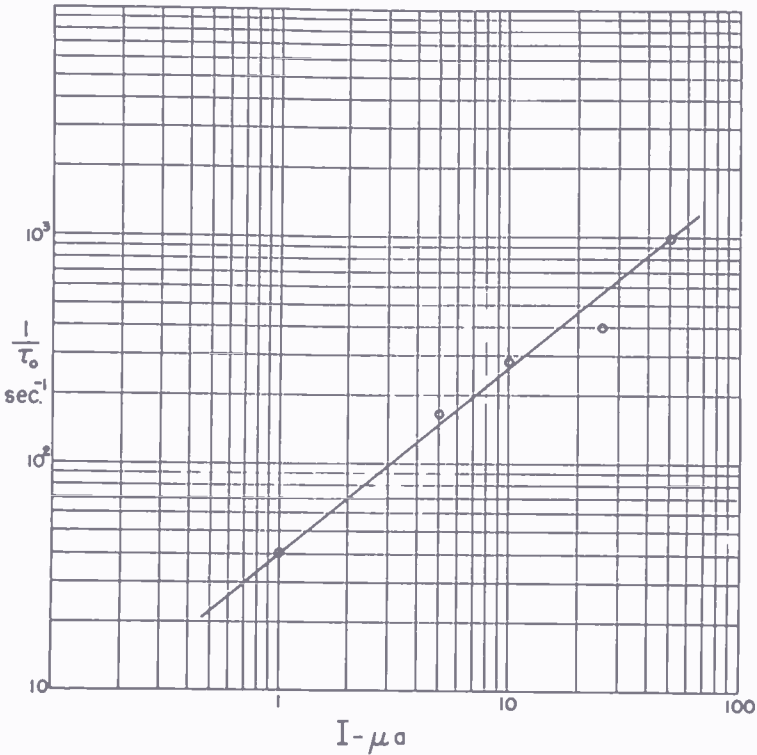


Fig. 6—Variation of Observed Time Constant τ_0 , with photocurrent I , crystal B.

where σ is the conductivity, R the Hall constant, V_H the measured Hall voltage, and H the magnetic field in oersteds.

Figure 7 shows the experimental arrangement. The crystal was strongly irradiated in order to reduce the impedances between electrodes as much as possible (to $\sim 10^6$ ohms). Spots of silver paste at the Hall electrodes served a similar purpose. A 15×10^6 -ohm potentiometer was used to balance the potential between Hall probes at $H=0$. A voltmeter (0.5 volts full scale and 2×10^8 ohms or greater input impedance) was used to measure the Hall voltages. Since potentials at points a, b, and c were known, a fairly accurate estimate of the electric field was obtained. A magnetic field of 5×10^3 oersteds was used.

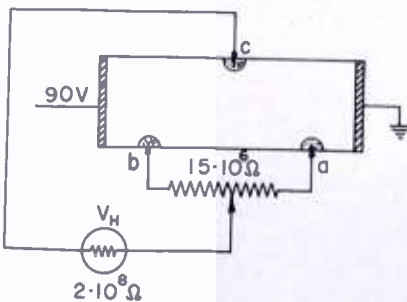


Fig. 7—Hall effect measurement.

Difficulties were experienced in obtaining a stable balance between Hall probes, and of even more concern, a nonreversing Hall potential with reversal of the magnetic field, at times was observed. Direct-current measurements were made and no correction or estimate has been made for possible interfering thermo- and galvano-magnetic effects.

Of the several crystals examined three are of particular interest. They gave Hall voltages that reversed with reversal of electric or magnetic field, were proportional to both the electric and magnetic field strengths, and were independent of the irradiation on the crystal. One crystal (not otherwise mentioned in this paper) gave a barely detectable Hall voltage, indicative of a mobility of 1 cm²/volt-sec. A mobility of 40 cm²/volt-sec. was measured for crystal A, and 200 cm²/volt-sec. for crystal B. Other crystals measured gave mobilities that fell between these values.

This spread of 200:1 of Hall mobility may be interpreted as: (1) a true variation of electron mobility from sample to sample; (2) a result of a combination of electron and hole conduction*; or (3) unaccounted for interfering effects.

Values of mobility reported in the literature for cadmium sulfide are 5 cm²/volt-sec. by Broser and Warminsky⁶, 10-40 cm²/volt-sec. by Fassbender and Lehmann⁷, and 40 cm²/volt-sec. by Gildart and Ewald⁸. All these were apparently measured in the high light region with no comments as to uniformity of potential distribution and photoresponse. Also they are values computed from quantum yield and time-constant data, rather than Hall measurements.

TEST OF EXPRESSION (1)

Correlated data for a test of Expression (1) have been obtained for two crystals. In the absence of more accurate knowledge or data on the mobility, the Hall mobility measured for each crystal will be used to compute the life time of a free carrier, τ , and this compared with the observed time constant, τ_{obs} . If the excitation density is high

* Preliminary tests for independent evidence of hole conductivity have given negative results.

⁶ I. Broser and R. Warminsky, "Theory of Luminescence and Electrical Conductivity of Cadmium Sulfide Crystals", *Ann. der Phys.*, Vol. 7, p. 288, 1950.

⁷ J. Fassbender and H. Lehmann, "Computation of Electron Mobility in Cadmium Sulfide Single Crystals from Attenuating Light Measurements", *Ann. der Phys.*, Vol. 6, p. 215, 1949.

⁸ L. Gildart and A. W. Ewald, "Electron Mobility and Luminescence Efficiency in Cadmium Sulfide", *Phys. Rev.*, Vol. 83, p. 359, 1951.

enough to minimize trapping effects, these two time constants should agree. From Table I, however, it is seen that the observed time constant exceeds the computed life time of a free carrier. A reasonable conclusion is that trapping is still effective even at these high excitation densities. Additional time is required to recombine some of the trapped electrons along with the conduction electrons. It is worth repeating that a test of Expression (1) carried out at low light intensities for either crystal A or B can result in a discrepancy between observed time constant and computed life time of as much as four orders of magnitude.

Table I

Crystal	<i>I</i>	<i>F</i>	θ	μ_H	τ	
	(microamperes at 90 volts)	(quanta/sec.)			(cm. ² /volt-sec.)	obs.
A (L = 0.7 cm.)	30	5×10^{13}	3.6	40	0.008	0.0005
B (L = 1.0 cm)	50	3×10^{13}	9.9	200	0.0012	0.00055

For convenience of comparing the present data with other measurements in the literature the observed time constants and quantum yields above may be used to compute mobilities of 2.2 and 92 for crystals A and B respectively. Both these values are lower than the directly measured mobilities. The discrepancies may, as in the case of the time constants, be ascribed to trapping effects.

If the present data on cadmium sulfide is interpreted in terms of the trapping effects discussed in the last paper of this group: deep traps are needed to account for the near linear photocurrent-irradiation characteristics, Figure 3; these traps must not be localized; but rather must be distributed more or less uniformly in energy to account for the variation of observed time constant with irradiation; and, finally, a concentration of shallow traps, larger in number than the deep traps, is needed to account for trapping effects still being present when the current-irradiation curve breaks from linear to half-power form. If the irradiation is assumed to be absorbed in a thickness of 10^{-4} cm., the concentration of free electrons may be computed to be $\sim 10^{16}$ cm⁻³ at the break point. The concentration of shallow traps would then have to exceed this value in order for trapping effects to be significant.

A final parameter, the capture of cross section of a primary center

for a free electron may be computed from the data presented:*

$$s = (vn_c \tau_{\text{obs}})^{-1}, \quad (3)$$

where v is the thermal velocity (10^7 cm/sec.) of a free electron, and n_c the concentration of free electrons (10^{16} cm $^{-3}$) at the break point. The capture cross section turns out to be 10^{-21} cm 2 for crystal A or six orders of magnitude smaller than atomic dimensions. A similar computation for crystal B gives a cross section of 10^{-19} cm 2 . It is this small cross section that must account in large part for the high sensitivity of cadmium sulfide crystals.

* Eq. (46), Ref. (1).

AN OUTLINE OF SOME PHOTOCONDUCTIVE PROCESSES*

BY

ALBERT ROSE

Research Department, RCA Laboratories Division,
Princeton, N. J.

Summary—An attempt is made to outline a variety of photoconductive processes in such form as to facilitate quantitative comparison with experimental data. The processes include space-charge-limited currents and volume-excited currents. The latter takes on a variety of forms depending on the presence and distribution of traps, the mobility of one or both kinds of carriers and the ease of replenishing these carriers at the electrodes. Most emphasis is placed on insulators and on trapping effects in insulators. The concept of a steady-state Fermi limit is introduced to aid the analysis. Also two time constants are separated out: the observed decay time for the photocurrent, and the mean life time of a free carrier. It is found that the following observed data can readily be accounted for: current-versus-light curves with exponents between 0.5 and 1.0; the lack of reciprocity between sensitivity and speed of response; and the low values of currents excited in thin evaporated insulating films by light or electron bombardment. The ratio of life time of a free carrier to the observed time constant is proposed as a figure of merit for a photoconductor. Other items discussed are infrared quenching, spectral response, nonuniform illumination of semiconductors and the effects of barrier fields on photoconductivity. It is suggested that these barrier fields may have a larger influence on photoconductivity by reducing capture cross sections than by shortening the effective length of photoconductor.

INTRODUCTION

ASOLID in thermal equilibrium has its electrons and holes distributed amongst available energy states in accordance with Fermi statistics. The deeper lying states are bound states — localized in space. The intermediate states may be free but completely filled. The higher lying states are free and unfilled. In thermal equilibrium, a fraction of the total number of holes and electrons are in free states and determine the “dark” conductivity of the solid. The absorption of light disturbs this distribution so that more electrons (and holes) are in free states and the conductivity is increased. Under steady-state conditions, the disturbance by light is balanced by various recombination processes that tend to return the electrons to their normal equilibrium distribution. The increase in

* Decimal Classification: 535.3.

conductivity brought about by the optically disturbed distribution is called photoconductivity.

To compute the magnitude of a photoconductive current one needs essentially only to know the increase in number of electrons* in the free states. But the number of electrons in the free states will, for a given rate of excitation, be proportional to their life time in the free states. This obvious relation has given rise to a more or less explicit expectation that there should be a reciprocity between photosensitivity and speed of response to intermittent light signals. Such a reciprocity, particularly amongst photoconducting insulators, has been the exception rather than the rule. Here, then, is one of the observations that a useful model must satisfy. The frequently used model of simple bimolecular recombination between free electrons and an equal number of positive centers from which these electrons were excited, does not fit.

The same simple bimolecular model leads to a photoconductive current increasing as the square root of the light intensity. For insulators, again, the usually observed current-versus-light curve has an exponent somewhere between 0.5 and 1.0 rather than 0.5. For example, crystals of CdS have shown exponents around 0.8 extending over three orders of magnitude of light intensity.* Such an exponent cannot, as has often been suggested, be compounded out of two currents, one increasing linearly with light and the other as the square root of the light intensity. Here, then, is a second observation which a useful model must satisfy.

A third observation of importance is the fact that the measured photocurrents are often as much as eight orders of magnitude smaller than one would compute from the known rate of excitation and the observed time constant (speed of response). It is clear that the speed of response is not a good measure of the life time of an electron in the free states. A useful model should clarify this discrepancy.

The several problems just enumerated are sufficient to point up the need for improved models — models that match known data well enough to make further comparison with experiment fruitful. Whether such models can at the same time be compact enough to guide experimental work is still not certain. What can profitably be done is to outline the properties of some of the simpler models in such a way that quantitative comparison with experimental data is facilitated. The need for and directions of further elaboration can then be readily assessed.

* The additional contribution of free holes is evident and will not be repeated in this introductory discussion.

* R. W. Smith, "Some Aspects of the Photoconductivity of Cadmium Sulfide", *RCA Review*, Vol. XII, No. 3, p. 350, September, 1951.

The simplest picture of photoconductivity is that in which the incident light creates free electrons and/or free holes, — each is drawn to its proper electrode; and the maximum photocurrent, since each photon can create one free pair, is equal to the incident photon current. This is the current which the classic works of Gudden and Pohl¹ sought to emphasize as the fundamental primary current as distinguished from the usual complex of secondary photoeffects that follow when light shines on a photoconductor. The present outline treats this primary current as only one of a number of possible fundamental photoconductive processes, and tries to outline the conditions for, and consequences of, each of these processes. Actually, the primary process is one of the least likely to be encountered. It is hemmed in by a narrow set of conditions which restrict both the probability of finding it and the magnitude of its current. Some of the other photoconductive processes are more frequent, more sensitive and *no less fundamental* for not satisfying the definition of "primary currents".

SPACE-CHARGE-LIMITED CURRENTS

The photocurrents drawn between two electrodes in a solid medium have frequently been compared with the electron current drawn between cathode and anode in a vacuum diode. While there are important parallels, the space-charge limitations imposed by the solid medium are particularly severe — enough so that the present discussion of photoeffects is mostly confined to currents in an electrically neutral medium, that is, to photoconductors that are uniformly illuminated between electrodes rather than illuminated at one end. When an insulator is illuminated at one end, the maximum current that may be passed is, except for electrode separations of less than a mil, generally limited by space charge to negligible values.

Let the photoconductor in Figure 1 be an insulator and let free electrons be generated at the cathode *K*. These electrons may, of course, be generated by cathode ray bombardment, α particles, or temperature, as well as by light. The maximum current that may be drawn through the insulator is given by Mott and Gurney² for the

¹B. Gudden, *LICHTELECTRISCHE ERSCHEINUNGEN*, Julius Springer, Berlin, 1928.

²N. F. Mott and R. W. Gurney, *ELECTRONIC PROCESSES IN IONIC CRYSTALS*, Clarendon Press, New York, 1940, p. 172. For voltages high enough to avoid space charge, Mott and Gurney's expression showing the current increasing linearly with voltage is apparently in error, since simple considerations would lead to a constant or saturated current just as in the vacuum diode case.

plane parallel case by

$$I = 10^{-13} \frac{V^2 \mu k}{L^3} \text{ amperes/cm}^2, \tag{1}$$

where μ is the mobility of electrons,
 k is the dielectric constant.

V and L are shown in Figure 1 and measured in volts and centimeters. This expression may be compared with the expression for the space-charge-limited current in a thermionic diode:

$$I = 2.3 \times 10^{-6} \frac{V^{3/2}}{L^2} \text{ amperes/cm}^2. \tag{2}$$

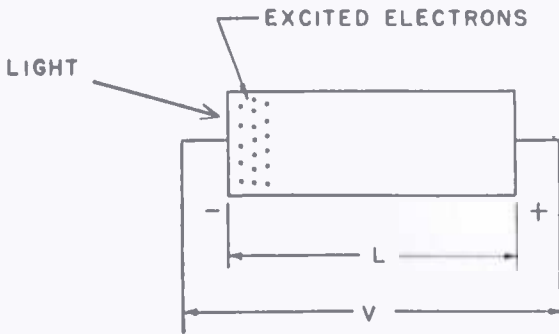


Fig. 1 — Space-charge-limited current.

It is immediately seen that the space-charge-limited currents in a solid medium are lower by seven orders of magnitude owing to the relative values of the constant factors alone. The source of this difference, as well as the different form of dependence on V and L , lies simply in the difference in the average velocity of an electron in the cathode-anode space. For the solid medium this velocity is $\frac{V}{L} \mu$; for the vacuum diode it is of the order of $10^7 V^{1/2}$. If these values for the average velocity are divided out of the two expressions, the results are substantially identical, namely:

$$\frac{I}{\text{electron velocity}} = 10^{-13} \frac{Vk}{L^2} \quad (\text{solid}),$$

$$\frac{I}{\text{electron velocity}} \cong 10^{-13} \frac{V}{L^2} \quad (\text{vacuum}).$$

The dielectric constant does not appear explicitly in the vacuum diode expression since its value of unity has already been inserted.

Since the form in which photoconductors are frequently tested departs markedly from the plane-parallel geometry, it is useful to have a ready means for evaluating the order of magnitude of space-charge-limited currents in a photoconductor of arbitrary geometry. This is obtained as follows:

$$I \cong \frac{Q}{T_r} \text{ amperes,} \quad (3)$$

where Q = charge in coulombs required to alter the potential of the "interior" of the photoconductor by V volts,

T_r = transit time (seconds) for carrier between electrodes.

But $Q = CV$,

where C = capacitance of "interior" of photoconductor, and

$$T_r = \frac{L}{E\mu} = \frac{L^2}{V\mu}. \quad (4)$$

With these values for Q and T_r , Equation (3) becomes

$$I \cong \frac{V^2 C \mu}{L^2}. \quad (5)$$

If Equation (5) is applied to the plane parallel case and if the capacitance of the "interior" for a square centimeter cross section is taken to be

$$10^{-12} \frac{k}{4\pi L} \text{ farads,}$$

that is, of the order of the capacitance of a central slice to either of the electrodes, the current becomes

$$I \cong 10^{-13} \frac{V^2 \mu k}{L^3} \text{ amperes per square centimeter.} \quad (6)$$

The close agreement with Equation (1) confirms the utility of this method of computing space-charge-limited currents.

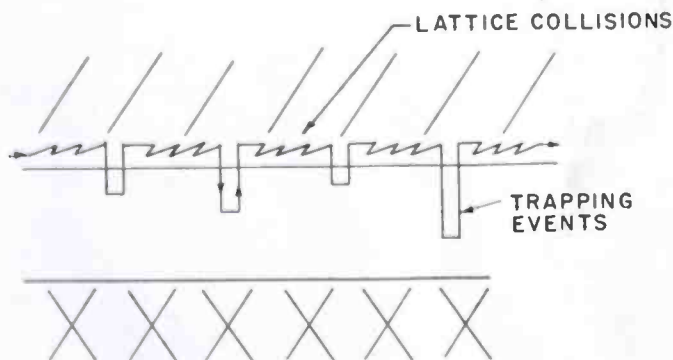
When Equation (5) is applied to a film, or a long slender crystal, a sufficient approximation to the capacitance of the interior is the free-space capacitance of the whole film or crystal, as if the electrodes were not present. The basis for this is that the current will be limited by the space charge of the middle sections which have negligible capacitance to the electrodes. Thus, a film will have a free-space capacitance in farads of the order of 10^{-12} times the geometric mean of its dimensions in centimeters. By way of example, 100 volts across opposite edges of a film one centimeter on a side will give a space-charge-limited current (using Equation (5)) of

$$I \cong \frac{10^4 \times 10^{-12} \times \mu}{1} \text{ amperes}$$

$$\cong 10^{-8} \mu \text{ amperes}$$

$$\cong 10^{-7} \text{ ampere for } \mu = 10 \text{ cm}^2/\text{volt-sec.}$$

Fig. 2 — Effect of traps on mobility.



Note that the thickness of film is not critical and does not enter into the expression as it would have if the plane parallel expression were used.

The value for the mobility (μ) used in this computation is of the order of the mobilities found in polar compounds. It is, however, a highly optimistic value since the effective mobility is likely to be many orders of magnitude lower as a result of trapping. The mobilities measured by the Hall effect are the normal mobilities of free carriers determined by collisions with the lattice. The mobilities effective for the present problem must include trapping because the maximum current is proportional to the speed with which the carriers can get through the crystal. Trapping lowers this speed and thereby increases the space charge.

Quantitatively, trapping is introduced into the mobility as follows:

$$\text{normal mobility} \equiv \mu_0 = \frac{\text{average distance travelled in direction of unit field in time between lattice collisions}}{\text{time between lattice collisions}}.$$

To include the effect of traps, the trapping time is added in the denominator and is apportioned amongst the lattice collisions. Since, for any appreciable trapping, the trapping time far exceeds the time between lattice collisions, the latter may be neglected. The conditions under which this approximation is valid will appear shortly. The result is

$$\begin{aligned} \text{mobility with trapping} &= \frac{\text{average distance travelled in direction of unit field in time between lattice collisions}}{\text{escape time per trap} / \text{number of lattice collisions between traps}} \\ &= \frac{\text{average distance, etc.} \times \text{time between traps}}{\text{escape time per trap} \times \text{time between lattice collisions}} \\ &= \frac{v e^{-b/T}}{v s N} \mu_0, \end{aligned} \quad (7)$$

where $v e^{-b/T}$ is the frequency of escape of an electron from a trap depth of b degrees Kelvin, s is the capture cross section of a trap for an electron, N is the number of traps per cubic centimeter, and v is the thermal velocity of an electron (10^7 cm/sec).

For reasons based on detailed balancing (see Appendix and Ref. (2), p. 108) the value of $\frac{v}{s}$ may be taken to be 10^{26} , and Equation (7) becomes

$$\mu = \frac{10^{19}}{N} e^{-b/T} \mu_0. \quad (8)$$

A lower limit for the trap density (N) based on crystal counter tests is of the order of $10^{15}/\text{cm}^3$. This value of trap density is likely to

permit a crystal to act as a counter for α particles. The scarcity of such counters, even among "good" crystals, suggests a more probable value of trap density of the order of $10^{16}/\text{cm}^3$ or higher, particularly for evaporated photoconductors. With this guide, Equation (8) becomes

$$\mu \leq 10^3 e^{-b/T} \mu_0 \quad (9)$$

Equation (9) says that trapping will lower the normal mobility when the trap depth is more than $7kT$ ($= 0.2$ volt at room temperature). For traps of $1/2$ volt depth and for room temperature,

$$\mu \cong 10^{-5} \mu_0$$

From the above, it is clear that in computing the space-charge-limited current for an insulator, that mobilities many orders of magnitude smaller than the normal mobility need be used and that the magnitudes of the space-charge-limited currents will be reduced accordingly. In the illustration used earlier of one hundred volts across opposite edges of a film one centimeter on a side, the space-charge-limited current will be less than 10^{-12} ampere when half-volt deep traps are present. Traps deeper than half a volt (and there is evidence from glow curve data on phosphors of such traps in ZnS for example) would make the space-charge-limited current practically unmeasurable.

If space-charge-limited currents are present, they should be easily identifiable by the marked saturation of the current-light curve as the current reaches its space-charge-limited value; by the dependence on applied voltage as V^2 ; and by the exponential increase of current with temperature, which rate of increase is also a good measure of the trap depth.

While it is argued here that space-charge-limited currents are ordinarily of negligible magnitude, there are several important exceptions which occur when the inter-electrode distance is 10^{-3} centimeter or less. The space-charge-limited current increases as the cube of the reciprocal spacing. P. K. Weimer^{3, 4} has reported drawing steady currents of a few tenths of a microampere through highly insulating films of amorphous selenium of the order of 10^{-3} centimeter thick. These currents are generated by blue light absorbed at the positive electrode in a tenth to a hundredth of the film thickness. The current

³ P. K. Weimer, "Photoconductivity in Amorphous Selenium", *Phys. Rev.*, Vol. 79, p. 171, 1950.

⁴ P. K. Weimer and A. D. Cope, "Photoconductivity in Amorphous Selenium", *RCA Review*, Vol. XII, No. 3, p. 314, September, 1951.

must then be carried through the film by holes. Weimer has reported also that at high light intensities and/or low applied voltages the initial current decreases with time owing to trapping of the holes. Further measurement on selenium films 3×10^{-3} centimeter thick at very high light intensities showed that the maximum current passed by the film tended to be independent of the light intensity, that it usually increased as the square of the applied potential, and that in most cases it varied rapidly (probably exponentially) with temperature. All of these properties are consistent with space-charge-limited currents. Some departures from space-charge-limited behavior are being investigated. The magnitude of the current and its temperature dependence both pointed to trap depths of about $\frac{1}{2}$ volt.

It is significant that in many similar tests by S. V. Forgue⁵ using various insulating sulphides, selenides and oxides that evidence for space-charge-limited photocurrents has been substantially lacking. Similarly, measurements by L. Pensak⁶ on bombardment induced conductivity in insulating silica films of the order of 10^{-4} centimeter thick have shown negligible currents when the bombarding beam *does not* penetrate the film. In both cases when the light or beam *does* penetrate the film, and space charge is not a limitation, large currents are observed. The conclusion is that either (1) *the traps are deep enough to make the space-charge-limited currents negligible, or (2) that the space-charge-limited current is already supplied in the dark by thermal generation at the electrodes giving rise to the observed dark current. The space-charge-limited current cannot be increased by adding optically excited carriers to the already present reservoir of thermally generated carriers.*

Another example of significantly large currents being drawn through a solid when the carriers are generated only at the electrodes occurs when currents are drawn through a crystal rectifier. Usually, the effective electrode separation (barrier thickness) is small enough, 10^{-6} to 10^{-4} centimeter, to allow milliamperes to be passed at a few volts. The so-called exhaustion layer barriers do not fall in the class of space-charge-limited currents since the exhaustion layer has a distribution of positive charges that neutralize the electron current carriers. The natural insulating barrier, however, is subject to space-charge limitations since the current is injected into the insulator from

⁵ S. V. Forgue, R. R. Goodrich and A. D. Cope, "Properties of Some Photoconductors, Principally Antimony Sulphide", *RCA Review*, Vol. XII, No. 3, p. 335, September, 1951.

⁶ L. Pensak, "Conductivity Induced by Electron Bombardment in Thin Insulating Films", *Phys. Rev.*, Vol. 75, p. 472, 1949.

either metal or semiconductor side. The insulator is essentially charge-free before injection.

In the case of crystal counters, like diamond and silver chloride, it is true that significant current pulses generated at one side of the crystal have been drawn through distances as large as millimeters. From all reports, however, the counting rates of these crystals decrease with time as trapping builds up a space charge so that the *steady-state* currents eventually become negligible. It would be interesting in the case of these crystal counters to actually try to measure the steady-state current as a function of temperature in order to get a measure of the trap depth.

One recent measurement⁷ of the currents that could be drawn through a two-millimeter thick crystal of ZnS when bombarded on one side by a low voltage beam gave currents of the order of 10^{-14} ampere with several hundred volts across the crystal. Since the properties of the observed current did not satisfy the properties of a space-charge-limited current, the latter must have been appreciably less than 10^{-14} ampere. The currents actually observed fit in better with the assumption of a volume or uniformly excited photoconductivity generated by luminescence excited by the bombarding beam. R. W. Smith* has already observed photoconductivity generated in a ZnS film as a result of bombarding a separate or electrically remote sample of ZnS.

VOLUME-EXCITED PHOTOCURRENTS

The term "volume-excited photocurrents" is used to define those photocurrents that result when an insulating sample is uniformly illuminated between electrodes. This is to distinguish the currents from those resulting when only one end of the insulating sample is illuminated. As has just been discussed, the latter currents are generally confined to small space-charge-limited values**. For volume-excited currents, with minor exceptions, positive and negative charges are equally distributed, the material is electrically neutral and space-charge effects do not enter in. The volume-excited currents may indeed be large even for large specimens.

In contrast to the relatively simply defined properties of space-charge-limited currents, the properties of volume-excited currents may

⁷ M. F. Distad, "Equilibrium Currents Induced in Zincblende by Electron Bombardment of Negative Electrode", *Phys. Rev.*, Vol. 80, p. 879, 1950.

* Unpublished work.

** This remark applies also to semiconductors in which only one sign of carrier is mobile but not to semiconductors in which both signs of carriers are mobile.

be quite varied. It becomes important to try to select the simplest terms in which these photoeffects may be described and to avoid mathematical complexities that may add only a degree of precision at the expense of clarity. The literature offers an abundance of data for which even first order interpretations would be profitable.

In the discussions that follow, the normal mobility, μ_0 , of an electron is taken to be $10 \text{ cm}^2/\text{volt-sec}$. This is an approximation to a very few experimental measurements for sulphides, lying in the range of one to $100 \text{ cm}^2/\text{volt-sec}$. and to one or two analytic estimates for polar materials in the range of one to ten. Data on the mobility of holes are similar but even more sparse. The variability of the normal mobility, in any event, is small compared with the variability of trapping effects and capture cross sections. Effects that vary no faster than a low power of the absolute temperature will either be neglected or referred to as slow variations. The temperature variations of the normal mobility or the thermal velocity are examples.

The symbol f , defined as the number of excitations per unit volume per second, will be used throughout to avoid repeated reference to quantum yields. Generally, photoconductors are sensitive only in the spectral range where they absorb substantially all of the incident light so that the quantum yield for the primary excitation process is substantially unity. For radiation in the visible spectrum, f may be converted to more familiar terms by these two relations:

$$10^{-16}f \doteq \text{number of lumens in the visible spectrum absorbed per unit volume,}$$

$$10^{-19}f \doteq \text{number of watts in the visible spectrum absorbed per unit volume.}$$

The photocurrent in each case will be written in the form:

$$\text{Number of electron charges passed per second} = G \times \text{number of photons absorbed per second,}$$

$$I/e = GF$$

$$= \frac{\tau}{T_r} F, \quad (10)$$

where F = total number of excitations per second = $f \times$ volume of photoconductor used. τ is the lifetime of a free carrier, and T_r is the transit time of a free carrier between electrodes.

This form has the advantage of conceptual simplicity as well as giving the information most frequently desired, namely, the number

of electron charges passed per incident photon. It has another advantage in that the value of τ can be used to compute a figure of merit. Thus, for a given photoconductor I , T_r , and F are observables from which a value of τ may be computed. If this value of τ is equal to the observed time constant for the photocurrent (that is, the time required for the photocurrent to decay to half its initial value after the light is interrupted), the maximum performance of the photoconductor is being obtained. If τ is less than the observed time constant, the fraction of maximum performance being obtained is given by the ratio of computed to observed time constants.

Ordinarily one would expect that the observed time constant would be equal to the life time of a free carrier, and it is this expectation which, from Equation (10), has given rise to the expectation that photosensitivity and speed of response are so related that the faster photoconductive materials should be less sensitive. In Equation (10), the faster materials would correspond to a smaller value of τ , and of sensitivity, provided speed of response and life time of a free carrier were one and the same thing. The fact that these two quantities are not necessarily the same will form a large part of the following discussions and will help to account for the ample experimental evidence that is not consistent with a reciprocity between sensitivity and speed of response.

The properties of photocurrents that will be discussed in each case will be first the magnitude of the sensitivity and its dependence on light intensity, temperature and applied voltage and second, the magnitude of the observed time constant and its dependence on light intensity, temperature and applied voltage. If the observed time constant and life time of a free carrier were the same, either one of these parts would suffice by itself.

1.0 Primary Photocurrents (Figure 3)

If one starts with an insulator which does not permit entry of carriers *from the electrodes into the insulator* and restricts the photocurrents to a range of values below that in which the space charge of the carriers offers any current limitations, the concept of light creating free electrons and holes and these carriers being drawn to their appropriate electrodes is physically quite sound. As Gudden and Pohl have pointed out,* the photocurrent should be proportional to the light intensity and insensitive to temperature. This will be true when the

* Actually the primary currents which Gudden and Pohl discussed were currents carried by electrons while the holes were thought to remain fixed. Under these conditions it is impossible to draw steady primary currents and their observations had to be limited to the measurement of initial transients.

voltage is high enough to *saturate* the photocurrent by pulling the carriers to their respective electrodes before they have a chance to recombine. The time constant need not, however, as they suggest, be "fast". The rise and decay time of the photocurrent will be of the order of the transit time of the slowest carrier through the insulator. If the mobility of the carriers is the normal mobility determined by lattice collisions, this time constant will usually be fast, depending of course on the geometry and applied voltage. If the mobility is lowered by trapping, the time constant may easily increase to milliseconds, seconds or longer.

In terms of the equation for photocurrent,

$$I/e = \frac{\tau}{T_r} \cdot F;$$

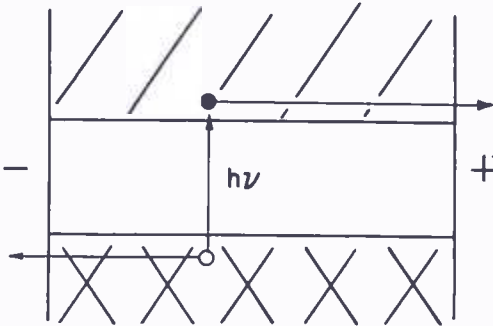


Fig. 3—Primary photo-effect.

the gain, $\frac{\tau}{T_r}$, is unity and independent of temperature, light intensity and applied voltage—assuming the voltage is high enough to saturate the photocurrent. Under these conditions, the observed time constant, the life time of a carrier, τ , and the transit time, T_r , are one and the same. As the voltage is increased in the saturation range, τ and T_r both decrease as the reciprocal voltage. The observed time constant should not change with light intensity and only slowly with temperature unless trapping is present.

All of the above remarks refer to the saturated primary current. If the applied voltage is not high enough to draw the carriers to their electrodes before they recombine, many of the relations are changed. Indeed, the photocurrents then become indistinguishable from the photocurrents to be described below under the heading of "secondary photocurrents", and will accordingly be discussed there since the treatment of secondary photocurrents has more general validity. In brief, an unsaturated primary photocurrent cannot be recognized as

a primary current. Only if the voltage is raised and the current saturates at a value close to unity gain is the designation "primary" reasonably justified.

Reasonable evidence for primary currents has been reported by Gudden and Pohl¹ for carefully selected natural crystals of ZnS and diamond and by Weimer³ for thin layers of amorphous selenium. Recent work on crystal counters⁸ has given evidence of primary currents in diamond, silver chloride and thallos bromide based on getting *saturated* yields that are of the same order as the number of secondary electrons to be expected from one alpha particle. While CdS has several times appeared in the list of counting crystals, there is evidence that its currents are usually of a secondary nature, that is, gains greater than unity. In fact, the ease and continuity with which selenium can grade from primary to secondary currents generally make one question the purity of some of the reported primary currents. *Physically, all that is needed to contaminate a primary photocurrent is to allow replenishing of the carriers at the electrodes, that is, entrance of carriers from metal to insulator.* And this may take place in continuously graded form.

One of the most likely examples of pure primary photocurrent should be that generated at a simple *P-N* junction in a semiconductor when it is biased in the back direction.⁹ The *P-N* junction is the insulator, while the *P* and *N* type semiconducting materials on either side are the electrodes. Even before light is introduced, the few free electrons on the *P*-side and the few free holes on the *N*-side that might act as replenishers are already drawn across as a saturated dark current. There is then no source of further replenishment when the light is introduced and creates free pairs of carriers within the *P-N* junction. These free pairs are drawn off as a saturated primary photocurrent. A formally possible source of replenishing in the case of the *P-N* junction exists at fields sufficiently high to excite electrons from the filled to the conduction band by field emission. Fields greater than 10^6 volts/cm would be needed before field emission would contribute appreciably to a secondary photoeffect.

On the other hand, the class of photocells consisting of metal-semiconductor rectifying contacts, biased in the *back* direction, can readily stray across the division from primary to secondary currents. The currents normally observed for these cells (grey selenium, Cu_2O , germanium, and CdS) are of the order of unity gain and can be

⁸ R. Hofstadter, "Crystal Counters", *Nucleonics*, Vol. 4, p. 2, 1949.

⁹ W. J. Pietenpol, "P-N Junction Rectifier and Photocell", *Phys. Rev.*, Vol. 82, p. 120, 1951.

saturated with small voltages. It is not difficult, however, to observe gains somewhat greater than unity, as for example, in the photo-transistor or in grey selenium¹⁰. A reasonable and already reported source for these gains is the secondary current resulting from electrons pulled out of the metal by approaching holes or trapped holes. A similar argument may be made for the secondary currents observed for the insulating amorphous selenium films used in the vidicon. Here, it is the trapped electrons near the signal plate that may pull out holes from the signal plate into the insulator.

2.0 Secondary Photocurrents

If free access of carriers from the electrodes into the insulator is allowed, a whole new set of photoconductive processes is generated. The photoevent that started with the liberation of a free pair of carriers is no longer terminated when these carriers reach their respective electrodes. Other carriers coming out of the electrodes take their place. The termination occurs when a free pair of carriers (electron and hole) recombines into their initial state before excitation. One prominent consequence is that gains far in excess of unity are now permitted.

The various possible processes are determined by combinations of the following conditions: one or both carriers replenished at the electrodes; one or both carriers are mobile; the absence or presence of traps and the energy distribution of traps when they are present; the photocurrents are small or large compared with the dark current. These processes will be discussed in increasing order of complexity.

2.1. Case of No Trapping (Figure 4)

A first example is defined by the following conditions:

- 1) Both carriers are replenished at the electrodes,
- 2) Both carriers are mobile,
- 3) Trapping is not present,
- 4) Dark current is negligible.

The density of free carriers is given by

$$\begin{aligned} \text{rate of excitation} &= \text{rate of recombination} \\ &= \frac{\text{equilibrium number of carriers}}{\text{life time of a carrier}}, \end{aligned}$$

$$f = \frac{n_0}{(vsn_0)^{-1}}$$

¹⁰ J. H. Sargrove, "The A. C. Behaviour of Barrier Layer Photo-Cells", *Proc. I.R.E. (Brit.)*, Vol. 7, p. 86, 1947.

$$= v s n_c^2, \tag{11}$$

where v = thermal velocity,

s = capture cross section of a hole for an electron,

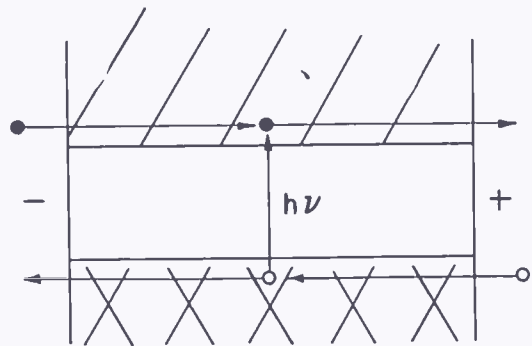
n_c = number of free electrons (or holes) per cm^3 ,

$\frac{1}{v s n_c}$ = time required for an electron to trace out a volume equal to that associated with one hole

= life time of an electron (τ)

= (in the absence of traps) observed time constant.

Fig. 4—Secondary photoeffect: no trapping, both carriers mobile and replenished at electrodes.



Since the transit time of a free carrier is given by

$$\frac{L^2}{V \mu_o}, \tag{12}$$

the photocurrent may be written

$$\begin{aligned} \frac{I}{e} &= \frac{\tau}{T_r} F = \left(\frac{1}{v s n_c} \right) \frac{F}{L^2 / V \mu_o} \\ &= \frac{V \mu_o}{L^2 v s n_c} F, \end{aligned}$$

and since, from Equation (11), $n_c = \left(\frac{f}{v s} \right)^{1/2}$,

$$I/e = \frac{V\mu_o}{L^2(vsf)^{1/2}} F. * \quad (13)$$

The sensitivity (gain factor) is proportional to applied voltage, is only slowly dependent on temperature, and is inversely proportional to the square root of the light intensity. It may be greater or less than unity. The observed time constant is

$$\tau_o = \frac{1}{vsn_o} = \left(\frac{1}{vsf} \right)^{1/2}, \quad (14)$$

and is independent of applied voltage and insensitive to temperature, but varies as the square root of the reciprocal light intensity.

The well-known properties of bimolecular recombination are readily recognizable in the above model. Attempts to use this model, however, to analyze the usual photoconductive currents run into immediate difficulties. Many photoconductors show a near linear rise of photocurrent with light intensity. R. W. Smith¹¹ has observed exponents of 0.8-0.9 for some samples of CdS extending over three orders of magnitude of light intensity.

Another discrepancy arises from the magnitude of observed currents. They are smaller than would be expected from an estimate of the gain factor. For the thin insulating targets of sulphide materials reported by S. V. Forgue⁴ the transit time of carriers through the target, using a mobility of 10 cm²/volt-sec., is of the order of 10⁻⁸ second. The observed time constants were of the order of 10⁻¹ second. If the observed time constant is identified with the life of a free carrier, the estimated gain would be of the order of 10⁷. Actually, gains of 10⁻² to unity were commonly observed. The same lack of sensitivity was observed by Pensak⁵ and by Anspacher and Ehrenberg¹² for bombardment induced conductivity measurements.

What is missing in the above picture is the presence and effects of trapping. From many sources, trap densities of 10¹⁵/cm³ and greater are to be expected. Since the density of photoelectrons is likely to range from 10¹⁵/cm³ downward, there is reason to expect that most of the excited photoelectrons will be trapped and that only

* Strictly, Equation (13) should contain the sum of electron and hole mobility rather than just the mobility of electrons.

¹¹R. W. Smith, "Some Aspects of the Photoconductivity of Cadmium Sulfide", *RCA Review*, Vol. XII, No. 3, p. 350, September, 1951.

¹²F. Anspacher and W. Ehrenberg, "Electron Bombardment Conductivity of Dielectric Films", *Proc. Phys. Soc. (A)*, Vol. 64, p. 362, 1951.

a small fraction will at any one time contribute to the photocurrent.

At very high current densities (conductivities greater than 10^{-3} ohm-cm), that is, when the number of free conducting carriers exceeds the number of traps, the photo properties just discussed for trap-free materials should hold. Some evidence to date indicates that CdS approaches this state at high light intensities¹¹.

2.2. Case of Trapping

2.2.1. General Remarks

It was pointed out that the inability of most insulating materials to act as counters indicated that trap densities well in excess of $10^{15}/\text{cm}^3$ were the rule. This is a relatively high density. It may be contrasted, for example, with the density of free carriers found in materials used for various charge storage purposes. A density of 10^7 carriers per cm^3 or eight orders of magnitude smaller than the trap density is a representative value. This large disparity is important in its effect on observed sensitivities and time constants. It is important also in allowing many simplifying approximations to be made in computing the photoconductive properties of insulators.

The effect of trapping may be regarded, as it was in the case of space-charge-limited currents, as a reduction in the average mobility of the total number of excited carriers. This point of view was preferred for space-charge-limited currents because the space charge build-up was directly proportional to the average drift velocity of *all* the excited carriers. In the present treatment of volume-excited currents, however, where space charge does not enter in, an alternative approach will be taken. The normal mobility, determined by lattice collisions, will be used and will be applied to only that fraction of the total number of excited carriers that is in the free states in order to compute the photoconductive current. The effect of traps is, of course, to reduce the fraction of total number of excited carriers in the free states. This approach has certain conceptual advantages as well as allowing a consistent treatment of time constants.

Most emphasis will be placed on a model in which carriers of one sign, for convenience of reference the holes, are immobile. The immobility may be an intrinsic property resulting from the deep lying position of the filled band or it may be an acquired property resulting from asymmetric trapping conditions. For example, if one starts with an insulator in which discrete states are more or less uniformly distributed in energy in the forbidden band, and in which the Fermi level lies in the middle of the forbidden band, the chances of trapping a free electron or a free hole are likely to be symmetric. That is, the

number and depth of traps, by assumption, are substantially the same for electrons and holes. If, now, high lying n-type centers are added, the Fermi limit will be shifted toward the conduction band*—electrons from the n-type centers settling into the deeper traps. The result will be a trapping asymmetry such that the traps for holes will be deeper than those for electrons. To a good approximation, then, one may take the holes as completely trapped and the electrons as distributed between the conduction band and trapping states. The holes become fixed primary centers from which electrons were excited and to which they eventually return. Because of the immobility of the holes, recombination will take place only between free electrons and fixed holes (primary centers). Recombination between trapped electrons and holes is highly unlikely. Even for trap densities as high as $10^{16}/\text{cm}^3$, the probability of finding an electron and hole trap at adjacent sites,

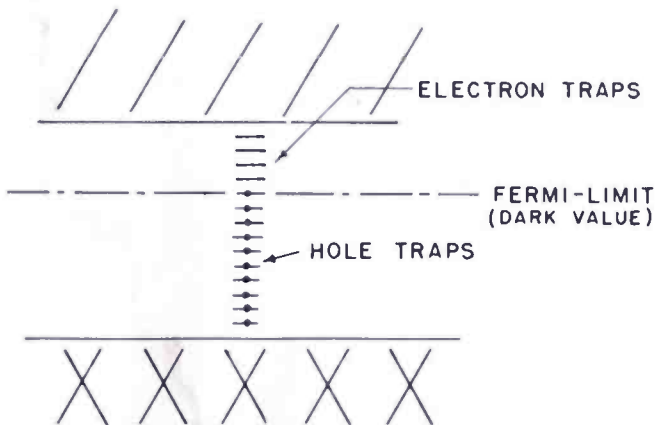


Fig. 5—Asymmetric trapping.

if these traps are randomly distributed, is negligibly small.

The picture presented at this point is that of an insulator in which light has created a number of hole-electron pairs. The holes are either immobile or rapidly and completely trapped. The electrons distribute themselves amongst the free states of the conduction band and the traps. Recombination takes place between the free electrons and the fixed holes.

The approximations here have been chosen in order to get a variety of easily calculable results and, at the same time, to retain the important properties of real insulators. A suggestion of the complexities inherent in the problem is given by the following expression for photocurrent obtained by Broser and Warminsky¹³ from a detailed con-

* By virtue of dissociation and lattice defects the Fermi limit is more likely than not to be "off-center".

¹³ I. Broser and R. Warminsky, "Theory of Luminescence and Electrical Conductivity of CdS Crystals", *Ann. der Phys.*, Vol. 7, p. 288, 1950.

sideration of kinetic reactions and from a different choice of approximations,

$$j = \frac{b_f E e}{2\beta (\alpha A + \kappa H)} \left\{ [\gamma \kappa H + \beta Z] \left[1 + 4\alpha A \beta Z \frac{\alpha A + \kappa H + \gamma}{(\gamma \kappa H + \beta Z)^2} \right]^{\frac{1}{2}} - [\gamma \kappa H - \beta Z] \right\} \text{ amperes/cm}^2$$

where α , β , γ and κ are constants for the various rates of excitation and recombination, A is the concentration of activators, H is the concentration of traps and Z is the rate of volume excitation by the incident light. Insofar as the present model is valid, a large measure of analytic compactness is achievable.

2.2.2. Computation of Current

In the steady state there is an equality between the rate of excitation by light and the rate of recombination. Thus

$$f = v s n_c n_p, \quad (15)$$

where n_p is the number per cm^3 of trapped holes which may be called primary centers and is equal to the number of free electrons (n_c) + the number of trapped electrons (n_t). From Equation (15)

$$n_c = \frac{f}{v s n_p}. \quad (16)$$

There is also, at the same time, a thermal exchange between free electrons and trapped electrons. *The rates of these exchanges do not affect the sensitivity; they may affect the observed time constant.*

The mean life time of an electron in the conduction band is

$$\tau = \frac{1}{v s n_p}. \quad (17)$$

It is the time a conduction electron takes to trace out a volume equal to the volume associated with a primary center. The transit time of a conduction electron between electrodes is given, as before, by

$$T_r = \frac{L^2}{V \mu_0}.$$

Thus, the gain factor is

$$G = \frac{\tau}{T_r} = \frac{V\mu_0}{L^2 v s n_p}, \quad (18)$$

and the photocurrent may be written as

$$\frac{I}{e} = GF,$$

or

$$I = e \frac{V\mu_0}{L^2 v s n_p} F. \quad (19)$$

This may be compared with the case for no traps where

$$I = e \frac{V\mu_0}{L^2 v s n_0} F. \quad (20)$$

The notable difference is in the appearance of either n_p or n_0 in the denominator. Since, as will be shown, n_p is the order of the number of traps (10^{15} or greater) and since n_0 may often be in the range of 10^7 to 10^{15} , there will, in general, be a large *desensitizing* effect of the traps varying from unity to 10^{-8} .

What has been computed thus far is the observed photocurrent. In this expression n_p is the only quantity that refers to the effect of traps. The observed time constant has not yet been computed. Before computing it, it will be useful to introduce a concept of the steady-state Fermi limit in order to get a ready means for estimating n_p and its variation with light intensity and temperature.

2.2.3. Steady-State Fermi Limit (Figure 6)

It was pointed out that in the steady state there was a thermal exchange between electrons in the conduction band and electrons in traps. This thermal exchange may actually become a thermal equilibrium provided the trapped electrons have access only to the conduction band and only by thermal excitation. The first condition is insured by the assumption that the holes are fixed so that recombination between free holes and trapped electrons is avoided. The second condition is closely approximated for strongly absorbed light which can be expected to excite electrons out of the filled band rather than out of traps.

To the extent that thermal equilibrium is valid, a Fermi limit is defined such that the states a few kT below this limit are substantially filled while those a few kT above the limit are substantially empty. For states more than a few kT removed from the Fermi limit, the fraction of states occupied (by electrons on the high side or holes on the low side) is given by the Boltzman factor $e^{-b/T}$ where b is the energy in degrees Kelvin between the Fermi limit and the states in question. Conversely, if one knows the occupancy of a group of states, the location of the Fermi limit is determined.

The occupancy of states in the conduction band is already set by the steady state equilibrium between optical excitation of electrons

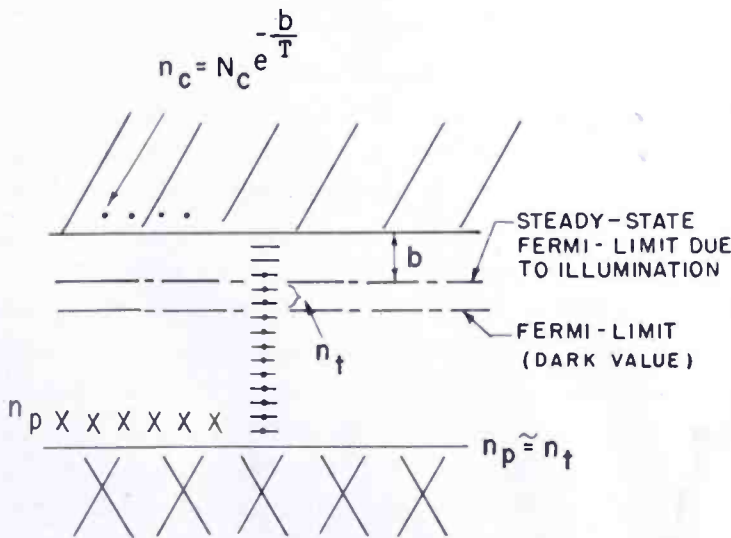


Fig. 6—Steady-state Fermi limit.

into the conduction band and recombination of these electrons with their primary centers. Now most of the electrons in the conduction band lie in states within a few kT of the bottom of the band. Thus, if one takes the number of these accessible states to be N_c ($\sim 10^{19}$ at room temperature) the occupancy fraction is n_c/N_c and the Fermi limit lies a distance b below the conduction band given by

$$\frac{n_c}{N_c} = e^{-b/T} \tag{21}$$

In brief review, the optical excitation determines the density of electrons in the conduction band; the ratio of this density to the density of available states determines the location of what is here called the steady-state Fermi limit to distinguish it from its normal

location in the dark; the states (traps) below the Fermi limit are substantially occupied; those above are substantially empty.

The problem set up was to find a measure of n_p . That measure is given by the number of electron traps lying below the steady-state Fermi limit because these traps, occupied by electrons, constitute the bulk of the excited electrons which number of excited electrons is equal to the number of primary centers n_p . Exceptions will occur when the concentration of shallow traps greatly exceeds the concentration of deep traps. (See, e.g., section 2.2.7.) The number of primary centers and its variation with light and temperature determine the sensitivity and its dependence on light and temperature.

2.2.4. Observed Time Constant (Figure 7)

Let a photoconductor be illuminated by a steady light and let a steady photocurrent be drawn. If the light is interrupted, the photocurrent will decay as the electrons in the conduction band recombine with their primary centers. It is clear that, if all that was involved was a recombination of free electrons with their primary centers, the time taken for the current to decay to half its initial value (observed time constant) would be equal to the average life time of a conduction electron. If, however, the conduction electrons are replenished by electrons out of the trapping states, the decay of the concentration of free electrons and of the observed current will be slowed up. In particular, before the current decays to half value a large number of trapped electrons, as well as half the initial number of conduction electrons, will have had to be recombined via the conduction band with primary centers. Whether or not significant replenishment takes place depends upon the relative rates of exchange between conduction electrons and trapped electrons on the one hand, and conduction electrons and primary centers on the other. If the rate of exchange with traps is large compared with the rate of exchange with primary centers, replenishment of conduction electrons by thermal release of trapped electrons will almost keep pace with the loss of conduction electrons by recombination with primary centers. In this case, one may consider the conduction electrons to be in thermal equilibrium with the trapped electrons *during the decay process*. This means that in order for the current to decay to half value the steady-state Fermi limit must drop by approximately one kT and that the electrons trapped in this kT slice of energy must be emptied via the conduction band into their primary centers. Since the number of electrons in these traps is usually large compared with the number of conduction electrons the observed time constant may be written with good approximation:

$$\tau_0 = \frac{\text{Number of electrons trapped in an energy slice } kT \text{ wide in the neighborhood of the steady-state Fermi limit}}{\text{Rate of recombination of conduction electrons with primary centers}}$$

$$= \frac{n_b T}{v s n_c n_p}, \tag{22}$$

where n_b is the number of traps per unit volume per unit energy range taken at the Fermi limit.

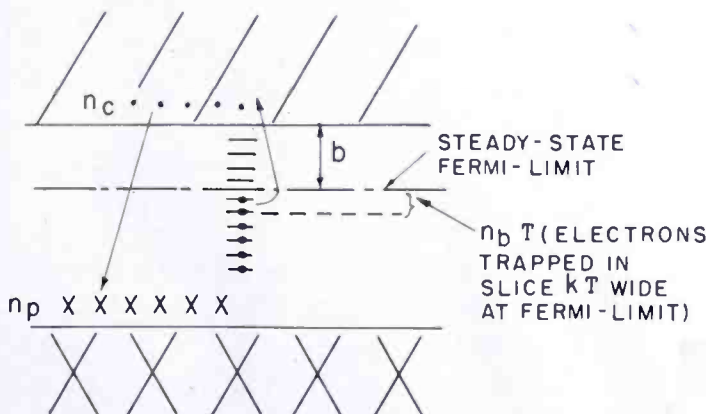


Fig. 7—Contribution of trapped electrons to observed time constant.

If the rate of exchange of conduction electrons with traps is small, say a tenth or less the rate of exchange with primary centers, the current will decay rapidly to a tenth its value or less before replenishment by trapped electrons becomes significant. The trap distributions that will lead to this condition will be discussed later. For the moment it must be emphasized that the ratio of the two rates of decay may be very large — of the order of the ratio of number of conduction electrons to number of trapped electrons. In particular, as will be shown shortly, the observed time constant for a uniform distribution of traps *with replenishment* is

$$\tau_0 \cong \frac{10^{-1}}{v s n_c}, \tag{23}$$

while for the absence of replenishment this time constant is

$$\tau_0 = \frac{1}{vsn_p} \quad (24)$$

Remembering that n_p may be orders of magnitude larger than n_c , the ratio of the two time constants may be similarly large. Since both time constants may occur in the same specimen after interruption of the light, a possible source is provided for the frequently observed strong separation of the current decay curve into a long and short component.

It is clear from the expressions for sensitivity and time constant that these quantities and especially their variation with light and temperature will be a function not only of the number of traps but also of their distribution in energy. From glow curve data on phosphors¹⁴ there is evidence that traps may be continuously distributed below the conduction band to a depth of as much as one volt.* The consequences of several representative distributions will be discussed separately below.

2.2.5. Uniform Distribution of Traps (Figure 8)

Let the traps be uniformly distributed in energy to a depth of about a volt below the conduction band and let the steady-state Fermi limit be *amidst* the trap distribution. The density of conduction electrons due to optical excitation is, as before,

$$n_c = \frac{f}{vsn_p} \quad (25)$$

Now it is immediately evident that n_p (the number of primary centers) remains almost constant while n_c varies over many orders of magnitude. For example, let the steady-state Fermi limit vary from 0.5 volt to zero volts below the conduction band. n_p will then increase by a factor of two. At the same time n_c will increase by the factor $e^{b/T}$ where b is half a volt. This factor is about 10^9 at room temperature. The result is that the photocurrent will vary as the 0.97 power of the light intensity or be almost indistinguishable from a linear function.

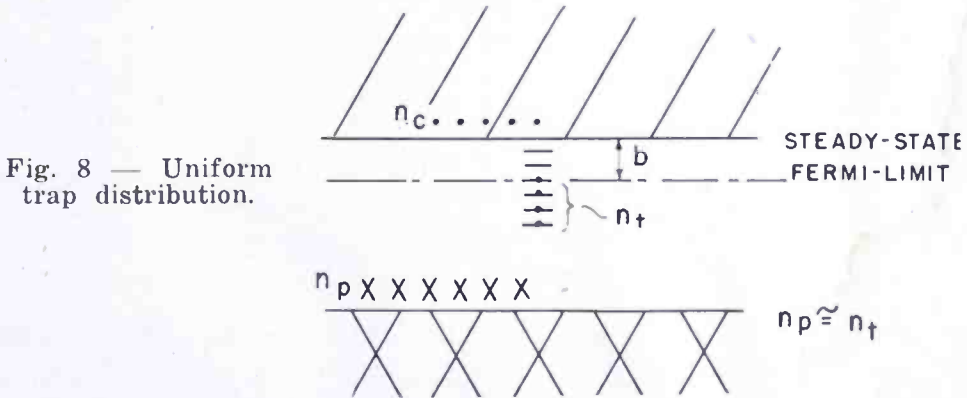
¹⁴ R. H. Bube, "Luminescence and Trapping in Zinc Sulphide Phosphors with and without Copper Activator", *Phys. Rev.*, Vol. 80, p. 655, 1950.

* It is not meant to imply here that the traps that are effective for luminescence are necessarily also effective for photoconductivity (see also Ref. (19)).

Next, let the temperature be varied while keeping the light intensity fixed. From Equation (25), n_c will change only if n_p changes.* But as long as the Fermi limit lies within the uniform trap distribution, n_p will undergo only small changes. Therefore, n_c is similarly restricted and, to a good approximation, the steady-state Fermi limit will change proportionately with the absolute temperature so that n_c in the relation

$$n_c = N_c e^{-b/T} \tag{26}$$

is maintained constant. That is, the photocurrent should be insensitive to temperature. In the second approximation the photocurrent will increase slowly with temperature (less than a factor of two in the range of 100°C above or below room temperature). This is of the



order of the changes in thermal velocity which are being ignored in the discussion.

The magnitude of the photocurrent is given, as before, by

$$I = e \frac{V\mu_0}{L^2 v s n_p} F. \tag{27}$$

The parameters of particular interest are the capture cross section, s , and the number of primary centers, n_p , which is substantially given by the number of traps. The capture cross section may vary from 10^{-12} cm² to values less than 10^{-20} cm². The density of traps is likely to exceed 10^{15} /cm³ and be bounded on the top side by the number of atoms (10^{23}) per cm³. Methods for measuring both these parameters are particularly desirable in order to characterize the sensitivity properties of a photoconductor.

* The capture cross section is assumed to be independent of temperature. The discussion of the effect of temperature dependence of the capture cross section is postponed until the trapping effects have been clarified.

To summarize, the assumption of traps distributed uniformly in energy leads to photocurrents that are insensitive to temperature; that increase linearly with light intensity; and that may vary from sample to sample over many orders of magnitude depending upon the number of traps and the capture cross section of primary centers for conduction electrons.

The expression for the observed time constant (assuming rates of exchange between conduction electrons and traps to be greater than between conduction electrons and primary centers) was given by

$$\tau_0 = \frac{n_b T}{v s n_c n_p} \text{ seconds,} \quad (28)$$

where n_b is the number of traps per cm^3 per unit energy measured in $^\circ\text{K}$. For trap distributions extending a half a volt to a volt below the conduction band, $n_b T$ is 1/20 to 1/40 the total number of traps since T at room temperature is 1/40 of a volt. Thus, to a sufficient approximation,

$$\tau_0 \cong \frac{10^{-1}}{v s n_c} \text{ seconds.} \quad (29)$$

The observed time constant should vary as the reciprocal conductivity or light intensity and should be insensitive to temperature. The time constant is *not dependent on the number of traps* but is dependent on the capture cross section. The observed time constant is larger than the life time of a conduction electron. The latter is given by

$$\tau = \frac{1}{v s n_p}.$$

Thus, the ratio of observed time constant to the average life time of a conduction electron is

$$\frac{\tau_0}{\tau} \cong 10^{-1} \frac{n_p}{n_c}, \quad (30)$$

and this ratio may take on values from unity to greater than 10^6 . This relation is valid only for $n_p \gg n_c$, so that $\tau_0 > \tau$. The observed time constant cannot be less than the life time of a conduction electron.

2.2.6. Fermi Limit Lying Above the Traps (See Figure 9)

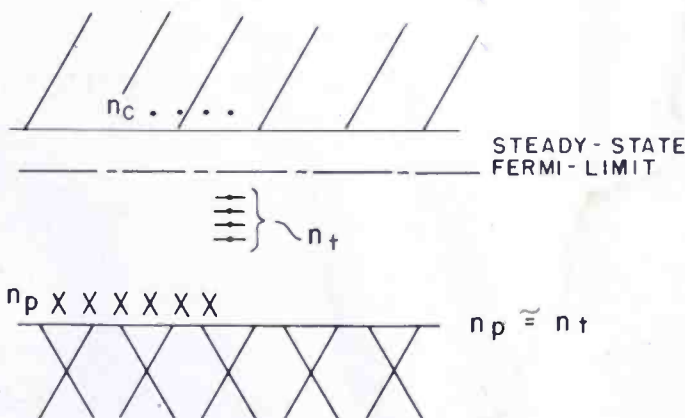
By inspection of Figure 9, and by use of arguments just employed

for the uniform trap distribution, it is evident that the photocurrent is still linearly dependent on light intensity and is even less sensitive to temperature. The observed time constant, however, is radically reduced since now, instead of having to recombine the conduction electrons plus the very much larger slice of trapped electrons near the Fermi limit, only the conduction electrons need to be recombined. The observed time constant is given by

$$\tau_0 = \frac{n_c}{vsn_c n_p} = \frac{1}{vsn_p}, \tag{31}$$

and is equal to the life time of a conduction electron. This time constant will not vary with light or temperature as long as the Fermi limit lies above the trap distribution.

Fig. 9—Steady-state Fermi limit lying above trap distribution.



2.2.7. Fermi Limit Lying Below the Trap Distribution (Figure 10)

Let there be a uniform distribution of traps extending from the conduction band to a depth b_0 below the conduction band, and let the steady-state Fermi limit be below b_0 at a depth b . The number of electrons in traps is then

$$n_t = \int_{b-b_0}^b n_b e^{-b/T} db$$

$$\doteq n_b^0 T e^{b_0/T} e^{-b/T}, \tag{32}$$

where n_b is the number of traps per cm^3 per unit energy depth. But, from the nature of the steady-state Fermi limit, the number of electrons in the conduction band is

$$n_c = N_c e^{-b/T}.$$

Accordingly, at a fixed temperature the number of electrons in traps is proportional to the number of free electrons,

$$n_t = \frac{n_b T}{N_e} e^{b_0/T} n_c = \alpha(T) n_c \tag{33}$$

If trapping is to be effective, the number of electrons in traps will exceed the number of free electrons, so that

$$n_p = n_t + n_c \doteq n_t = \alpha(T) n_c \tag{34}$$

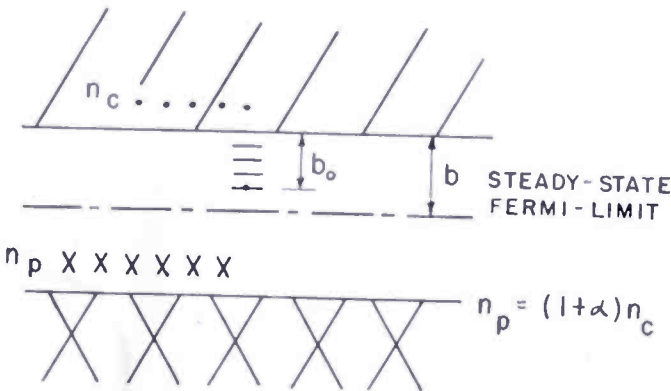


Fig. 10 — Steady-state Fermi limit lying below trap distribution.

Thus, in the expression already derived for the concentration of electrons in the conduction band,

$$n_c = \frac{f}{v s n_p},$$

the value of n_p may be inserted from Equation (34) giving

$$n_c = \left[\frac{f}{v s \alpha(T)} \right]^{1/2} \tag{35}$$

Of chief significance is the change in form such that n_c or the photocurrent now increases at the *square root* of the light intensity rather than linearly. The square-root form is obtained even though the reacting groups n_c and n_p are highly unequal; that is, $n_p \gg n_c$, just as they were for traps below the Fermi limit. The difference is that now n_p changes proportionately with n_c .

The temperature dependence of the photocurrent is given by $\alpha(T)$

or, from Equations (33) and (35),

$$n_c \sim e^{-b_0/T}.$$

That is, the photocurrent increases exponentially with temperature at a rate determined by the trap depth, b_0 .

The observed time constant is determined by the time necessary to empty half the trapped electrons, since these exceed the number of free electrons.

$$\begin{aligned} \tau_0 &\doteq \frac{n_c + n_t}{vsn_c n_p} \\ &\doteq \frac{n_t}{vsn_c n_t} \\ &= \frac{1}{vsn_c}. \end{aligned} \tag{36}$$

The observed time constant is the same as it would be in the absence of traps even though the traps have lowered the sensitivity by the ratio

$$\frac{n_c}{n_p} \doteq \frac{1}{\alpha(T)}.$$

The observed time constant also is larger than the life time of a free electron by the factor $\alpha(T)$.

2.2.3. Fermi Limit Lying in a Void in the Trap Distribution (Figure 11)

As long as the number of electrons trapped in states below the Fermi limit exceeds those in the conduction band and in shallow traps, the photocurrent will be linearly dependent on light intensity and insensitive to temperature. The observed time constant, also, will be invariant with light intensity. Its magnitude, however, will be increased by the number of electrons in shallow traps since these must now be recombined along with the conduction electrons. The number of electrons in shallow traps is given as in the previous case by $\alpha(T)n_c$, and if these exceed the number in the conduction band, the observed time constant is

$$\tau_0 = \frac{\alpha(T)n_0}{vsn_c n_p}$$

$$= \frac{\alpha(T)}{vsn_p} \tag{37}$$

That is, the observed time constant will exceed the life time of a free electron by the ratio $(\alpha(T))$ of electrons in shallow traps to those in the conduction band. This ratio is temperature dependent and decreases exponentially with temperature since

$$\alpha(T) \sim e^{b_0/T}$$

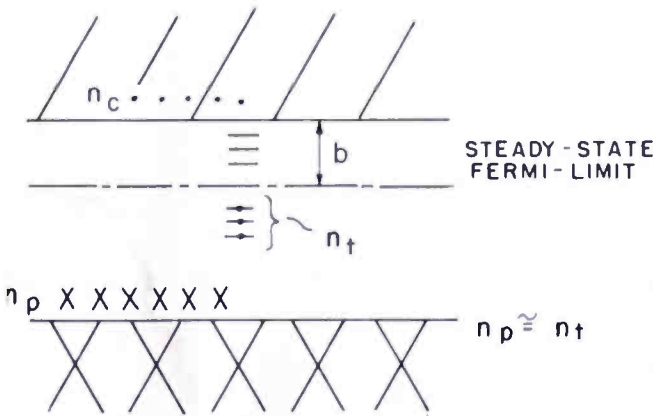


Fig. 11 — Steady-state Fermi limit lying in void in trap distribution.

where b_0 is a mean depth for shallow traps. While the time constant should decrease with increasing temperature, the sensitivity should be substantially constant, being determined by the larger fixed number of electrons in deep traps.

As the light intensity is increased the Fermi limit approaches the level of shallow traps. If the number of these traps exceeds the number of deep traps, the electrons trapped above the Fermi limit will exceed those trapped below. At this point, the current-versus-light curve will bend into a square-root form, and the photoconductive properties will duplicate those discussed in the previous section, namely, sensitivity increasing exponentially with temperature, and time constant invariant with temperature.

2.2.9. Exponential Trap Distribution (Figure 12)

Let the traps be distributed in exponentially decreasing numbers below the conduction band such that the energy distribution is given by

$$n_b db = A e^{-b/T_1} db.$$

The temperature T_1 is used here to indicate a temperature higher than room temperature. Physically, T_1 might be the temperature at which the traps were "frozen in" as the crystal cooled and, accordingly, its value is likely to be 1000°K or higher.

The number of electrons trapped below the Fermi limit is, as before, equal to the number of traps below the Fermi limit and is a good approximation of the number of primary centers. Thus

$$\begin{aligned} n_p &\cong \int_b^\infty A e^{-b/T_1} db, \\ &= AT_1 e^{-b/T_1}. \end{aligned} \tag{38}$$

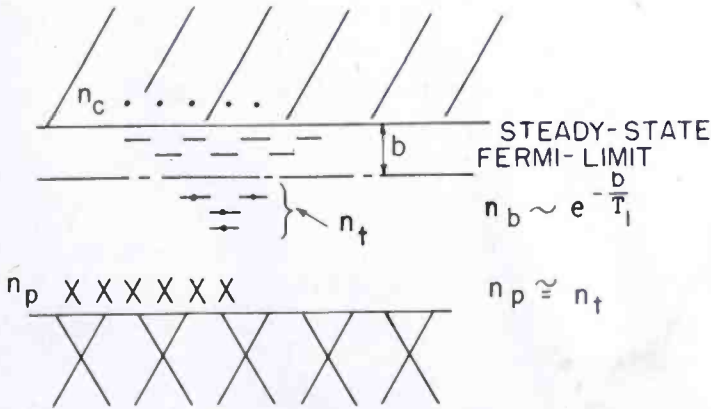


Fig. 12—Exponential trap distribution.

If this value for n_p is used in the expression for the number of conduction electrons,

$$\begin{aligned} n_o &= \frac{f}{vsn_p} \\ &= \frac{f}{vsAT_1 e^{-b/T_1}}. \end{aligned} \tag{39}$$

The value of the Fermi limit b is given, as usual, by

$$n_o = N_o e^{-b/T_1},$$

or

$$b = T \ln \frac{N_c}{n_c}. \quad (40)$$

Using this value for b in Equation (39) gives

$$n_c = \frac{f}{vsAT_1 \left(\frac{n_c}{N_c} \right)^{T/T_1}}, \quad (41)$$

from which

$$n_c = \left(\frac{f}{vsAT_1 N_c^{-T/T_1}} \right)^{\frac{T_1}{T+T_1}}. \quad (42)$$

If $T_1 = T$, n_c (and the photocurrent) increase as the square root of the light intensity. If $T_1 = 1000^\circ\text{K}$, the photocurrent increases as the 0.75 power of the light intensity. If $T_1 = 2000^\circ\text{K}$, the photocurrent increases as the 0.9 power of the light intensity. In brief, an exponential trap distribution, which is a physically reasonable expectation, can yield a range of exponents between 0.5 and 1.0 for the current-versus-light curve depending on the temperature at which the traps were "frozen in". Since exponents in the range of 0.7 to 0.9 are frequently observed, the exponential trap distribution would appear to be favored.

Equation (42) is not valid for characteristic temperatures T_1 less than T . In this case the number of electrons trapped above the Fermi limit exceeds the number trapped below and the exponent retains its value 0.5.

To get the temperature variation of photocurrent, Equation (42) is rewritten as

$$n_c = \left(\frac{f}{vsAT_1} \right)^{\frac{T_1}{T+T_1}} N_c^{\frac{T}{T+T_1}}, \quad (43)$$

from which the factor $N_c^{\frac{T}{T+T_1}}$ is seen to contribute the major part of the temperature dependence. A representative set of values for this factor is listed using $T_1 = 1000^\circ\text{K}$ and $N_c \cong 10^{19}$.

T	$\frac{T}{N_c T + T_1}$
100°K	10 ^{1.7}
200°K	10 ^{3.2}
300°K	10 ^{1.4}
400°K	10 ^{5.3}
500°K	10 ^{6.1}

For this choice of T_1 , the photocurrent is seen to increase by a factor of about ten per 100°C. If T_1 were chosen to be 2000°K the factor would be about 3 per 100°C. These rates of change do not compare unfavorably with some observed current-temperature curves.

The expression for the observed time constant, emphasizing the contribution from trapped electrons, is

$$\tau_0 = \frac{n(b)T}{vsn_c n_p} \quad (44)$$

In the present case

$$n(b) = Ae^{-b/T_1},$$

$$n_p \cong AT_1 e^{-b/T_1}.$$

With these values in Equation (44),

$$\tau_0 = \frac{T/T_1}{vsn_c} \quad (45)$$

\cong the time constant to be expected in the absence of traps.

Here, also, as was the case for a uniform distribution of traps, the presence of traps makes a large reduction in photosensitivity with little effect on the observed time constant.

2.2.10. General Comments on the Effect of Traps

The presence of traps has three first order effects on the properties of a photoconductor. The photosensitivity is reduced many orders of magnitude, namely, by the ratio of conduction electrons to trapped electrons; the observed time constant is likely to remain unaffected but may be decreased by the same ratio of free to trapped electrons; and the form of the current-versus-light curve is shifted from the 0.5 power, to be expected in the absence of traps, toward unity. The desensitizing effect is not particularly dependent on the energy distribution of traps. The time constant is dependent in the first order

on the energy distribution, since one of the factors in the time constant expression actually contains this distribution. Voids in the energy distribution of traps may lead to very short time constants approaching the life time of a free carrier. A concentration of traps localized in energy may lead to a marked increase in time constant. This should be particularly striking in its effect on the time constant versus temperature. If the temperature is raised and the steady-state Fermi limit passes through this localized concentration of traps, the time constant will be observed to go through a maximum, increasing at first and then decreasing. (The figure on page 134 of Mott and Gurney suggests this behavior for heating KCl.) Data reported by R. H. Bube¹⁹ for ZnS shows such a maximum with increasing temperature.

The time constant, in general, is orders of magnitude larger than the life time of a free carrier. This difference accounts for the lack of the expected reciprocity between speed of response and sensitivity and leads to inefficient performance of photoconductors. The departure from reciprocity is clearly shown in the data on CdS crystals. Here, for a large range of light intensity, the current increases nearly enough linearly to say that the sensitivity remains substantially constant. The time constant, on the other hand, rapidly increases toward low light intensities.

The lack of efficiency just referred to is illustrated by adding traps to an initially trap-free solid. One might have hoped that in exchange for the large desensitizing effect of the traps that the speed of response would have been correspondingly increased. Except for specialized trap distributions, this improvement in speed of response does not follow. If the observed time constant remained equal to the life time of a free carrier, the exchange would have been carried out accurately. For this reason the ratio of the life time of a free carrier to the observed time constant has been proposed as a figure of merit for a photoconductor. The life time of a free carrier is readily computed from the relation

$$I/e = \frac{\tau}{T_r} F,$$

where all of the quantities are observables except τ .

Any reasonably uniform distribution of traps leads to a current-versus-light curve that is very close to linear. Only by assuming an exponential distribution (or one of comparable nonuniformity, such as, for example, the Fermi limit lying below the bulk of the trap

distribution) can the power of the current-light curve be moved toward values around 0.7. Since many curves lie near this value, an exponential-like distribution appears to be needed analytically. Fortunately, it is also a physically reasonable distribution. The more refractory materials, by virtue of having their traps frozen in at a higher temperature, ought to be more nearly linear than the low temperature materials. Also, those materials that have a more nearly linear current-light curve ought to be less dependent on temperature. This last statement refers, of course, only to the contribution of trapping to temperature effects. A number of other sources of temperature effects exist and need to be considered. These are the variations of mobility, capture cross section, absorption edge and chemical state. In particular, since trapping effects can furnish the basis only for an increase of current with temperature but not for a decrease, the latter observation is good evidence for a temperature dependent capture cross section.

In summary, traps added above the steady-state Fermi limit lead to the square-root form of the current-light curve, temperature dependent photocurrents and observed time constants in excess of the life time of a free carrier; traps added below the steady-state Fermi limit lead to the linear form of the current-light curve, temperature independent photocurrents and observed time constants approaching the life time of a free carrier. The trap density, in order to be effective, should be in excess of $N_0 e^{-b/T}$, where b is the trap depth below the conduction band.

The contribution of the present picture of trapping can be emphasized by comparing its consequences with those of the simple bimolecular recombination model without traps. The bimolecular recombination model gives a photocurrent that increases as the square root of the light intensity; a time constant that is proportional to the reciprocal conductivity and is equal to the life time of a free carrier. The photosensitivity depends only on the capture cross section of primary centers (holes) for free electrons. The present trapping model gives a current that increases more nearly as the first power of the light intensity, a time constant that may be proportional to the reciprocal conductivity but, in general, may take on a varied behavior depending on the trap distribution, and a time constant that usually is large compared with the life time of a free carrier. The photosensitivity depends on the ratio of trapped to free electrons as well as on the capture cross section.

While the present trapping model is consistent with a large part of the experimental data on photoconductivity, further independent

and quantitative checks are needed. There are, moreover, the observations of nonohmic photocurrents, of photocurrents that saturate with voltage with no change in time constant, and of photocurrents that increase faster than linearly with light intensity, all of which observations fall outside the present model of trapping.

2.2.11. High Light Intensities

Throughout the previous discussion of trapping effects, the assumption has been that the number of trapped carriers far exceeded the number of free carriers in the conduction band. This should be true over most of the working range of a photoconductor and allows many convenient and simplifying approximations to be made. At very high light intensities, or more accurately at very high current densities, the number of electrons in the conduction band may exceed the number of trapped electrons. The trapping may then obviously be ignored and the problem treated as a simple bimolecular recombination problem. The virtue of pressing a photoconductor into this range is that the transition point, that is the conductivity at which the current-versus-light curve changes from substantially linear to square-root form, can be an immediate measure of the total number of traps. Namely, the total trap density can be of the order of the density of electrons in the conduction band. Also, at this transition point or higher, a direct measure of capture cross section of the primary centers may be made since the other parameters in the expression for observed time constant are known, namely,

$$\tau_o = \frac{1}{vsn_o} = \tau, \quad (46)$$

n_o taken at or above the transition point.

The above remarks hold for a reasonably uniform distribution of traps in energy or even for the exponential distributions that lead to exponents for the current-light curve greater than 0.5. A trap distribution that would weaken the above conclusions is one already discussed in which there is a high concentration of shallow traps superposed on an otherwise uniform distribution. While the low-light characteristics would be derived from the uniform part of the distribution, the high-light characteristics would be determined by the high concentration of shallow traps. In particular, as the light intensity is increased, the current-versus-light curve will bend into a half-power form at a level of excitation where the number of trapped

electrons (shallow traps) still exceeds the number of electrons in the conduction band. The result is that the observed time constant, measured in the half-power range, would be larger than the life time of a conduction electron by the ratio of trapped to free electrons.

2.2.12. Comparison with Experimental Data

At this point an attempt will be made to apply these expressions to data obtained from CdS crystals¹¹ in the range of photoconductivities from 10^{-9} to 10^{-2} ohm-cm⁻¹ and for evaporated Sb₂S₃ pickup tube targets⁴ in the range of 10^{-12} to 10^{-9} ohm-cm⁻¹. In both cases the photocurrents observed are generally much larger than the dark currents.

Typical CdS crystals have shown a nearly linear current-versus-light curve up to the range of 10^{-3} to 10^{-2} ohm-cm⁻¹ at which point the curve bends over into a square-root form. This would define the total trap density to be in the order of 10^{16} traps/cm³. Measurements on one crystal showed also the linear dependence of time constant on the reciprocal conductivity to be expected from a uniform or exponential trap distribution. From this data on time constant a capture cross section of primary centers was computed to be 10^{-21} cm².

The agreement between the present model for trapping and the results for CdS lies in:

- 1) The linear current-versus-light curve.
- 2) A reasonable basis for the lack of reciprocity between sensitivity and speed of response.
- 3) Proper sensitivity using a figure for trap density which is already reasonable from other sources.

What would aid in establishing this agreement would be independent observations on the number and distribution of traps.

In the case of Sb₂S₃, current-versus-light curves have been observed to have an exponent in the neighborhood of 0.7. If one interprets this on the basis of an exponential distribution of traps, the characteristic temperature of the trap distribution from Equation (42) is about 700°K. This same characteristic temperature, from Equation (43), should yield a twenty fold increase in photocurrent in the range of 300°K to 400°K. The observed increase reported by Forgue⁴ is very nearly the same.

The observed quantum yields for Sb₂S₃ targets 10^{-3} centimeter thick with ten volts across the target are of the order of unity. Under these conditions, also, the observed time constant is about 10^{-1} second. If this time constant were the actual life time of a free electron, the quantum yield that should be observed may easily be computed to be

$$\frac{\tau V \mu_0}{L^2} = 10^7.$$

The ratio of computed to observed quantum yields is also the ratio of trapped to free electrons. Since, under pickup tube operating conditions, the free electron concentration is of the order of $10^7/\text{cm}^3$, the concentration of trapped electrons would be $10^{14}/\text{cm}^3$. This concentration of trapped electrons is less than that computed for CdS and yet, for the same electrode spacing and applied field, CdS would be expected to show a quantum yield over six orders of magnitude higher than Sb_2S_3 . This difference must be taken up by the capture cross section which for Sb_2S_3 may be computed from Equation (45) to be 10^{-13} cm^2 to be compared with 10^{-21} cm^2 already computed for CdS.

2.2.13. Capture Cross Sections

Since the large difference between CdS and Sb_2S_3 sensitivities lies in the capture cross section of primary centers for free carriers, both theoretical and experimental attention ought to be paid to this parameter to try to get a better understanding of it. It is not usual, however, for data on photoconductivity to be couched in these terms. Some capture cross sections have been reported and some may be computed from the literature. They show the large range of values that may be encountered. Mott and Gurney² compute a cross section of 10^{-15} cm^2 for F-center traps in KCl. This is of the order of atomic cross sections. Haynes and Shockley¹⁵ report a cross section of 10^{-18} cm^2 or less for capture of a free electron by a free hole in germanium. Since both carriers are free, the small value is not at all unexpected. Data published by von Hippel and Rittner¹⁶ on Ti_2S may be used to compute a cross section of 10^{-19} cm^2 for capture of a free hole into its ground state. This value is based on a hole mobility of unity and a thermal velocity for free holes of 10^7 centimeters per second. Von Hippel uses a hole velocity of 10^5 centimeters per second to compute a cross section of 10^{-17} cm^2 . Similar data by Pick¹⁷ on PbS may be used to estimate a capture cross section of 10^{-22} cm^2 . Capture cross sections for CdS observed explicitly by R. W. Smith¹¹, Fassbender,¹⁸

¹⁵ J. R. Haynes and W. Shockley, "Investigation of Hole Injection in Transistor Action", *Phys. Rev.*, Vol. 75, p. 691, 1949.

¹⁶ A. von Hippel and E. Rittner, "Thalious Sulphide Photoconductive Cells", *Jour. Chem. Phys.*, Vol. 14, p. 370, 1946.

¹⁷ H. Pick, "Concerning Photoconductivity in Lead Sulphide", *Ann. der Phys.*, Vol. 3, p. 255, 1948.

¹⁸ J. Fassbender, "Concerning the Photoelectric Properties of Cadmium Sulphide Single Crystals", *Ann. der Phys.*, Vol. 5, p. 33, 1949; also J. Fassbender and H. Lehmann, "Computation of Electron Mobility in CdS Single Crystals from Attenuating Light Measurements", *Ann. der Phys.*, Vol. 6, p. 215, 1949.

and Broser and Warminsky¹³ range around 10^{-22} cm². Comparably small values are needed to fit data of R. H. Bube¹⁹ for ZnS.

Capture cross sections of atomic dimensions are, of course, readily understandable. In fact, it may be argued that the capture cross section may be larger than atomic dimensions by two or three orders of magnitude (as in Sb₂S₃) if the capturing center is charged and surrounded by a coulomb field. This would especially be true for materials in which the carrier mobility is low, of the order of unity. The cross sections that need clarification are those that are seven orders of magnitude *smaller* than atomic dimensions.

A formal method for getting small capture cross sections is to surround the primary center with a potential barrier. For such a barrier, one would expect an increase in temperature to increase the capture cross section, increase the speed of response and decrease the photosensitivity. Considerable work is needed to fit this in with observed photoconductive currents that both increase and decrease with temperature depending on the material and the temperature range.

The barrier field, preventing recombination, need not be of atomic dimensions surrounding each primary center. It may occur over larger dimensions of a solid owing to fluctuations of the Fermi level set up by a nonuniform distribution of traps and impurities. Such fields would be structure sensitive and not characteristic of the material. The large variations in sensitivities observed in CdS crystals suggest this picture.

2.2.14. Infrared Quenching

Thus far the holes have been assumed to be completely trapped. If this assumption is relaxed to allow a finite density of free holes, the contribution of these holes to the current will make no significant change in the previous discussion. An increase in current of the order of a factor of two is all that is involved. On the other hand, if the capture cross section of a free hole for a trapped electron is large compared with that of a trapped hole for a free electron (the only recombination considered till now) the free electron \rightarrow trapped electron \rightarrow free hole path for recombination may dominate the time constant. Broser and Warminsky¹³ take the stand that the trapped electron \rightarrow free hole is a much more probable transition than the free electron \rightarrow trapped hole. Their argument is that the electron is trapped at an imperfection in the lattice while a hole is trapped at an impurity

¹⁹ R. H. Bube, "A Comparative Study of Photoconductivity and Luminescence", *Phys. Rev.*, Vol. 83, p. 393, 1951.

site. The lattice imperfection gives a large transition probability by offering a series of intermediate states through which the electron may sift down rapidly without radiation. The impurity site, involving a single radiation transition, leads to a smaller transition probability.

While it may be difficult to separate out which recombination path the conduction electrons normally take, it is interesting that infrared quenching fits in quite naturally with the picture of infrared creating free holes which recombine rapidly with trapped electrons, and in that way drain off the conduction electrons. The part that fits very nicely is that the first effect of infrared will be to add to the current by a slight amount due to the addition of more carriers (free holes). The quenching or draining off of conduction electrons necessarily will take a finite time to build up because the first holes that recombine with trapped electrons do not immediately reduce the number of conduction electrons. The probability of a small number of conduction electrons finding a small number of vacancies in the electron traps will be correspondingly small. Only after the free holes build up enough vacancies among the trapped electrons will free electrons be drawn off sufficiently fast to show quenching. It is a common observation that infrared gives the current a slight jog in the positive direction just before its quenching shows up. Similarly, when the infrared is interrupted the current jogs in the negative direction.*

The present picture for infrared quenching would lead one to expect also that the infrared would have more effect on the conductivity excited by weakly absorbed radiation than on that excited by strongly absorbed radiation. The strongly absorbed radiation already is producing free holes and, in a sense (see next section), is already doing some self-quenching. The addition of infrared would accordingly be less effective.

2.2.15. Spectral Response

A frequent characteristic of the spectral response for photoconductors illuminated uniformly between electrodes shows a sharp peak just at or before the wave-length at which strong optical absorption, presumably absorption by the host crystal lattice, takes place. The sensitivity on the blue side of this peak drops off to a relatively constant or slowly decreasing value. The spectral response curves published by Frerichs²⁰ for CdS are an example.

* See, for example, A. E. Hardy, "The Photoconductivity of Zinc Cadmium Sulfide as Measured with a Cathode-Ray Oscilloscope", *Jour. Electro-Chem. Soc.*, Vol. 87, p. 1, 1945.

²⁰ R. Frerichs, "The Photoconductivity of Incomplete Phosphors", *Phys. Rev.*, Vol. 72, p. 594, 1947.

The suggestion has several times been made (see for example, Fassbender¹⁸) that the rapid fall on the blue side of the peak follows from the absorption of blue in a very thin layer giving rise to a high concentration of carriers and the consequent reduction in sensitivity derivable from the usual bimolecular recombination arguments. It would appear that this argument can be stated more broadly and without reference to any model. If the current-versus-light curve has an exponent less than unity, a peak is to be expected at the absorption edge that is easily calculable from the known exponent and rate of change of absorption constant with wave length. If the exponent is unity, no peaking is contributed by this argument. R. W. Smith¹¹ has observed nearly linear curves for both strongly absorbed blue light and green light near the absorption edge for CdS.

An alternate explanation for the peak can be that the thin surface layers constitute a different and less sensitive photoconductor (for example, more traps) than the volume. Independent tests would, of course, be needed to establish this picture.

It is interesting that a third argument can be made using the concept of rapidly recombining free holes already discussed for infrared quenching. Light whose energy is just short of the absorption edge will tend to excite electrons from localized states lying just above the filled band. The holes left behind are then already trapped. Blue light, on the other hand, will excite from the filled band to the conduction band. This leaves free holes which, although they are rapidly trapped, will have some opportunity for recombining with trapped electrons. The result is, in a sense, a smaller quantum yield for the primary photo excitation. That is, only a fraction of the holes generated survive and are able to support photocurrents. If this argument is valid, the ratio of photocurrents at the peak to those on the blue side is a measure of the contribution of free holes to the recombination processes. A test of this argument would appear to be that materials which show infrared quenching should also show a spectral peak at the absorption edge.

If the spectral response curve is taken by illuminating one end of the crystal rather than by uniform illumination, the photocurrents from the strongly absorbed wave lengths will rapidly approach either zero or the small amplitude permitted by the space-charge-limited current formula. Spurious exception to this can occur if, as suggested and observed by R. W. Smith, the blue light causes luminescence in the longer wave lengths which can penetrate the whole crystal and give rise to volume-excited photocurrents, or if the potential distribution is nonuniform and localized at the illuminated end.

2.3. Case of Trapping and One Carrier not Replenished at the Ends (Figure 13)

It was assumed in the previous discussion of trapping effects that both carriers could be replenished at the ends of the photoconductor by free charges moving in from the electrodes. Since it was argued shortly that one of the groups of carriers (holes) would be substantially completely trapped it was not significant to demand that this carrier be replenished at the electrode. Allowing the holes some freedom of movement introduced a small, but not important, addition to the current and a possibly large contribution to recombination. The present discussion takes on from this point and assumes that the holes are not replenished at the ends. At low voltages little change results from this added restriction. The life of a conduction electron still is determined by recombination with a hole. At higher applied voltages, however, the slowly migrating holes will tend to be drawn off into the cathode before they suffer recombination with an electron. This results

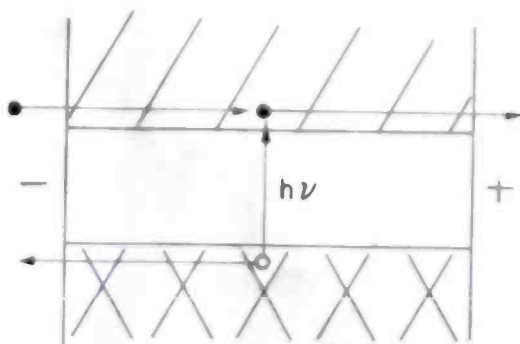


Fig. 13—Both carriers mobile but only one carrier is replenished at the ends.

in a striking saturation of the current-voltage curve. The holes, instead of having a life time independent of applied field, now have a life time inversely proportional to the field. If one returns to the expression for photocurrent,

$$I = e \frac{\tau}{T_r} F, \quad (47)$$

in which τ is the mean life of a conduction electron and T_r is the transit time of the electron, as before,

$$T_r = \frac{L^2}{V\mu_{e0}}, \quad (48)$$

where μ_{e0} is the normal mobility of an electron. But τ does not now

have a value determined by recombination and independent of applied field. Each hole that is drawn out means also the loss of one electron (in order to preserve charge neutrality). The mean life of an *excited* electron is equal to the mean life of a hole. The latter is given by the transit time of a hole or by

$$\frac{L^2}{V\mu_h} \quad (49)$$

Here μ_h is the mobility of a hole including the effects of trapping. Now the life of a *conduction* electron is equal to only a fraction of the life of an *excited* electron; an excited electron spends most of its time trapped and only a small part of its time free. The fraction of total excited time spent as a free electron is given by the ratio of free electrons to total number of excited electrons or by $\frac{n_c}{n_p}$. Thus, the mean life of a conduction electron is

$$\tau = \frac{n_c}{n_p} \frac{L^2}{V\mu_h} \quad (50)$$

Inserting the values of T_r and τ , just obtained in Equation (47) gives

$$I = e \left(\frac{\frac{n_c}{n_p} \mu_{eo}}{\mu_h} \right) F \quad (51)$$

But $\frac{n_c}{n_p}$ is the factor needed to convert the normal mobility (μ_{eo}) of an electron into the mobility as determined by trapping (μ_e). The photocurrent then becomes*

$$I = e \frac{\mu_e}{\mu_h} F \quad (52)$$

That is, the gain factor is the ratio of mobilities of electrons and holes. If there are no traps, these are the normal mobilities. If there is

* The hole current contribution has been neglected here since μ_e was assumed $\gg \mu_h$. If the hole current is included this equation becomes

$$I = e \frac{\mu_e + \mu_h}{\mu_h} F.$$

trapping, these are the mobilities as determined by trapping.

This is the voltage-saturated current referred to at the start of this section. It has the same form as the expression for photocurrents in germanium even though germanium is a low resistance semiconductor and the present model is an insulator. It is highly suggestive also of the form of expression first obtained by Hilsch²¹ in 1937 in his argument for the origin of the gain factor in secondary photocurrents and for the fact that secondary as well as primary currents could be saturated with applied voltage. The model used by Hilsch made use of both electronic and ionic dark currents. What is common to all of these models and what gives rise to the saturation effect is a field-dependent life time of a primary center. If this dependence is linear, τ and T_r both change at the same rate with applied voltage and the current remains constant or saturated. If the dependence is greater than linear, the current should be observed to go through a maximum and actually decrease with increase in voltage-negative resistance.

2.4. High Dark-Current Photoconductors

The present outline has been concerned chiefly with relatively insulating materials in which the photocurrent is large compared with the dark current. Many photoconductors (PbS, Tl₂S, grey Se, germanium, etc.) have a sufficiently high dark current ($\sigma > 10^{-5}$ ohm-cm⁻¹) that they are normally operated with photocurrents appreciably less than the dark current. Under these conditions, the photocurrent, being a small perturbation on the dark current, should vary linearly with light intensity. The data reported by von Hippel and Rittner on Tl₂S is a good example. A second consequence of working with high dark current materials is that trapping effects are either absent or substantially reduced since already in the dark the number of free carriers becomes comparable with the number of trapped carriers. PbS, Tl₂S and germanium at room temperature closely satisfy the relation

$$I/e = \frac{\tau}{T_r} F,$$

using the observed time constant for the average life of a carrier τ . At lower temperatures trapping may again become significant. [See last section and Ref. (25)]

²¹ R. Hilsch and R. Pohl, "Stationary Photoelectric Primary and Secondary Currents in Crystals, Particularly in KH-K Br Mixed Crystals", *Z. f. Phys.*, Vol. 108, p. 55, 1937; also F. Stockmann, "Theory of Photoelectric Conduction in Mixed Conductors", *Z. f. Phys.*, Vol. 128, p. 185, 1950.

2.4.1. Nonuniform Illumination

An interesting element of novelty enters in when both carriers are mobile in a high dark current material and nonuniform illumination is used. In the case of insulators it was pointed out, for example, that illumination at one end or in a narrow interior slice would result in photocurrents severely limited by space charge. In the present case of high dark current and both carriers mobile this is not true. If one considers a narrow interior slice illuminated, *the free electrons and holes do not move off* in opposite directions. If they did, the severe space-charge limitation would be effective. Rather, one of the groups of carriers created by light moves in its proper direction but takes with it enough carriers of the opposite sign to maintain charge neutrality. The photo- and transistor-effects in germanium are the striking examples.²² The holes injected by light, or by an emitter, take with them an equal number of electrons. The extra electrons accompanying the holes do not remain identified as the same electrons, but only as a statistical excess.

Since the excess number of holes and electrons created by light move together, one would compute zero photocurrent if the photocurrent were computed as in the insulator case by a movement of charge. The computation is made here on the basis of a slice of increased conductivity created by light. This slice of increased conductivity lowers the total resistance and allows an increased current to flow. The total charge passed is proportional to the life time of this slice which, in turn, is given by the transit time of the holes to the cathode. The electric field used to compute the transit time is the *field within this slice of increased conductivity* and is smaller than the field in surrounding sections. For very high light intensities (conductivities of the slice large compared with the surrounding sections) this transit time becomes correspondingly long. While the photocurrents here are computed differently from those in an insulator, *it is significant that both methods of computation lead to identical results.* In particular,

the gain in the case of the high dark current semiconductor is $\frac{\mu_e + \mu_h}{\mu_h}$ just as it was for the insulator where both carriers were mobile, but one of them (the holes) was not replenished at the electrodes.

The conditions under which one carrier takes along a compensating charge of carriers of the opposite sign can be outlined by considering an illuminated interior slice of semiconductor. For the sake of argument, let the extra carriers created by light move off in opposite

²² W. Shockley, *ELECTRONS AND HOLES IN SEMICONDUCTORS*, D. Van Nostrand Co., Inc., New York, N. Y., 1950.

directions. As they separate they rapidly build up a space charge. Now, if one allows this space charge to be neutralized by ordinary ohmic conduction, the neutralization will be carried out by that sign of carrier that contributes most to the dark conductivity. Since the relaxation time of a semiconductor is about $(10^{12} \sigma)^{-1}$ seconds, the neutralization will take place in less than a microsecond for a high-conductivity semiconductor and, except in special cases, will take place orders of magnitude more rapidly for carriers of one sign compared with carriers of the other sign. In the case just cited, for example, both the space charge created by movement of the photoelectrons and that created by movement of the photoholes will be neutralized by electron conduction (for an n-type semiconductor). The result is that the cluster of photoelectrons disappears and the cluster of photoholes is surrounded by an equal number of extra electrons.

The criterion of whether the photocurrent results from actual movement of electrons and holes in opposite directions or from the slice of increased conductivity, as just discussed, would appear to depend on the relative values of transit time of carriers and relaxation time of the semiconductor. For an insulator (transit time \ll relaxation time) one would expect the carriers to move in opposite directions; for a good semiconductor (transit time \gg relaxation time) one would expect the slice of increased conductivity. In either case, the photocurrent is the same.

An interesting test for hole mobility in an insulating photoconductor is suggested by the above discussion. Let a photoconducting insulator be uniformly illuminated by a bias light. This converts it into a semiconductor. Now add the same number of lumens focussed on a narrow interior slice of the photoconductor not more than a tenth of its length. If the holes are mobile, the increase in current should be comparable with the bias current. If the holes are not mobile, the increase in current can at the most be one tenth of the bias current. A long, thin crystal would be best suited for this test.

2.5. Nonuniformities

There is ample evidence in the literature to support the statement that when a potential is applied across an insulator, the major part of that potential usually appears at the metal-insulator interface. It is not safe to assume that the field in the main body of the insulator is given by the applied potential and length of specimen. Probe measurements by R. W. Smith¹¹ and R. H. Bube¹⁰ on CdS, CdSe and ZnS crystals have borne out these statements. Not only is the potential distribution nonuniform but it can change with light intensity and

applied voltage. In a small percentage of cases, either by deliberate treatment of the electrodes or by accident, specimens have been obtained that do show a reasonably uniform and stable potential distribution and are suitable for making quantitative measurements.

In the case of relatively high conductivity evaporated films (PbS, Tl_2S , grey Se) there has been much speculation in the literature to the effect that the microcrystalline boundaries constitute insulating barriers in which the main seat of the photoeffect lies. This picture is supported by tests of high frequency impedance properties, light probe measurements and the fact that the two semiconductors brought into contact generally form a high resistance contact.

While the presence or absence of barriers is of interest in making quantitative interpretations of observed photoeffects, it is not immediately true that their presence alters the physics of the photo-processes. In particular, barriers thicker than 10^{-4} cm. can be regarded already as acting like long insulating specimens. The carriers must migrate through these barriers just as they would through normally thick specimens.

If the barriers are thick and occupy the fractional length ϑ of the interelectrode distance, the following formal effects are to be noted. For a given uniform light intensity incident on the crystal, the amount of useful light is reduced by the factor ϑ ; the gain (referred to the useful light absorbed) is increased by the factor ϑ^{-2} since the gain goes as L^{-2} ; and the net observed photocurrent is increased by the factor ϑ^{-1} . These statements follow from the fact that the effective length of photoconductor is ϑL instead of L . While the barriers reduce the effective length of specimen, this is true only in so far as the barrier resistance is high compared with the resistance of the rest of the specimen, namely at low and intermediate light intensities. At high light intensities, as the barrier resistance becomes comparable with that of the rest of the specimen, the effective length of photoconductor increases toward its nominal length. The effect on the current-light curve would be to give it a spuriously low slope.

Some emphasis has been given, in British publications on PbS²³ and recently by Rittner²⁴, to the barrier effects of P-N junctions. It is difficult to see how such junctions can play a significant role, particularly in PbS and other photoconductors where the gain is of the order of unity. If one uses the P-N junction in the back direction it

²³ L. Sosnowski, J. Starkiewicz and O. Simpson, "Lead Sulphide Photoconductive Cells", *Nature*, Vol. 159, p. 818, 1947.

²⁴ E. S. Rittner, "Concerning the Theory of Photoconductivity in Infra-red Sensitive Semi-conducting Films", *Science*, Vol. 111, p. 685, 1950.

provides the barrier insulation needed. A P-N junction in the back direction, however, is limited to a primary photoeffect or a gain of unity. If there are a number of these P-N junctions in series the effective gain per junction is reduced by the reciprocal of their number. Moreover, if the P-N junction is the seat of the photoeffect, it intercepts only a small fraction of the total light incident on the crystal and would have to yield a gain much greater than unity in order to compensate for the lack of light. If the P-N junction is used in the forward direction it *can* offer gains greater than unity but now it offers very little barrier resistance. Moreover, the dark current ought to rise exponentially with applied voltage, at least while the barrier is effective. This is usually not the case.

A test for the presence of barriers can be derived from the expression for photocurrent,

$$I = e \frac{\tau}{T_r} F.$$

If one operates a photoconductor at high light intensities, where trapping is negligible and $I \sim F^{1/2}$, the τ in the above equation, defined as the life time of a free carrier, should also be equal to the observed time constant. It was mentioned earlier that the observed time constant may be equal to or greater than the life time of a carrier, but not less than it. If the observed time constant in this test turns out to be actually smaller than τ , the reasonable conclusion is that the transit time T_r , computed on the basis of the nominal length of photoconductor was too large. The effective length should be shorter and would be a measure of the shortening effect of barriers.

It is interesting to note that data published by H. Pick¹⁷ on PbS and by von Hippel and Rittner¹⁶ on Tl_2S satisfy the above expression for photocurrent providing a mobility of unity is used for the free carriers in computing the transit time. If this is the proper value for the mobility, the agreement means that the reported data needs neither traps nor barriers to reconcile it with simple expectations. Data published recently by A. W. Ewald,²⁵ however, show that as Tl_2S is cooled, both the sensitivity and speed of response decrease. The rate of decrease is consistent with traps whose mean depth is 0.2 volt.

The nonuniformities discussed above are all nonuniformities along the length of photoconductor. An interesting possibility arises if one assumes that the lateral free surfaces of the photoconductor form a

²⁵ A. W. Ewald, "On the Photoconductivity of Thallous Sulphide Cells", *Phys. Rev.*, Vol. 81, p. 607, 1951.

barrier field due to the presence of surface states. If strongly absorbed light is used, and free pairs are created in this barrier field, the two signs of carriers will be separated by the barrier field to the width of the barrier. The photoconductor would still be substantially electrically neutral, but the physical separation of carriers could give rise to spuriously large time constants and small capture cross sections. This same argument can be applied to interior or volume fluctuations in Fermi limit (relative to the conduction band) arising from non-uniform distribution of traps and impurities. Probable sources for the appearance of these fluctuations have been given both for highly conducting²⁶ and for highly insulating²⁷ materials. Although the energy level diagram appears similar to that drawn for the usual barrier arguments, the usual barrier properties are not made use of here. Rather, the local fields are used to separate holes and electrons to generate the abnormally small capture cross sections. Another way of stating the distinction is that the barrier properties are used in parallel rather than in series with the current. While the usual barrier argument requires that the conducting sections be highly conducting relative to the photocurrents drawn, the present use of barrier fields to reduce capture cross section is not subject to the same restriction. The material may be insulating and vary locally in the degree of insulation.

In brief review, the most likely effect of barriers in series with the current is to shorten the effective length of photoconductor without altering the physics of the photoprocess. Barriers need not be introduced if the general expression, Equation (10), is satisfied without them. Internal or surface barrier-like fields may readily occur and be responsible for the unusually small capture cross sections observed in many sensitive photoconductors.

CONCLUDING REMARKS

The present treatment of traps offers an interpretation for the following observations:

- a. Current-light curves with exponents in the range of 0.5-1.0.
- b. Lack of expected reciprocity between sensitivity and speed of response including both the observations of change of sensitivity without changes in speed of response and changes in speed of response without changes in sensitivity.

²⁶ H. M. James, "Conduction in Photoconductive PbS Films", *Science*, Vol. 110, p. 254, 1949.

²⁷ G. H. Wannier, "On the Energy Band Structure of Insulators", *Phys. Rev.*, Vol. 76, p. 438, 1949.

- c. Temperature dependence of photocurrent extending from constant to exponential.
- d. Currents through thin layers of insulators excited by light or electron bombardment as much as eight orders of magnitude smaller than would be expected in the absence of traps.
- e. The high sensitivity of some photoconductors.
- f. The apparent variation of mobility with light intensity or temperature reported by other workers (Fassbender, CdS, and Ewald, Tl_2S).

The introduction of a steady-state Fermi limit has facilitated the computation of the effects of various trap distributions. The validity of this concept depends on the agreement of further experimental work with the computed results.

Emphasis has been placed on the capture cross section of primary centers for free carriers and on the extraordinarily small values of this cross section in sensitive photoconductors. Local barrier-like fields are cited as a likely cause for these small cross sections. Temperature dependence of the cross section is apparently needed to account for photocurrents that decrease with increasing temperature.

ACKNOWLEDGMENT

The present discussion was prompted and guided mainly by the work reported in the preceding papers. In addition, the writer has had frequent discussions of the subject matter with H. W. Leverenz, G. A. Morton, D. O. North and E. G. Ramberg.

APPENDIX

Computation of v/s

The value of v/s will be computed for two quite different special cases and shown to be the same. From this, it is assumed that its value is the same in all cases.

Intrinsic Semiconductor

Let the width of forbidden zone be equal to $2b$. Then, under thermal equilibrium, the rate of recombination will be equal to the rate of thermal excitation:

$$n_c^2 vs = N_c ve^{-2b/T}.$$

$$\text{But } n_c = N_c e^{-b/T}.$$

Therefore, $\frac{v}{s} = N_c v \cong 10^{26}$ at room temperature

$$\cong 10^{26} \left(\frac{T}{300} \right)^2 \text{ at temperature } T.$$

Impurity Semiconductor

Let the donor impurities be at a level b below the conduction band and let the temperature (for convenience of computation) be such that half the donors are ionized. That is, the Fermi limit lies also at the level b below the conduction band. Let the number of donors be N_p . Then, under thermal equilibrium,

$$n_c \frac{N_p}{2} v s = \frac{N_p}{2} v e^{-b/T}.$$

$$\text{But } n_c = N_c e^{-b/T}.$$

Therefore
$$\frac{v}{s} = N_c v \cong 10^{26} \text{ at room temperature.}$$

List of Symbols and Some Convenient Relations

- n_c number of conduction electrons/cm³
- n_t number of trapped electrons/cm³
- n_p number of primary centers (holes)/cm³
- $n_p = n_c + n_t$
- n_b number of traps/cm³ per unit energy depth
- N_c number of energy levels in bottom slice of conduction band a few kT wide

$$N_c \cong 10^{19} \left(\frac{T}{300} \right)^{3/2} / \text{cm}^3$$

- b energy in degrees Kelvin
(electron volts = $b/11,600$)
- T absolute temperature
- μ_0 normal mobility determined by lattice collisions
- μ mobility determined by trapping
- I current in amperes
- F total number of optical excitations per second
- f number of optical excitations/sec/cm³
- τ average life time of a free carrier
- τ_0 observed time constant (time for photocurrent to decay to half value)

- T_r transit time of free carrier between electrodes
 G gain factor = number of carrier transit times per carrier
 life time = $\frac{\tau}{T}$
 e electron charge (coulombs)
 L distance between electrodes
 V potential between electrodes
 v thermal velocity ($\sim 10^7 \left(\frac{T}{300}\right)^{1/2}$ cm/sec)
 s capture cross section of primary center for free carrier (cm²)
 σ conductivity (ohm-cm)⁻¹
 $\sigma = n_c e \mu_0$

σ	n_c (for $\mu_0 = 10$)	$\frac{n_c}{N_c}$ (at room temp.)	$\frac{b}{11,600}$	(energy difference in electron volts between bottom of conduction band and Fermi limit at room temperature)
1	10 ¹⁸	10 ⁻¹	0.058	
10 ⁻³	10 ¹⁵	10 ⁻⁴	0.23	
10 ⁻⁶	10 ¹²	10 ⁻⁷	0.40	
10 ⁻⁹	10 ⁹	10 ⁻¹⁰	0.56	
10 ⁻¹²	10 ⁶	10 ⁻¹³	0.75	

STUDIES OF EXTERNALLY HEATED HOT CATHODE ARCS*

Part I. — Modes of the Discharge

BY

L. MALTER, E. O. JOHNSON AND W. M. WEBSTER

Research Department, RCA Laboratories Division,
Princeton, N. J.

Summary—It is shown that in a gas discharge in cylindrical diodes with inner hot cathode, the discharge can take on a number of possible forms. At low current values the "anode-glow" mode occurs, provided the pressure exceeds some minimal value. In this case the potential in the tube is close to that of the cathode over all of the tube except for a thin film adjacent to the anode surface. The potential rises steeply in this film to above ionization potential. The light appears to come from the anode surface only.

At higher current values the discharge goes over into the "ball of fire" mode in which the light comes from a definitely defined region which may be very small in volume and appear to float in space. The potential is a maximum within the ball and all excitation and ionization occur therein. The balance of the tube (except close to cathode and anode) is filled with a plasma which acts as a conductor to transport electrons from cathode to anode.

At a current value equal to about half the cathode emission, the discharge goes over into a form in which ionization (and excitation) occur through all of the tube with the exception of a thin sheath around the cathode. Since this form of discharge has been studied extensively by Langmuir, it is here designated as the "Langmuir" mode.

At a current equal to the cathode emission, a temperature-limited form of discharge sets in.

Data and results are presented for plasma and floating potentials, electron temperature, plasma density and glow distribution for the various forms of discharge.

I. INTRODUCTION

EXTERNALLY heated hot cathode arcs have received attention from several workers. Various forms of the discharge have been reported. Thus, e.g., Langmuir¹ has described a discharge in which a distinct cathode fall is approximately equal to the arc drop (the potential difference between cathode and anode). Compton and

* Decimal Classification: R337.1.

¹I. Langmuir, "The Interaction of Electron and Positive Ion Space Charges in Cathode Sheaths," *Phys. Rev.*, Vol. 33, p. 954, June, 1929.

Eckart² and Druyvestyn and Penning³ have described a form of discharge in which the potential rises from the cathode to a pronounced maximum and then falls off to a lower value at the anode. They have explained the phenomenon of the low-voltage arc in terms of this discharge. Druyvestyn and Penning³ also make mention of a form of discharge in which the major portion of the arc drop is concentrated in a thin sheet close to the anode.

It is the purpose of this study to attempt to establish some order in this field; to determine the conditions under which the various forms of discharge occur; to account for the transitions from one form of discharge to another; to collect information regarding the fundamental processes occurring in each form; and to study such other matters of interest as arise from the study of the above-mentioned points.

In the studies, cylindrical diodes were employed with central hot cathodes. The cathodes were of two types—indirectly heated oxide cathodes, and directly heated tungsten or tantalum filaments. The former types were employed for two reasons: (1) the light emission from the cathode did not obscure the discharge glow, and (2) a uni-potential cathode was achieved without special circuitry. Metallic cathodes were employed where definite information regarding the saturated cathode emission was desired. It was found that the data obtained from tubes which were identical except as regards cathode, were very similar. As a consequence the tubes were usually built in pairs, one with oxide cathode, the other with metallic filament. Each was used to collect data and the results combined in arriving at conclusions.

II. VISUAL OBSERVATIONS

In order to establish the forms of discharge to be studied, visual observations are described which may be made on a simple cylindrical diode, with an inner hot cathode, as the anode current is increased. The cathode-anode spacing is about one centimeter, and the gas pressure is somewhere between 0.5 and 10 millimeters of mercury. The studies were all made with noble gases. The circuit employed is shown in Figure 1.

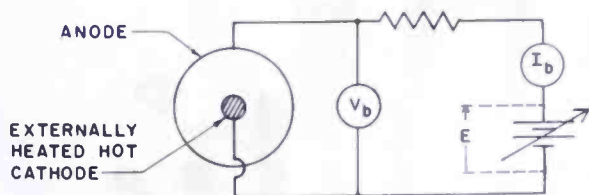
² K. T. Compton and C. Eckart, "The Diffusion of Electrons Against an Electric Field in the Non-Oscillatory Abnormal Low Voltage Arc", *Phys. Rev.*, Vol. 25, p. 139, February, 1925.

³ M. J. Druyvesteyn and F. M. Penning, "The Mechanism of Electrical Discharges in Gases of Low Pressure", *Rev. Mod. Phys.*, Vol. 12, p. 148, April, 1940.

The current through the tube is increased from zero by increasing E . When E is less than the ionization potential, V_i , I_b is extremely small and first becomes appreciable as E approaches V_i . When E slightly exceeds V_i , a discharge occurs in which the glow appears to come from the anode surface only.³ This form of discharge is denoted as the "anode-glow" mode. As I_b is further increased, the discharge remains in the anode-glow mode until a certain value of current is reached and then breaks into the form described in the next paragraph.

At the critical condition, the discharge abruptly changes into a form in which the glow occupies an extended region whose shape and location depend primarily on the pressure. At lower values of pressure, the luminosity comes from a region several millimeters thick which "hugs" a portion of the anode. At higher pressures the glow is detached from the anode and appears to float in space as a glowing region of luminosity. At pressures of several millimeters the luminosity comes from a sphere. In argon at 6 millimeters, the luminous sphere has a compact blue core about 1 millimeter in diameter. This

Fig. 1 — Circuit for diode tests.



is surrounded by a pale rose shell, the intensity of which diminishes with distance from the core. This is called the "ball-of-fire" mode. Since the discharge mechanism for the glows with delimited boundaries appears to always be the same, the designation is retained for all discharges in which the glow is of this type, whether they are ball-shaped or not.

When the current is increased above a value which is approximately half the available cathode emission,* the character of the discharge changes abruptly to another form in which the glow fills all of the tube except for a narrow cylinder around the cathode. This is here referred to as the "Langmuir" mode, since it appears to correspond to the form of discharge described by Langmuir,⁴ in which electrons and ions travel in opposite directions through a thin layer at the cathode. Langmuir designates such a region as a "double sheath." The phe-

* The reason for the transition at this value of anode current will be developed analytically in Part II of this series.

⁴ I. Langmuir, "The Interaction of Electron and Positive Ion Space Charges in Cathode Sheaths", *Phys. Rev.*, Vol. 33, p. 954, June, 1929.

nomena in the vicinity of the cathode in discharges of this form have been studied in detail by Druyvestyn and Warmoltz.⁵

Finally, when the anode current attains in value the available emission from the cathode, the glow changes in color and appears to fill the entire tube. The emission is then temperature limited.

It should be pointed out that only in certain tubes, for certain gases and at certain pressures can one observe clean-cut processes such as described above. In most tubes, over certain current ranges, the discharge shifts, in some cases in a regular, in others in a highly erratic fashion from one mode of discharge to another. It is believed that, for the most part, these instabilities find their origin in the inability of the discharge to satisfy its boundary conditions in any one discharge mode. The details of mechanisms involved are not presently understood and will not be discussed here.

Furthermore, at low pressures of the order of 100 microns, one does not usually observe the anode-glow mode. At low currents the glow takes place in a thick shell inside the anode. As the current is increased this shell expands inward and quickly assumes the Langmuir-mode characteristics. At lower pressures, below about 50 microns, the discharge starts immediately in the Langmuir mode. Since so much of the early work in the hot cathode arc field was done in mercury vapor, at low pressures, it is understandable that such phenomena as the anode glow were not generally observed and studied.

Actually, operation at pressures below about 300 microns is generally accompanied by large oscillations in voltage and current. It cannot be said, as a rule, that cleancut operation is occurring in any one mode. For these reasons, this study was largely concerned with pressures in excess of 300 microns.

The various forms of discharge will now be discussed in more detail, with presentation and analysis of data and formulations of "pictures" of the processes taking place.

III. VOLT-AMPERE CHARACTERISTICS

The details of tube No. 1 are shown in Figure 2. It contained helium at 500 microns pressure. The cold probes were used for determinations of electron temperature and plasma density by the double probe method of Johnson and Malter.⁶ The hot probe was used for determination of plasma potential.

⁵ M. J. Druyvesteyn and N. Warmholtz, "Ein neuer Dunkelraum in der Nähe einer Gluhkathode in einer Bogenentladung", *Physica*, Vol. IV, p. 51, January, 1937.

⁶ E. O. Johnson and L. Malter, "A Floating Double Probe Method for Measurements in Gas Discharges", *Phys. Rev.*, Vol. 80, p. 58, October 1, 1950.

In some cases an alternating-current voltage was applied to the tube in the manner indicated in Figure 3. On the oscilloscope one obtains a plot of current versus voltage as shown in Figure 4.

From observations in a similar tube with an oxide cathode, it is possible to identify the various regions of the characteristic of Figure 4 with the modes of discharge described in the preceding section. They are

- A-B-C anode-glow,
- D-E ball-of-fire,
- F-G Langmuir distribution,
- G-H temperature-limited.

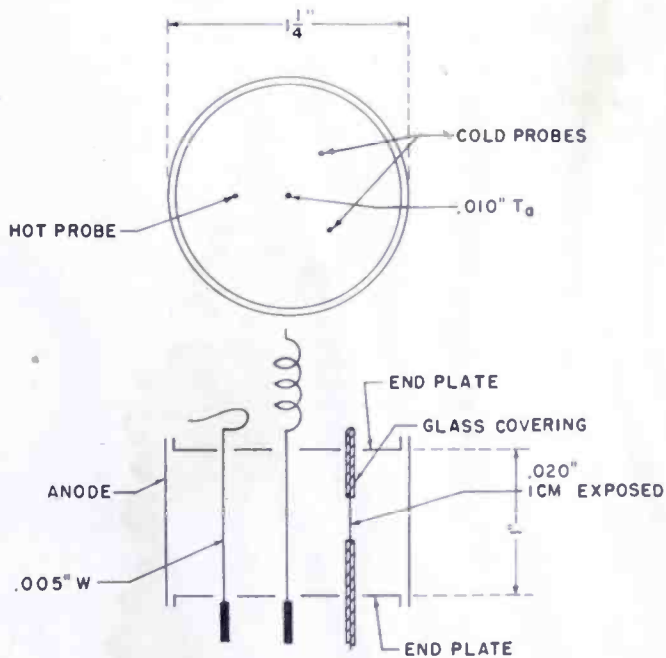


Fig. 2 — Experimental diode study tube.

Region D-B is a ball-of-fire mode which appears as a continuation of region E-D as the current is diminishing and is thus an indication of a path hysteresis effect in the discharge phenomena.

IV. SPACE POTENTIAL DISTRIBUTION

The potential distributions between cathode and anode corresponding to the different forms of discharge will now be discussed. While considerable data which originally led to the formulation of these concepts remains to be presented, it seems best to describe the distributions at this point. In this way it will be possible to present

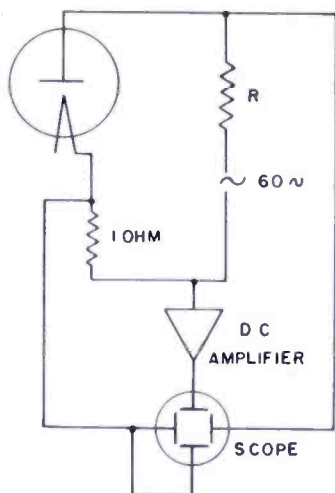


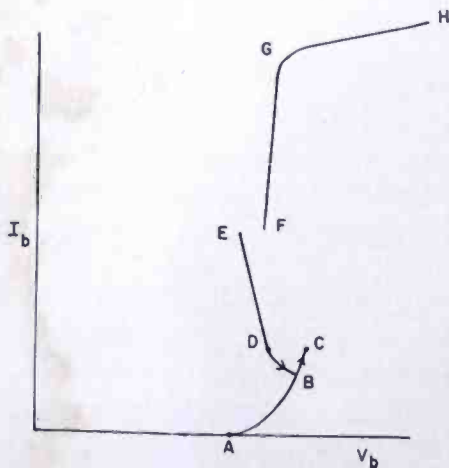
Fig. 3—Test circuit for observation of diode voltage-current characteristics.

the supporting evidence more concisely and pertinently. Visual observations furnish useful clues to these potential distributions in that it is hard to conceive of ionization occurring without attendant excitation. Thus regions of intense glow indicate regions in which ions are being formed. Readers are reminded, however, that ions have a mean life time which is long compared to that of an excited atom. As a result, ions can diffuse from the region of glow and exist elsewhere in large numbers.

(a) Anode-Glow Mode

The fact that the glow appears at the anode surface only, indicates that excitation and ionization are occurring in a layer very close to the anode. The cathode emission is space-charge limited since the anode current is far less than the total available emission. Thus, there must be a retarding field at the cathode. The potential falls from the cathode to a potential minimum and then rises slowly to a point near

Fig. 4—Volt-ampere characteristic of hot-cathode gas-discharge diode.



the anode beyond which it rises steeply to a value in excess of the ionization potential at the anode surface. The slow rise through the plasma is required to impart sufficient directed velocity to the electrons in the plasma to sustain the circuit current. The postulated potential distribution is shown in Figure 5a. This distribution differs from that shown by Drayvestyn and Penning³ in that they do not show the potential minimum close to the cathode.

In this distribution, the ionization occurs in a layer very close to the anode. The probability of cumulative effects is not large. As a consequence, it is not surprising that the anode potential should exceed the ionization potential. Ions produced near the anode fall back into

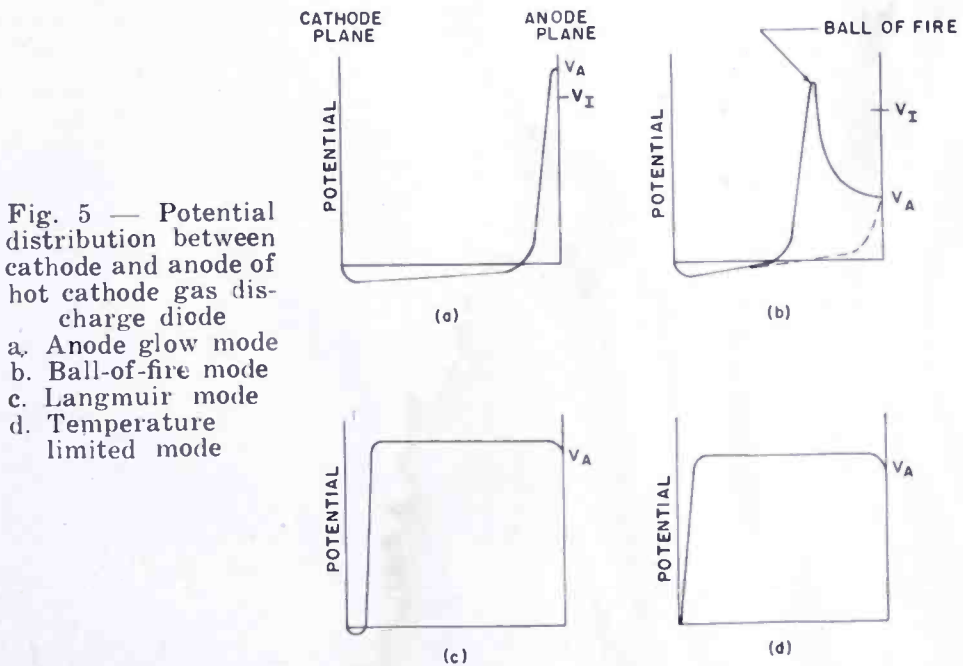


Fig. 5 — Potential distribution between cathode and anode of hot cathode gas discharge diode
 a. Anode glow mode
 b. Ball-of-fire mode
 c. Langmuir mode
 d. Temperature limited mode

the plasma. Due to the retarding field at the cathode they cannot escape to that electrode. They can thus be lost only to insulating supports or probes, or by recombination.

An analysis of the anode glow mode (to be presented in paper II of this series) shows that as the anode potential and current increase, the ion production at the anode increases. The ions produced flow away from the anode to the plasma in the opposite direction to the electron current flowing out of the plasma to the anode. Thus in this region there is a double sheath of the form described by Langmuir.⁴

Upon increasing the anode current, an abrupt transition from the anode-glow mode to the ball-of-fire mode is observed. Analysis of the

anode sheath and the plasma region immediately adjacent to it has suggested two mechanisms which may be responsible. The first has to do with the inability of the plasma (in the anode region) to carry the anode current. This occurs when the random electron current close to the anode is less than the anode current. The latter is determined largely by the external potential source and circuit resistance. The second mechanism is concerned with the instability of the electron sheath at the anode in the presence of the ions there generated. In both cases a critical ratio of ion current entering the plasma to electron current leaving is defined as a criterion for the transition. Since the critical values associated with the two mechanisms are very nearly the same, experiment, while essentially substantiating both, has failed to select between them. These criteria will be discussed in detail in the later paper.

(b) *Ball-of-Fire Mode*

In this case the anode potential is less than the ionization potential. In some cases *negative* arc drops have actually been observed, i.e., cases in which the anode was negative with respect to the cathode, while a sustained discharge was present. This required the use of tungsten filamentary cathode (high work function) and a nickel anode upon which had been evaporated controlled amounts of barium, thus producing a low work function anode. The resultant contact potential difference favored low, and even negative, arc drops. The discharge is actually maintained by thermal energy from the cathode.

In the "ball" itself, the potential must exceed the resonance potential if not the ionization potential. Measurements by Druyvestyn⁷ with a movable probe indicate that the potential has a maximum value in the ball and falls off toward both cathode and anode. The authors postulate a potential distribution in a plane through cathode, ball of fire, and anode as shown by the solid line in Figure 5b. This differs from the Druyvestyn distribution in having a potential minimum near the cathode. Such must be the case since the cathode is again in a space-charge-limited condition. Druyvestyn also shows the potential rising much more rapidly between the cathode and the ball. Evidence will be presented below indicating that the plasma potential is close to that of the cathode, even at a distance only 2 millimeters outside the ball. It may be that the movable probe in Druyvestyn's studies disturbed the discharge and thus affected the readings.

In a plane rotated 180° from that which passes through the ball of

⁷ M. J. Druyvesteyn, "Der Niedervoltbogen", *Zeit. fur Phys.*, Vol. 64, p. 781, September 22, 1930.

fire, the postulated potential distribution is as shown by the broken line of Figure 5b. The ionization occurs only at and near the crest of the ball. The ions there produced, travel to the balance of the tube under the influence of the existing fields and by a diffusion process. Along radii whose potential distribution is described by the dashed curve of Figure 5b, current flows from the cathode to the anode under the influence of the slight gradient. A sheath forms at the anode, its thickness being determined by space-charge current-flow relations. Thus, in regions of the tube removed from the ball of fire, the plasma acts as a conductor enabling electron current to flow from cathode to anode with low applied potentials. An application of the use of a plasma to achieve a continuously controllable, low arc drop gas tube has been described by E. O. Johnson.⁸

(c) Langmuir Mode

Since, in this case, the glow pervades the tube with the exception of a region around the cathode, the potential distribution would appear to be of the form shown in Figure 5c.

Once again a potential minimum exists near the cathode. The major portion of the tube is above ionization potential. If the integrated random current near the anode surface exceeds the circuit current, a potential drop occurs at the anode which results in the return of some electrons to the plasma.

The region of the cathode fall has been designated by Langmuir¹ as a double sheath. Electrons and positive ions move through it in opposite directions. It is observed that as a rule the cathode is surrounded by a fairly well defined region of several millimeters thickness which is usually dark, but may in certain cases be of a different brightness from the plasma. Druyvestyn and Warmoltz⁵ have studied this usually dark region and have shown that it is much thicker than the space-charge-limited region and that at its inner boundary the potential drops slightly, and that the charge density rises considerably as one moves outward through the boundary. They explain the results as arising largely from elastic encounters of electrons which emerge from the double sheath (space-charge region) with velocities corresponding to the cathode fall.

Since this type of discharge has been studied quite thoroughly by previous workers, it will not be given so much attention as other modes of the discharge.

⁸ E. O. Johnson, "Controllable Gas Diode", *Electronics*, Vol. 24, p. 107, May, 1951.

(d) Temperature-Limited Case

The postulated potential distribution in this case is shown in Figure 5d. The potential rises steeply from the cathode to a high value of space potential and then falls at the anode to a value in excess of the ionization potential.

V. SPACE POTENTIAL — HOT PROBE STUDIES —
ARC DROP — ELECTRON TEMPERATURE

*a. Anode Glow Mode***Case 1 — Tube No. 1**

In the study of this as well as of the other cases, many measure-

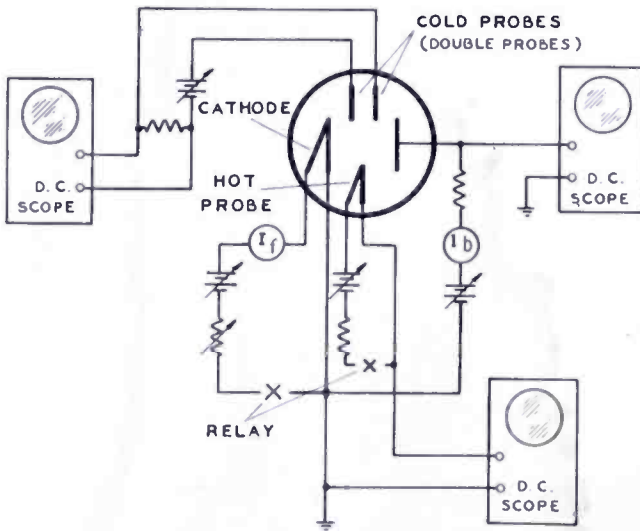


Fig. 6 — Test setup for study of gas discharge diode with unipotential cathode.

ments were made with tube No. 1 (see Figure 2). In order to eliminate the effects of potential drop along the cathode and hot probes, these were operated in the circuit shown schematically in Figure 6.

The relays employed were such that by connecting their four contacts in parallel, they could readily handle the maximum 6 amperes of current in the 0.010-inch Tantalum filament and the 2 amperes of the 0.005-inch tungsten probe. The relays were driven by 60-cycle alternating current, and by means of suitable phasing networks (not shown) could be adjusted so that both relays were open over the same period, thus enabling measurements to be made when the cathode and hot probe were both equipotentials. The off times of the heating currents were several hundred microseconds, occurring at a repetition

rate of 120 per second. The filament cooling during the off periods was computed and found to be negligible.

The filament heating current, I_f , was set at various average values, and determinations were made of the following qualities during the off periods: (1) floating potential; (2) plasma potential with hot probe; (3) arc drop; (4) electron temperature (measured with the double probes);⁶ (5) cathode emission. The floating potential was determined with the "hot" probe unheated, the potential with respect to ground being measured with a direct-current oscilloscope. The plasma potential was determined by heating the hot probe until its potential "locked." This is the potential at which emitted electron

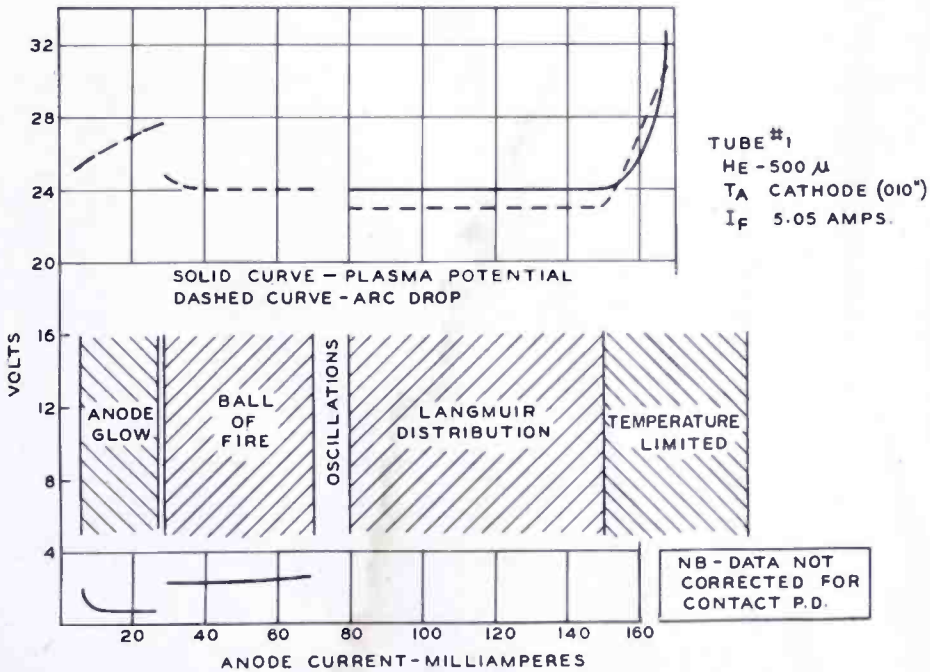


Fig. 7—Arc drop and plasma potential of hot-cathode gas-discharge diode operating in various modes.

current and electron current arriving to the probe from the plasma just balance. Heating the probe beyond this point causes its potential to go slightly positive with respect to the plasma, but by an amount which is negligible in comparison with the quantities being measured.

Figure 7 is a plot of arc drop V_b and plasma potential as a function of anode current. (These have not been corrected for contact difference of potential.)

In the anode-glow case, it is seen that the arc drop exceeds the ionization potential of helium (24.5 volts) as is to be expected from the picture previously presented. Furthermore, as the current increases, the required increase in plasma density is achieved by an

increase in the arc drop. The plasma potential is very close to cathode potential, also in accordance with this picture.

If this picture is correct, electrons released by ionizing collisions will be drawn by the field to the anode and hence, all the plasma electrons must originate at the cathode. It would then be expected that the plasma electron temperature would be close to that of the cathode. Double probe measurements showed that such is actually the case. A typical double probe characteristic is shown in Figure 8. For this case the electron temperature $T_e = 2900^\circ \text{ K}$. The cathode temperature in this case was about 2600° K .

Rapid methods for determining plasma density and random plasma currents from double probe data have been described by Malter and Webster.⁹ Application of these methods yields in this case: (1) plasma density, $n = 3.3 \times 10^9$ per cubic centimeter; (2) random electron current, $j_{eo} = 4.6 \times 10^{-3}$ ampere per square centimeter. These are the values in the vicinity of the probes.

It is of interest to compare the random current flowing through the cylindrical surface in which the probes lie, with the directed current through the same surface. The latter current is the anode current in this case and is 8 milliamperes. The random current through the plane of the probes is given by

$$\begin{aligned} I_r &= 2\pi r_p \left(\frac{2}{\pi} h \right) j_{eo} \\ &= 4 \times 0.76 \times 2.5 \times 4.6 \times 10^{-3} \\ &= 35 \text{ milliamperes.} \end{aligned}$$

In the expression above it is assumed that the axial distribution is sinusoidal. This accounts for the factor $2/\pi$. It is seen that at a point about midway between cathode and anode, the random current density exceeds the directed current density by a factor greater than four. The anode current must equal the random current at the point where the potential rises steeply near the anode. This is so since beyond this point there is no return flow of electrons. The necessary decrease of random current to a value of 8 milliamperes near the anode is brought about by a decrease in plasma density as the anode is approached. An analysis of the actual plasma distributions will be contained in a later paper of this series.

⁹ L. Malter and W. M. Webster, "Rapid Determination of Gas Discharge Constants from Probe Data", *RCA Review*, Vol. XII, No. 2, p. 191, June, 1951.

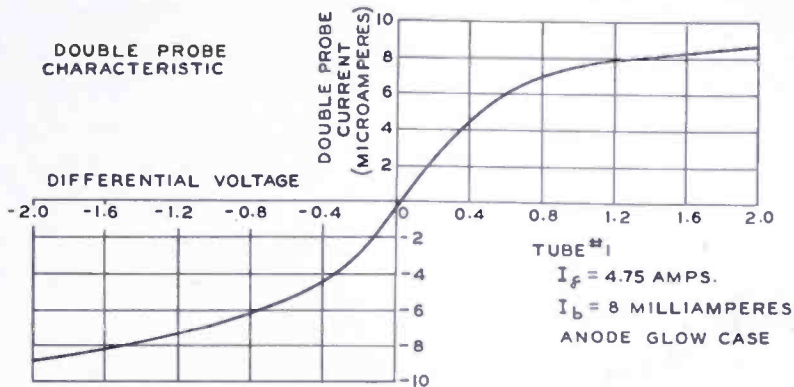


Fig. 8—Double probe characteristic of test diode operating in anode glow mode.

Case 2 — Tube No. 2

This tube is similar to No. 1 except that the cathode is of the oxide type and the ends are made of mica. The tube was filled with helium at 1 millimeter pressure. This enables one to operate at much higher levels of cathode emission, so that operation can be extended to higher currents. What is more important, the light emission from the cathode does not, in this case, prevent visual observation of the glow.

The volt-ampere characteristic of this tube is plotted in Figure 9. The upper curve shows the arc drop as a function of anode current. The characteristic is seen to be similar to that of Figure 7 for the case

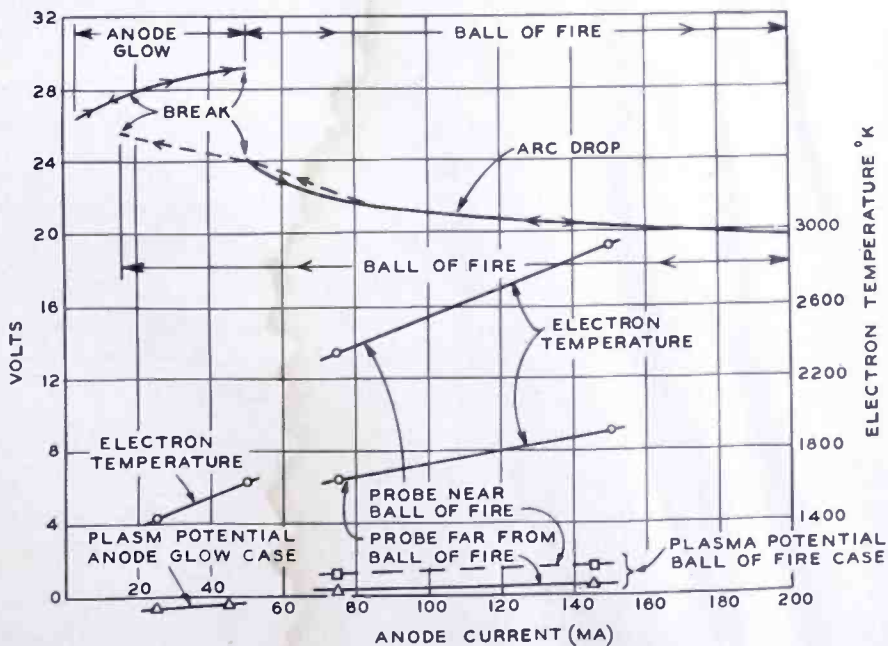


Fig. 9—Volt-ampere characteristic of test diode.

of a tantalum cathode. The arrows indicate the direction of current increase and decrease. The hysteresis effect in the breaks between anode-glow and ball-of-fire modes is very marked in this case. The lower curves show the plasma potential. These were obtained by measurement of floating potential and determination of wall potential (difference between plasma and floating potentials) by the double-probe method of Malter and Webster. It is seen that in the anode-glow case, the plasma potential (not corrected for contact potential difference) is, at a point midway between cathode and anode, actually below that of the cathode. Furthermore, the electron temperatures (shown in Figure 9) are seen to be only slightly above the temperature of the oxide cathode. These results are in good concordance with the picture of the anode glow case previously presented. The plasma electrons are entirely those emitted by the cathode and their slightly higher temperature may be attributed to the energy which they gain in the very weak plasma field.

b. Ball-of-Fire Mode

Case 1 — Tube No. 1

At a current of about 29 milliamperes (see Figure 7) the discharge goes over into the ball-of-fire form. Because of the intense light from the tungsten filament, the position of the glowing region could not be ascertained. However, observations in oxide cathode tubes (tube described in Case 2) indicate that the ball of fire avoids probes. The data are believed to represent conditions far removed from the ball of fire.

Between 29 and 70 milliamperes, the discharge remains in this state. It is seen (from Figure 7) that the arc drop is now below the ionization potential, and the plasma potential (away from the ball of fire) is still not far removed from cathode potential.

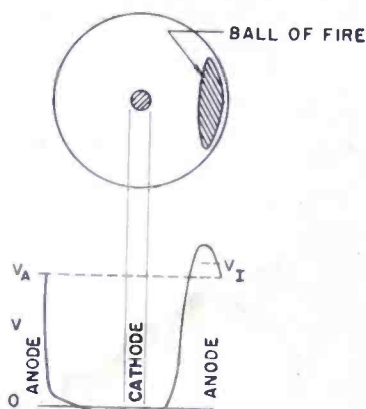
Double-probe data at a current of 40 milliamperes yielded the following results: $T_e = 3150^\circ \text{ K}$, $n = 2.1 \times 10^{10}$ per cubic centimeter, $j_{co} = 29.2 \times 10^{-3}$ amperes per square centimeter.

From the above studies and the results of others, it appears that the potential distribution through the tube has the form shown in Figure 10.

The ion generation occurs entirely within the ball of fire (either by single electron impacts or by multiple processes). These ions travel to other parts of the tube under the influence of the fields and density gradients.

At higher pressures and with heavier gases, the arc drop can assume very low values (true low-voltage arc), but qualitatively the picture is undoubtedly the same. It would seem that there must be

Fig. 10 — Typical ball-of-fire discharge in cylindrical diode and corresponding radial distribution of potential.



considerable current flow from cathode to anode along paths which do not pass through the ball of fire. That such is actually the case is demonstrated by the following experiment.

Case 2 — Tube No. 3

This tube had the form shown in Figure 11. The anode of this tube was made of four sections subtending at the axis approximately 30° , 60° , 90° , and 180° . If the discharge was started when only the 30° segment was connected, the ball of fire would assume a position close to that segment, as shown in the Figure 11, and retain that position even when the other segments were then connected into the circuit.

In test No. 1, the tube was connected as shown in Figure 12. The current to each segment was about 50 milliamperes. The potential assumed by each of the segments was: $V_{30^\circ} = 5.8$ volts, $V_{60^\circ} = 1.4$ volts, $V_{90^\circ} = 0.7$ volts, and $V_{180^\circ} = 0$ volts. Each segment assumed the potential which would just permit a current flow determined by the resistor R and potential source. (These currents are all very nearly alike.) In accordance with this picture, the plasma potential should drop off as one moves away from the ball of fire, and consequently less anode potential should be required to collect current as one moves in the same direction. Such is seen to be the case.

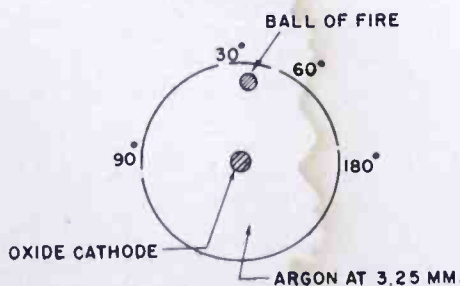


Fig. 11—Experimental multi-segment diode for study of ball-of-fire mode.

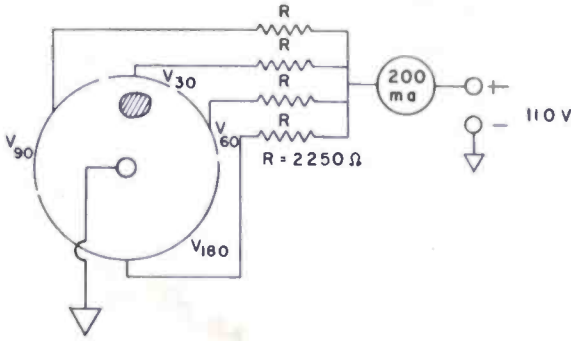


Fig. 12 — Test circuit for study of tube of Figure 11.

In test No. 2, the 60° and 90° electrodes were permitted to float. The ball of fire was stationed near the 30° electrode, and the current to the 180° electrode, I_{180} , was measured as a function of the electrode potential. The results are plotted in Figure 13. It is seen that I_{180} has an appreciable value when $V_{180} = 0$, and then rises rapidly and substantially saturates at $V_{180} \approx 0.5$ volt. This is just the behavior that would be expected from the potential plot portrayed in Figure 10. At $V_{180} \approx 0.5$ volt the 180° electrode is at plasma potential and so collects the entire random plasma current which approaches it. It will be recognized that this is something very similar in principle and in operation to the Plasmatron described by Johnson.⁸ In that device, the conducting plasma is generated by means of a discharge between

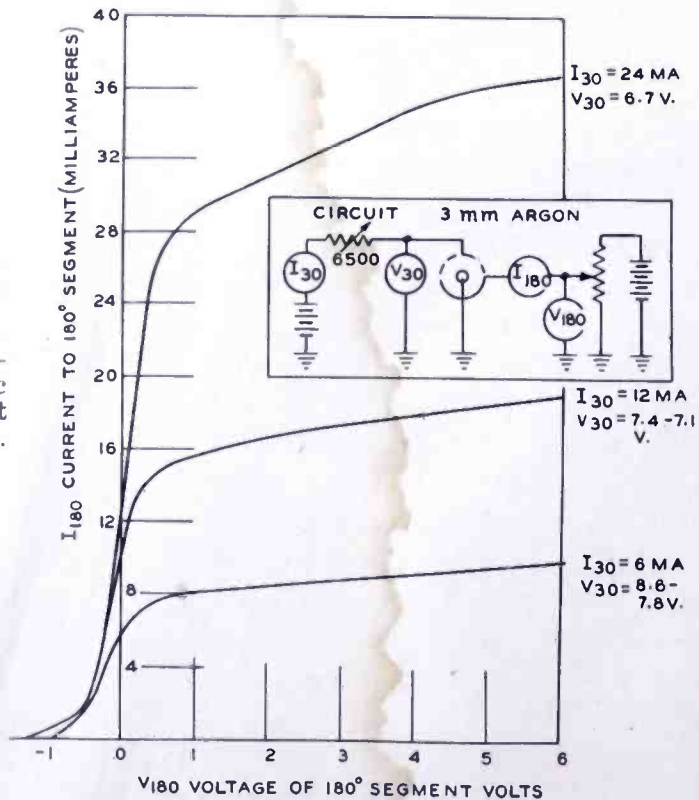


Fig. 13 — Volt-ampere characteristic of multi-segment tube of Figure 11.

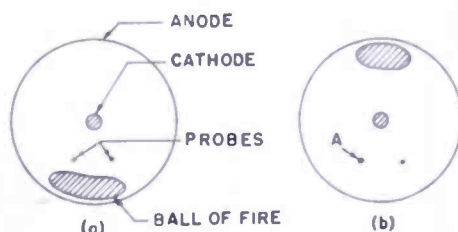
an auxiliary cathode and anode. In this case the auxiliary discharge occurs between the cathode and the 30° electrode. This provides the conducting plasma for transport of electrons between the same cathode and the 180° electrode.

Case 3 — Tube No. 2

This tube is similar to tube No. 1 of Figure 2 except that an oxide cathode replaces the one of tantalum, and the helium filling was at a pressure of 1 instead of 0.5 millimeter.

The results for the ball-of-fire case are presented (in part) in Figure 9. The arc drop is seen to be substantially below the ionization potential. Plasma potential and electron temperatures at the probes were found to depend upon the position of the ball of fire. It was found that there were several stable positions of the ball of fire and that the ball could be placed in any one of these by means of a magnet.

Fig. 14—Positions of probes and ball of fire in two cases studied.



The ball would remain in the particular spot after the removal of the magnet. Data were taken with the ball in the two positions indicated in Figure 14.

From the curves of Figure 9 it is seen that the plasma potential and electron temperature are both higher near the ball of fire. (The data were taken at probe A.) It is amazing that at a distance of only 2 millimeters from region of visible glow, plasma potential is still less than 2 volts, although it may well rise to values in excess of 20 volts within the ball. This indicates that the potential rise near the ball of fire is exceedingly steep.

Data for the various cases studied are included in Table I. It is seen that the plasma density and random electron currents increase at about the same rate as the anode current. A comparison of the random current data with those for the anode glow case (see section IIIa) indicates that here too, the random current and plasma density must fall off rapidly as the anode is approached. This is essential, since in accordance with the postulated picture, the major portion of





the anode current is due to saturated current arising from collection of electron flow out of the plasma into the anode sheath.

Case 4 — Tube No. 4

This tube contained an oxide cathode and was filled with argon at a pressure of 8 millimeters. It was unstable at low current values but at an anode current of 200 milliamperes, stable operation occurred in the ball-of-fire mode. The ball was a very tight blue sphere about 2 millimeters in diameter which "floated" about midway between cathode and anode.

The ball of fire normally floated on a radius opposite the median

Table 1 — Discharge Characteristics for Various Modes and Operating Conditions

TEST	I_p	ARC DROP	NATURE OF DISCHARGE	T_e °K	n $\frac{\text{IONS}}{\text{p CM}^3}$	J_{oe} $\frac{\text{AMP}}{\text{CM}^2}$
1	25	28.3	ANODE GLOW	1430	1.1×10^{10}	10.5×10^{-3}
2	50	29.0	ANODE GLOW	1630	2.86×10^{10}	30×10^{-3}
3	75 ma	24.5	BALL OF FIRE GLOW 	1650	2.86×10^{10}	30×10^{-3}
4	75 ma	24.5	COMPUTED AT DENSER REGION 	2350	1.9×10^{11}	190×10^{-3}
5	150 ma	20.5	GLOW 	1910	7.6×10^{10}	80×10^{-3}
6	150 ma	21	GLOW 	2930	3.5×10^{11}	450×10^{-3}

line of the probes. Under these conditions the following results were obtained:

$$V_f = -2.8 \text{ volts (floating potential),}$$

$$V_w = 4.1 \text{ volts (wall potential),}$$

$$V_{\text{plasma}} = +1.3 \text{ volts,}$$

$$n_o = 3.3 \times 10^{10} \text{ per cubic centimeter,}$$

$$T_e = 7500^\circ \text{ K.}$$

It is seen that electron temperatures greatly in excess of that of the cathode exist even far from the ball of fire. This may be attributed to two factors: (1) high-energy electrons enter the plasma from the ball of fire; and (2) the higher gas pressure results in a higher plasma resistivity, hence higher electric fields from which the cathode electrons may acquire energy. By moving the ball of fire closer to the probes (with a magnet) electron temperatures as high as $13,800^{\circ}$ K. were observed.

c. Langmuir Mode

Case 1 — Tube No. 1

Referring to Figure 7, it is seen that for the operating conditions there involved, the tube leaves the ball-of-fire mode at anode currents of 70 milliamperes, but does not definitely enter into the Langmuir mode until a current of 80 milliamperes is reached. The transition between these two modes appears to be marked by instabilities in all cases.

In the Langmuir mode (see Figure 5c) the plasma potential is higher than the arc drop. This is in accordance with Langmuir's picture. It is further found in this case that there is no definite value of floating potential. The potential which a floating electrode assumes is a marked function of its size and location and of anode current. Langmuir has postulated that the region around the cathode is a double sheath within which electrons and ions are moving in opposite directions. The potential rises rapidly in this sheath to the high value of plasma potential. In this tube, this will result in the presence within the plasma of various categories of electrons: those which have traveled from the cathode without collision; cathode electrons which have suffered collisions; and electrons produced by ionization within the gas. Since floating potential is that potential at which electron and ion currents to the electrode balance, and since the electrode shape and position determine the proportions of the different categories of electrons which arrive at it, it is not surprising that there is no definite "floating potential." Under these conditions there can be no "electron temperature," at least not for all the electrons. This was borne out by double-probe studies. These showed no evidence of saturation. The unsaturated characteristic is what would be obtained if a major portion of the electrons present were cathode electrons which had been accelerated through the cathode fall and which had experienced on the way through the cathode fall and plasma, an insufficient number of elastic and inelastic collisions to "acquire a temperature." The region

of the cathode fall or double sheath is, however, a region in which a considerable number of collisions of ions with atoms do occur (at the pressures in which the tests were run). This is evidenced by the fact that there was no disturbing cathode heating due to ion bombardment. This indicates that the ions, while "falling downhill" to the cathode experience enough collisions to transfer a major portion of the energy corresponding to the cathode fall, to the atoms of the gas.

d. Temperature-Limited Case

In this case (see Figure 7) the arc drop and plasma potential rise rapidly. The current may actually continue to increase, due in part to Schottky effect, and in part to cathode heating by ion bombardment. The latter phenomenon makes studies in this region difficult. There is no observable dark region around the cathode as was the case for the Langmuir mode. As a consequence the electrons and ions can travel through this sheath without making collisions. This is what makes possible cathode heating by ion bombardment. This case can be looked upon as a transition between the externally heated hot cathode arc and the glow discharge and will receive no further attention here.

VI. SUMMARY

It has been shown that a gas discharge between an externally heated hot cathode and a positive electrode takes on a number of possible forms.

At the lowest currents the discharge assumes the anode-glow mode. The tube drop occurs in a thin sheath close to the anode, all the ionization and excitation occurring very close to the anode. The light emission appears to come from the anode surface. With the exception of the anode sheath region, and a narrow region around the cathode, the remainder of the tube is filled with a plasma whose potential is close to that of the cathode. The electron temperature within this plasma is close to that of the cathode.

When the ion production close to the anode surface exceeds a critical value, a plasma forms at that point which detaches itself to a greater or lesser extent from the anode. The ionization and excitation occur within this detached region referred to as the ball of fire. The ions produced within the ball serve to provide a plasma throughout the remainder of the tube. This plasma serves as a conductor permitting electron current to flow from cathode to anode at potentials less than that required for ionization or excitation. All the ionization

occurs within the ball of fire where the potential rises to its maximum value. Away from the ball of fire the plasma potential is close to that of the cathode. It is believed that the nonoscillating low-voltage arc is always a ball-of-fire discharge.

At a discharge current about half that of the cathode emission the discharge breaks into the Langmuir mode. In this mode the arc drop is concentrated largely in a double-sheath surrounding the cathode. The balance of the tube (except for a thin sheath at the anode) is filled with a plasma whose potential, as a rule, exceeds that of the anode slightly.

When the cathode emission is saturated the discharge fills the entire tube. This discharge is referred to as the temperature-limited mode.

RCA TECHNICAL PAPERS†

Second Quarter, 1951

Any request for copies of papers listed herein should be addressed to the publication to which credited.

- "All Electronic Thickness Gauge for Very Thin Metal Foils", J. Guy Woodward, *RCA Licensee Bulletin LB-835* (June 27) 1951
- "Application of Polarity Diplexing to Microwave Relay Systems", C. A. Rosencrans, *TV Eng.* (June) 1951
- "Backtalk", A. N. Goldsmith, *Electronics* (June) (Letter to the Editor) 1951
- "A Bandpass Mechanical Filter for 100 KC", L. L. Burns, Jr., *RCA Licensee Bulletin LB-829* (April 12) 1951
- "A Brief Review of Diode Detectors", R. L. Kuehn, *Audio Eng.* (June) 1951
- "Cabinets for High-Quality Direct Radiator Loudspeakers", H. F. Olson, *Rad. and Tele. News* (May) 1951
- "Code Transmission and Reception", John B. Moore and David S. Rau, Section of RADIO ENGINEERING HANDBOOK, Keith Henny, McGraw-Hill Book Company, Inc., New York, N. Y., 4th Edition 1951
- "Controllable Gas Diode", E. O. Johnson, *Electronics* (May) 1951
- "Direct-Reading Noise-Factor Measuring Systems", R. W. Peter, *RCA Review* (June) 1951
- "A Diversity Receiving System for Radio Frequency Carrier Shift Radiophoto Signals", J. B. Atwood, *RCA Review* (June) 1951
- "An Editing Machine for Magnetic Tape Recording", D. C. Yarnes, *Broadcast News* (May-June) 1951
- "Filter Design Simplified, Part II", B. Sheffield, *Audio Eng.* (May) . 1951
- "Filters for Amateur TVI", A. M. Seybold, *Radio-Television Service Dealer* (April) 1951
- "Graphexon Writing Characteristics", A. H. Benner and L. M. Seiberger, *RCA Review* (June) 1951
- "Grid Current and Grid Emission Studies in Thyratrons—the Trigger-Grid Thyatron", L. Malter and M. R. Boyd, *Proc. I.R.E.* (June) 1951
- "High-Speed Ten-Volt Effect", R. M. Matheson and L. S. Nergaard, *RCA Licensee Bulletin LB-833* (May 25) 1951
- "High-Speed Ten-Volt Effect", R. M. Matheson and L. S. Nergaard, *RCA Review* (June) 1951
- "A High-Voltage Cold-Cathode Rectifier", E. G. Linder, *RCA Licensee Bulletin LB-827* (April 10) 1951
- "Horizontal Pulling, Part 2", J. R. Meagher, *Rad. and Tele. News* (April) 1951
- "Luminescence of Three Forms of Zinc Orthophosphate: Manganese", A. L. Smith, *RCA Licensee Bulletin LB-834* (June 6) 1951
- "Material-Saving Picture Tube", L. E. Swedlund and R. Saunders, Jr., *Electronics* (April) 1951
- "Measurement of Dissipation in Plate of Horizontal-Deflection Output Tube", *RCA Application Note AN-150*, RCA Tube Department, Harrison, N. J. (May) 1951
- "Metal Evaporator Uses High-Frequency Heating", Robert G. Picard and J. E. Joy, *Electronics* (April) 1951
- "A Method of Determining the Tracking Capabilities of a Pickup", H. E. Roys, *Broadcast News* (May-June) 1951
- "Methods to Extend the Frequency Range of Untuned Diode Noise Generators", H. Johnson, *RCA Review* (June) 1951
- "New Horizontal Deflection Circuit", R. K. Seigle, *Rad. and Tele. News* (June) 1951

† Report all corrections or additions to RCA Review, Radio Corporation of America, RCA Laboratories Division, Princeton, N. J.

- "New Lightweight Pickup and Tone Arm", L. J. Anderson and C. R. Johnson, *Broadcast News* (May-June) 1951
- "New Professional Tape Recorder", W. E. Stewart, *Audio Eng.* (April) 1951
- "A New Television Studio Audio Console", R. W. Byloff, *RCA Review* (June) 1951
- "A Note on 'Network Representation of Input and Output Admittances of Amplifiers'," F. W. Smith, *Proc. I.R.E.* (April) (Letter to the Editor) 1951
- "On Extending the Operating Voltage Range of Electron Tube Heaters", J. Kurshan, *RCA Licensee Bulletin LB-831* (May 11) 1951
- "Permanent Magnet Lenses", J. H. Reisner, *Jour. Appl. Phys.* (May) 1951
- "The Perturbation Calculus in Missile Ballistics", R. Drenick, *Jour. Frank. Inst.* (April) 1951
- "Practical Considerations in the Use of Television Super Turnstile and Super-Gain Antennas", H. E. Gihring, *RCA Review* (June) 1951
- "Practical Solution to the Screen Light Distribution Problem", C. R. Underhill, Jr., *Jour. S.M.P.T.E.* (June) 1951
- "Precision AM Frequency Monitor", R. S. McKinney, *Broadcast News* (May-June) 1951
- "Radio Broadcasting", Carl G. Dietsch, Section of RADIO ENGINEERING HANDBOOK, Keith Henny, McGraw-Hill Book Company, Inc., New York, N. Y., 4th Edition 1951
- "Rapid Determination of Gas Discharge Constants from Probe Data", L. Malter and W. M. Webster, *RCA Review* (June) 1951
- "Remote Control for Television Receivers", G. F. Rogers, *RCA Licensee Bulletin LB-828* (April 11) 1951
- "A Solution to the Magnetic Tape Timing Problem", D. R. Andrews, *Broadcast News* (May-June) 1951
- "Some Extensions of Elementary Plasticity Theory", F. Edelman and D. C. Drucker, *Jour. Frank. Inst.* (June) 1951
- "A Storage Oscilloscope", L. E. Flory, J. E. Dilley, W. S. Pike and R. W. Smith, *RCA Review* (June) 1951
- "The Television Casting Director", W. I. Kaufman, *Televiser* (April) 1951
- "Television Service. Part XII—Visible Symptoms of Hum Trouble", J. R. Meagher, *RCA Rad. Serv. News* (April-May) 1951
- "Television Studio Acoustics", M. Rettinger, *Audio Eng.* (April) 1951
- "Television Transmitter Monitoring", R. A. Boot and I. E. Goldstein, *Broadcast News* (May-June) 1951
- "A Tristimulus Photometer", G. C. Sziklai, *Jour. Opt. Soc. Amer.* (May) 1951
- "Video Relay Switching Layouts", C. R. Monro, *Broadcast News* (May-June) 1951
- "A 45-degree Reflection-Type Color Kinescope", N. Rynn and P. K. Weimer, *RCA Licensee Bulletin LB-830* (April 30) 1951

NOTE—Omissions or errors in these listings will be corrected in the yearly index.

AUTHORS



A. DANFORTH COPE received the B.A. degree from Colgate University in 1938, later engaging in graduate study in Physics at Yale University. He joined the Radio Corporation of America in 1941 as manufacturing process and development engineer working with special purpose, phototube, and television camera tube types at the Harrison, N. J. and Lancaster, Pa. tube plants. In 1949 Mr. Cope transferred to the RCA Laboratories Division at Princeton, N. J. where he is engaged in research on television camera tubes.

STANLEY V. FORGUE received the B.S. degree in Physics in 1939 and the B.E.E. and M.S. degrees in 1940 from the Ohio State University. He was a graduate assistant in the Physics Department of this university from 1939 to 1940. While taking additional graduate work he was a research engineer at the Ohio Engineering Experiment Station from 1940 to 1941 and a research fellow in the Ohio State Research Foundation from 1941 to 1942. Since then he has been with the RCA Laboratories at Harrison and Princeton, N. J. He is a Member of the Institute of Radio Engineers, the American Physical Society, Sigma Xi, Tau Beta Pi, Pi Mu Epsilon and is a Registered Professional Engineer.



ROBERT R. GOODRICH, II, was graduated from Harvard University with the degree of A.B. in Physics in 1928 and received the degree of S.M. in Communication Engineering from the same university in 1930. He joined the RCA Victor Division in Camden, N. J. in 1930. In 1942 he transferred to the RCA Laboratories Division in Princeton, N. J. where he is engaged in electronic research.

EDWARD O. JOHNSON received the B.S. degree in Electrical Engineering from Pratt Institute of Brooklyn in 1948. From 1941-1945 he served as an electronic technical in the U. S. Navy. In 1948 he joined the RCA Laboratories Division, Princeton, N. J., where he is now engaged in work on gaseous electronics. Mr. Johnson is a Member of the Institute of Radio Engineers.





DONALD MACKEY received the B.S. degree in electrical engineering from the University of Idaho in 1937. Upon graduation, he joined the RCA Victor Division at Camden, N. J. as an engineering trainee. In 1938 he joined the Home Instrument Department, specializing in the design of coils and transformers until 1943. From 1943 to 1944 he was engaged in the design of Loran receiving equipment. In 1944 he joined the newly formed Parts activity as manager of the Coil Development Group, and in that capacity is currently responsible for the design of high-frequency transformers and printed-circuit com-

ponents. Mr. Mackey is a Member of Sigma Tau and an Associate Member of Sigma Xi.

LOUIS MALTER—(See *RCA Review*, Volume XII, No. 2, June 1951, page 286.)

ALBERT ROSE received the A.B. degree from Cornell University in 1931 and the Ph.D. degree in Physics in 1935. From 1931 to 1934 he was a teaching assistant at Cornell University and since 1935 he has been associated with RCA Laboratories Division at Princeton, N. J. Dr. Rose is a Fellow of the Institute of Radio Engineers and a Member of the American Physical Society.



EARL SASS received the B.S. degree in Electrical Engineering from the University of Nebraska in 1945 and is presently engaged in evening graduate study at the University of Pennsylvania. Upon graduation in 1945, he joined the Parts activity of the RCA Victor Division at Camden, N. J. where he was engaged in the design of high-frequency coils and transformers until June 1947. From 1947 to August 1951, he specialized in the development of television tuners. Since August 1951, he has been with the Color Television Products Development Section of the Home Instrument Department. Mr. Sass is a

Member of Sigma Tau and Pi Mu Epsilon.

ROLAND W. SMITH—(See *RCA Review*, Volume XII, No. 2, June 1951, page 288.)

WILLIAM M. WEBSTER—(See *RCA Review*, Volume XII, No. 2, June 1951, page 288.)



PAUL K. WEIMER received the B.A. degree from Manchester College in 1936, the M.A. degree in Physics from the University of Kansas in 1938, and the Ph.D. degree in Physics from Ohio State University in 1942. During 1936 to 1937 he was a graduate assistant in physics at the University of Kansas. From 1937 to 1939, he taught physics and mathematics at Tabor College, Hillsboro, Kansas. Since 1942 he has been engaged in television research at RCA Laboratories Division at Princeton, N. J. Dr. Weimer is a Senior Member of the Institute of Radio Engineers, and a Member of the American Physical Society and Sigma Xi.



